

NEW APPROACHES FOR QUANTITATIVE GLYCOMICS USING
MASS SPECTROMETRY

by

SHUJUAN TAO

(Under the Direction of Ron Orlando)

ABSTRACT

The ability to quantitatively determine changes in glycan expression is an essential component of comparative glycomics. However, the quantitative analysis of N-glycans is often hindered by the lack of consistent analysis across laboratories due to the lack of quantitation strategies available. This study describes multiple improved relative quantitation approaches to facilitate studies of comparative glycomics while providing insight into their strengths and weaknesses, so that glycomic investigators can make an educated choice of the strategy that is best suited for their particular application.

Chapter 1 is an introduction of glycomics and the application of mass spectrometry in this field. Also, it briefly describes the currently available techniques for quantitative glycomics as well as the challenges.

Chapter 2 describes a novel method for relative quantitation of N-glycans by isotopic labeling using ^{18}O -water during the enzymatic release process. The 2 Da mass shift for the labeled species can be differentiated from their unlabeled counterparts by using high resolution mass spectrometers, such as Fourier Transform Ion Cyclotron Resonance (FT-ICR) mass spectrometers.

Chapter 3 describes a Selected Reaction Monitoring (SRM) approach coupled with Hydrophilic Interaction Liquid Chromatography (HILIC) separation for relative quantitation of isomeric N-glycans with different sialic acid linkages. By using a novel superficially porous particle Penta-HILIC column, sialylated N-glycan isomers differing in α 2-3 and α 2-6 linkages can be resolved chromatographically. Thus, the relative quantitation of each sialic acid linkage isomer can be obtained from a straightforward LC-MS experiment.

Chapter 4 describes the evaluation of an ^{15}N -labeled monoclonal antibody (mAb) as an internal standard for quantitative glycomics. This ^{15}N -labeled mAb reference is aimed at providing an internal standard on the glycoprotein level for quantitative glycomics, especially for the quality control of the Immunoglobulin G (IgG) pharmaceutical product batch to batch.

Chapter 5 describes a targeted discovery glycomics strategy for global glycomics using scheduled Selected Reaction Monitoring (SRM) coupled with HILIC separation. This hypothesis driven glycomics approach utilizes the predictability of HILIC separation and the sensitivity and selectivity enhancement of SRM detection, which enables high through-put and consistent identification and quantification of diverse glycans expressed in different biological systems.

INDEX WORDS: Mass Spectrometry, Quantitative Glycomics, Stable Isotopic Labeling, Permethylated, Reductive Amination, Hydrophilic Interaction Liquid Chromatography, Selected Reaction Monitoring, Sialic Acid Linkage, Monoclonal Antibodies, Human Serum

NEW APPROACHES FOR QUANTITATIVE GLYCOMICS USING
MASS SPECTROMETRY

by

SHUJUAN TAO

B.S., Wuhan University, 2008

A Dissertation Submitted to the Graduate Faculty of The University of Georgia in Partial
Fulfillment of the Requirements for the Degree

DOCTOR OF PHILOSOPHY

ATHENS, GEORGIA

2014

© 2014

SHUJUAN TAO

All Rights Reserved

NEW APPROACHES FOR QUANTITATIVE GLYCOMICS USING
MASS SPECTROMETRY

by

SHUJUAN TAO

Major Professor:	Ron Orlando
Committee:	I. Jonathan Amster
	John Stickney

Electronic Version Approved:

Julie Coffield
Interim Dean of the Graduate School
The University of Georgia
August 2014

DEDICATION

To Mom and Dad, who are always there for me and encourage me to go on every adventure, especially this one. I love you both and owe you everything!

ACKNOWLEDGEMENTS

Foremost, I would like to express my sincere gratitude to my advisor Prof. Ron Orlando for the continuous support of my Ph.D. study and research, for his patience, motivation, enthusiasm and immense knowledge.

Besides my advisor, I would like to thank Dr. Barry Boyes for his lectures that helped me improve my knowledge in the area and his advice that helped me sort out the technical details for my work. Also I would like to thank Dr. Joshua Sharp for sharing his knowledge and experience.

My sincere thanks also go to the rest of my thesis committee: Prof. Jon Amster, and Prof. John Stickney, for their encouragement, insightful comments, and hard questions.

I thank my colleagues and friends: Dr. Rongrong Huang, Jessie Saladino, Dr. DJ Johnson, Dr. Evelyn Rampler and Yulun Chiu, for their assistance, encouragement with my work and all the fun we have had in the last six years. In particular, I am grateful to Jesse Hines for showing me how to break down the instrument to pieces and put it back together. Also I thank Emily Betchy, her editorial advice and revision were essential to the completion of this dissertation and I wish her the best luck with her studies.

Last but not the least, I owe my gratitude to those whose names are not mentioned but have made this dissertation possible and my graduate experience has been one that I will cherish forever.

TABLE OF CONTENTS

	Page
ACKNOWLEDGEMENTS	v
CHAPTER	
1 INTRODUCTION AND LITERATURE REVIEW	1
Glycosylation and biological significance	1
Analytical techniques for N-glycan Analysis	3
Quantitative glycomics	18
Important study objects	21
Synopsis of completed research	24
References	28
2 A NOVEL METHOD FOR RELATIVE QUANTITATION OF N-GLYCANS BY ISOTOPIC LABELING USING ¹⁸ O-WATER	37
Abstract	38
Introduction	38
Experimental Section	40
Results and Discussions	43
Conclusions	54
References	54
3 AN LC-SRM APPROACH FOR THE SEPARTATION AND QUANTITATION OF SIALYLATED N-GLYCANS LINKAGE ISOMERS	57

Abstract	58
Introduction.....	58
Experimental Section	61
Results and Discussions	64
Conclusions.....	77
References.....	78
4 EVALUATION OF AN ¹⁵ N-LABELED MONOCLONAL ANTIBODY (MAB) AS AN INTERNAL STANDARD FOR QUANTITATIVE GLYCOMICS	81
Abstract.....	81
Introduction.....	81
Experimental Section	84
Results and Discussions	86
Conclusions.....	99
References.....	99
5 TARGETED GLYCOMICS BY SCHEDULED SELECTED REACTION MONITORING (SRM) WITH HILIC SEPARATION FOR GLOBAL GLYCAN PROFILING.....	101
Abstract.....	101
Introduction.....	101
Experimental Section	104
Results and Discussions	106
Conclusions.....	119
References.....	119

6 CONCLUSIONS.....	121
APPENDICES	
A SUPPLEMENTAL INFORMATION TO CHAPTER 2.....	124
B SUPPLEMENTAL INFORMATION TO CHAPTER 3.....	127
C SUPPLEMENTAL INFORMATION TO CHAPTER 4.....	133
D SUPPLEMENTAL INFORMATION TO CHAPTER 5.....	142

CHAPTER 1

INTRODUCTION AND LITERATURE REVIEW

Glycosylation and biological significance

Glycosylation is the most abundant and structurally diverse type of posttranslational modification, which occurs in up to half of all gene products in a non-templated manner.¹ As a matter of fact, all cells in nature are coated with a dense shell of glycans, which is important for their biological processes and functions.² Previous studies indicate that approximately 60% of total human proteins are glycosylated.³ The generality of protein glycosylation enhances the structural and functional diversity of proteins in biological systems. Thus, it gains people's interests world-wide.

The biosynthesis pathway of protein glycosylation occurs in the lumen of the Golgi apparatus, which is ruled by the activities of series enzymatic reactions that are specific to each glycoconjugate class and the availability of nucleotide sugars.¹ In the human genome, there are at least 250 glycosyltransferases, and it has been estimated that about 2% of the total human genome is directly involved in glycan assembly, including biosynthesis, degradation and transport.^{4,5} The biosynthesis of those nucleotide sugar donors is regulated by nucleic acid, glucose, energy metabolism, and specific transporters for compartmentalization.⁶ Thus, glycosylation of proteins is dependent on both the type and the status of the cells in which they are synthesized. The deficiency of glycosylation may have tremendous effects on biological function and various diseases.^{7,8} Hence, alteration of glycosylation has been studied extensively in many diseases for diagnostic and prognostic purposes.

Glycomics emerged at the end of the 20th century, which is analogous to genomics and proteomics.⁶ Glycomics is the comprehensive study of the significance of glycome expression in biological systems.¹ Generally, there are five classes of glycans: (i) N-linked glycans which are attached to a nitrogen of asparagine side-chains; (ii) O-linked glycans, which are attached to the hydroxyl oxygen of serine, threonine, tyrosine, hydroxylysine, and hydroxyproline side-chains, or to oxygens on lipids such as ceramide; (iii) C-linked glycans, which are a rare form of glycosylation where a sugar is added to a carbon on a tryptophan side-chain; (iv) Glycosaminoglycans (GAGs), which are long unbranched polysaccharides containing a repeating disaccharide unit; and (v) Glycophosphatidylinositol (GPI) anchors, which link lipids to the carboxyl terminus of proteins and serve to anchor these proteins to cell membranes. All these glycans share the same basic structural units—monosaccharides. Some of the most common monosaccharides are listed in **Table 1.1** with their symbolic representations. The complexity of glycans arises not only from the variety of the monosaccharides, but also from the sequence they built up and the linkages between each unit. Thus, the profiling of glycomics requires that: (i) all types of glycans can be detected and quantified; (ii) isomers can be separated; and (iii) components can be assigned to a particular structure, including the overall topology of the molecule and all linkages.⁸ Structural complexity and dynamic glycan patterns of biological samples hamper comprehensive glycomic studies. In this work, we mainly focused on the study of N-glycan analysis.

Table 1.1 Common monosaccharides.

Symbol	Abbreviation	Name
	Fuc	fucose
	Gal	galactose
	GalN	galactosamine
	GalA	galacturonic acid
	GalNAc	N-acetylgalactosamine
	Glc	glucose
	GlcN	glucosamine
	GlcA	glucuronic acid
	GlcNAc	N-acetylglucosamine
	IdoA	iduronic acid
	Kdn	2-keto-3-deoxy-nonulosonic acid
	Man	mannose
	ManN	mannosamine
	ManA	manuronic acid
	ManNAc	N-acetylmannosamine
	NeuAc	N-acetylneuraminic acid
	NeuGc	N-glycolylneuraminic acid
	Xyl	xylose

Analytical techniques for N-glycan analysis

N-glycans refer to the oligosaccharides attached to the N4 atom of asparagine residues in polypeptides. Usually the glycosylation sites can be predicted by the sequon Asn-Xaa-Ser/Thr (where Xaa can be any amino acid except proline). However, recently, N-glycosylation sites have been found at noncanonical Asn-Xaa-Cys sequences as well.⁹ All of the N-glycans are comprised of a common trimannosyl-chitobiose core (Man₃GlcNAc₂). Each mannose residue on

the non-reducing termini can be extended. Based on the branch extension composition, mature N-glycans are classified into three subtypes: high-mannose, hybrid and complex (**Figure 1.1**).

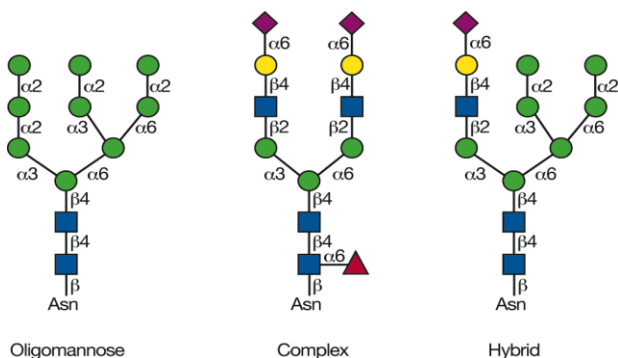


Figure 1.1 Common cores of different types of N-glycans

Intact N-glycans can be released both chemically and enzymatically from their peptide backbone. However, the chemical hydrolysis release of N-glycans is not widely used due to the concern of the destruction of the peptide backbone and the potential to degrade the oligosaccharides. The most widely used enzyme for releasing intact N-glycans is Peptide N-glycosidase F (PNGase F), which cleaves between the innermost GlcNAc and asparagine residues of most N-linked glycans from their peptide backbone, except those containing a 3-linked fucose attached to the reducing terminal GlcNAc residue.¹⁰ For these rare cases, PNGase A can be used to release those glycans.¹¹ The PNGases are amidases that release glycans as intact glycosylamine, rapidly converting them to native oligosaccharides especially at low pH.

Derivatization of Glycans

Glycans released from any biological samples can give a complex sample pool due to the structural diversity. Additionally, the abundance of each glycoform often presents at low levels, which puts pressure on the separation and detection of analytical technologies. Thus, the analysis

of glycans often requires appropriate derivatization prior to chromatographic separation and/ or mass spectrometric detection.¹² For the last few decades, various approaches for glycan derivatization have been developed to achieve higher resolution of separation and greater sensitivity, such as reductive amination, Michael addition, hydrazide labeling, permethylation, etc.

Permethylation

As one of the most important types of full derivatization employed in glycan analysis,¹³ permethylation of oligosaccharides results in conversion of all hydrogens on hydroxyl groups, amine groups, and carboxyl groups to methyl groups¹⁴ (**Figure 1.2**), yielding a hydrophobic derivative. The procedure was originally introduced by Hakomori in 1964,¹⁵ and utilized the dimethyl sulfoxide anion (DMSO⁻) to replace protons from oligosaccharides with methyl groups. This original procedure was modified later on by different groups^{14,16,17} to improve its rapidity, experimental simplicity, effectiveness and purity of reaction products. Those procedures are referred to as “in-solution permethylation”. More recently, Novotny and his colleagues introduced a miniaturized approach with packing of sodium hydroxide powder in microspin columns or fused-silica capillaries, which has been termed “solid-phase permethylation”,¹⁸ permitting effective derivatization in less than a minute at microscale.

Permethylation of oligosaccharides prior to MS analysis has been widely adopted due to several reasons. (i) Permethyated glycans have much higher ionization efficiency compared to native ones due to the increase in hydrophobicity of the molecules for both ESI and MALDI.¹⁹⁻²¹ Specifically, with ESI, the hydrophobic characteristics of permethylated oligosaccharides are less solvated and have a higher surface activity in the precursor electrospray droplet enabling significant enrichment in the progeny droplets that are further desolvated and eventually produce

gas-phase charged molecules. With MALDI, permethylated oligosaccharides have increased volatility which leads to better ionization. (ii) Permethylation can stabilize the labile sialic acid residues in acidic oligosaccharides to minimize the in-source or post-source decay.²² (iii) Permethylation gives more uniform ionization for both neutral and acidic glycans enabling simultaneous detection in positive mode. (iv) For structure characterization, the glycosidic bond cleavage during tandem MS leads to underivatized “scar” sites, reflecting the linkage positions. Furthermore, the tandem mass spectra of permethylated glycans contain a higher abundance of cross-ring fragments than their native counterparts, which allow a higher probability of structure assignment for branching and linkage isomers, as well as the presence of configurational and conformational isomers.²³⁻²⁷ (v) For relative quantitation, the incorporation of a stable isotope can be realized during the process of permethylation (*vide infra*).

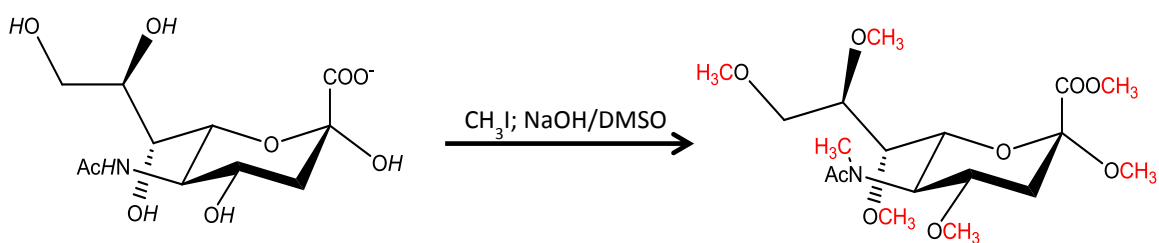


Figure 1.2 Derivatization of oligosaccharides by permethylation.

Despite these benefits derived from permethylation, there are also some drawbacks when applying this derivatization technique. First of all, the m/z shift due to permethylation is variable for different sized glycans. Secondly, 100% conversion has been proven difficult and is variable for different glycans, which can be problematic for quantitative analysis. For example, a 0.1 % change in the permethylation efficiency can result in a 3 %-10 % efficiency difference depending

on the number of methylation sites. Last but not least, permethylation is unsuitable for the analysis of biologically important glycans containing partially methylated sialic acids.²⁸

Reductive amination

Reductive amination is another prominent technique which has been widely utilized for glycan derivatization. In this reaction, glycans with a free reducing end can be labeled using a reagent containing a primary amine group by a two-stage process. For the first step, a stable Schiff's base is formed when the carbonyl carbon of the acyclic reducing sugar is attacked by the tag reagent in a nucleophilic manner. After formation of the Schiff's base, the resulting imine group is reduced simultaneously by a reducing reagent to yield stable, labeled glycans²⁹ (**Figure 1.3**).

Reductive amination has been widely used to introduce a chromophore or a fluorophore into the glycans for sensitive detection techniques such as UV or fluorescence absorption.^{30,31} Additionally, a direct quantitation based on the UV or fluorescence absorbance intensity can be achieved due to the stoichiometric attachment of one label per glycan. For MS detection, significant (over 50-fold) signal enhancement has been observed versus native counterparts with several tagging reagents, which have basic functional groups to provide a location for proton attachment.^{32,33}

Various amines have been applied to labeling glycans, such as 2-aminobenzamide (2-AB),³⁴ 2-aminobenzoic acid (2-AA),³⁵ 2-aminopyridine (PA),³⁶ 2-aminonaphthalene trisulfonic acid (ANTS),³⁷ and 1-aminopyrene-3,6,8-trisulfonic acid (APTS).³⁸ Many of them are available in commercial kits for convenience and effectiveness.³⁹⁻⁴¹ Among those, the 2-AB labeling has been studied most thoroughly and comprehensive databases have been developed for 2-AB labeled glycans in HPLC separation.⁴²⁻⁴⁴ Recently, it was reported that procainamide (ProA) can

be used to enhance glycan MS response compared to 2-AB labeled glycans.⁴⁵ Hence, procainamide is favored for derivatization of N-glycans through reductive amination in this work.

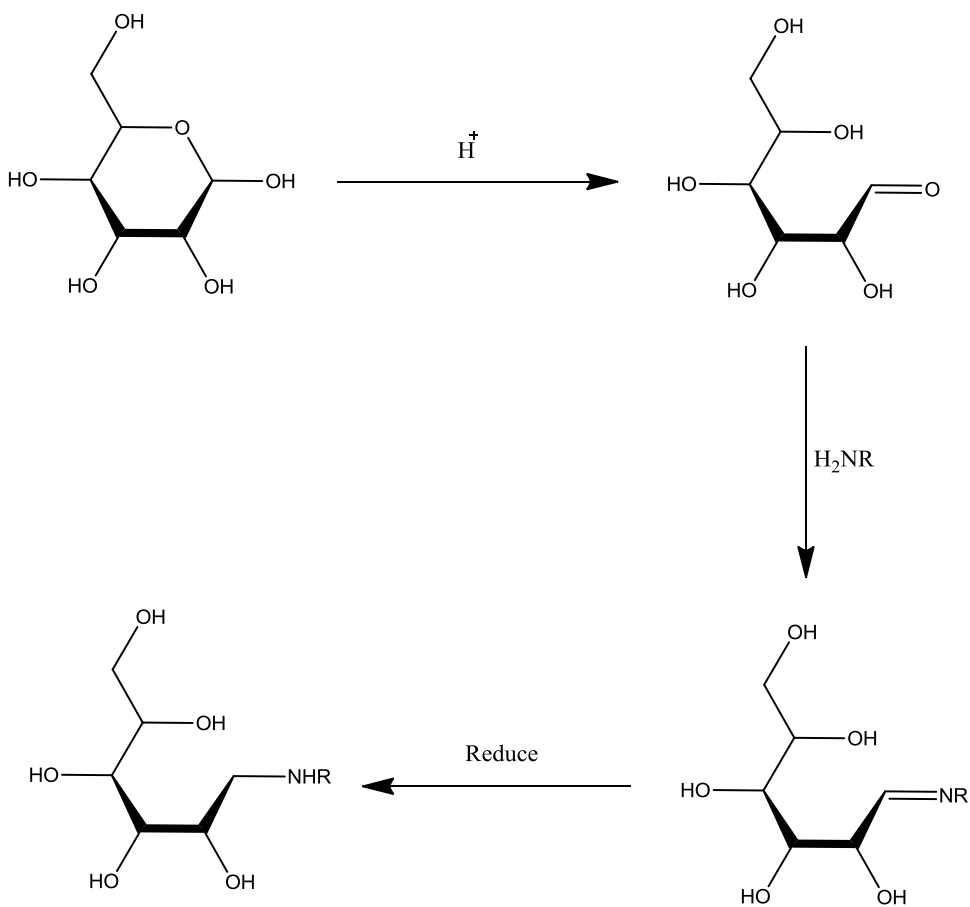


Figure 1.3 Derivatization of oligosaccharides by reductive amination.

Separation of glycans by liquid chromatography

The heterogeneity of glycosylation makes the glycan pools from biological sources the most complex and challenging samples. The structural diversity of oligosaccharides usually includes composition, sequence, anomeric character, linkage position, and branching pattern, resulting in different isomers. Numerous studies have demonstrated that structural configurations

of glycans are critical for their functional roles.⁴⁶⁻⁴⁸ While discrimination of glycans with different molecular masses can be easily achieved by MS techniques, the differentiation of various isomers is still problematic even with tandem MS. The separation of glycoforms prior to MS analysis offers great potential for individual structure characterization and quantitation. Moreover, the on-line separation of glycans can enhance MS detection due to chromatographic enrichment of low abundant glycoforms to yield optimum amounts and concentrations and reduce the ionization suppression of other components present. Hence, various types of separation techniques have been extensively investigated and the separation of glycans remains a very interesting field. Among those methods, reverse-phase (RP), porous graphitized carbon (PGC) and hydrophilic interaction chromatography (HILIC) have been mostly used for the separation of permethylated and fluorescently labeled glycans.

Reversed phase liquid chromatography (RPLC)

Due to the distinct advantages of permethylation in MS, such as remarkable increase of ionization efficiency and the potential of detailed structure characterization with tandem MS, it is reasonable to combine those merits with chromatographic separation of hydrophobic derivatives. Despite the hydrophilic nature of glycans, permethylation renders oligosaccharides more hydrophobic, enabling their retention and analysis in RP chromatography. Delaney and Vouros⁴⁹ were one of the first to explore the possibility of separating permethylated derivatives with a C18 (octadecyl silane-derivatized) column for oligosaccharides. More recently, Novotny and Mechref have investigated this method further by using chip-based RP microfluidic liquid chromatography of permethylated N-linked glycans for the discovery of a cancer-biomarker.⁵⁰ Furthermore, Mechref has transferred this separation strategy to comparative glycomic profiling of isotopically permethylated N-glycans using peak areas.⁵¹ Interestingly, Valmu and colleagues

have noticed that increase of column temperature improved the chromatographic resolution and increased retention time of permethylated oligosaccharides on C18 columns,⁵² which might be due to the hydrophobic nature of permethylated glycans and changes in the conformation of stationary phase as temperature increases.⁵³

Reduction of glycans is usually performed prior to permethylation to prevent anomerism (of α - and β -anomers).^{52,54} However, it increases sample handling and consequently sample loss during the preparation. Another disadvantage of permethylation is that glycans are no longer suitable for exoglycosidase studies after being permethylated. Due to the limiting factors of anomerism and enzyme accessibility of permethylated glycans, researchers also attempted to attach a chromophore or a fluorophore to hydrophilic glycans making the derivatives sufficiently amenable to RPLC.^{55,56} These derivatization approaches enable glycan analysis on the same LC-MS platform to be used for proteomic analyses, as well as benefit from all merits of RPLC. However, the choice of a particular tag to give sufficient retention on a RP column seems to result in resolving the glycans with similar structures, due to the fact that the tag-imparted hydrophobicity shifts the overall retention.

Porous graphitized carbon (PGC) liquid chromatography

PGC has arisen as a useful addition to the LC-based techniques due to its excellent separation of isomeric glycans.⁵⁷ Although the mechanism is not well understood, it is accepted that PGC stationary phases undergo “mixed-mode” interactions with oligosaccharides, involving hydrophobic and partitioning,⁵⁸ as well as ionic/adsorption.^{59,60} Thus, PGC has been applied for the separation of native glycans,⁶⁰ reduced glycans,⁶¹ labeled glycans,⁶² and permethylated glycans.⁵⁴ Within PGC, analyte interaction with the stationary phase is dependent upon the type

and positioning of functional groups, together with molecular contact with the planar graphite surface.

Many studies have repeatedly demonstrated the separation ability of PGC with glycans.⁵⁷ In particular, some of them focused on the studies of isomeric glycans as shown in the following examples. Kawasaki et al. successfully separated three Man5 isomers from RNase B in reduced form using PGC followed by characterization with tandem MS.⁶³ Costello et al. were able to differentiate permethylated Man7 isomers with PGC and tandem MS identification.⁵⁴ Moreover, separation of isomers with core/antenna fucosylation was achieved within the same method, combining the benefits of chromatographic separation and informative fragmentation of permethylated glycans to facilitate linkage, branch, and sequence assignment.⁵⁴

Although PGC exhibited remarkable separation power towards glycan isomers, problems with highly sialylated glycans permanently retained on PGC stationary phase were reported.⁵⁹ Nevertheless, the performance of PGC can be greatly influenced by the mobile phase pH, the ionic strength, and the column temperature, which makes it less reproducible and often leads to severe retention time shifts.⁵⁹ Furthermore, the “mix-mode” separation mechanism makes the retention less predictable.⁶⁴ Last but not least, although it has been used for decades, only limited improvements in the carbon stationary phases have been obtained, which hampers further development and applications for PGC.

Hydrophilic interaction liquid chromatography (HILIC)

HILIC was first introduced by Alpert in 1990⁶⁵ for the separation of peptides, nucleic acids, carbohydrates and other polar compounds. Although lacking a thorough theoretical explanation, it has been widely accepted that HILIC retention is primarily caused by the partitioning of analytes between the acetonitrile-rich mobile phase and a water-enriched layer

adsorbed onto the hydrophilic stationary phase⁶⁶ (**Figure 1.4**). In other words, the more hydrophilic the analyte, the more the partitioning equilibrium is shifted towards the immobilized water layer on the stationary phase increasing analyte retention. Due to the fact that HILIC allows the use of the hydrophilic nature of glycan molecules for selective solute-solvent interactions, it is not surprising that HILIC has gained such popularity in glycan separation.⁶⁷

For HILIC separation, acetonitrile (ACN) and water are the most favored mobile-phase components. Moreover, volatile additives such as ammonium acetate and ammonium formate (lower than 100 mM) are typically used to modify the mobile phase pH and ionic strength. However, unlike RPLC and PGC liquid chromatography, the designed stationary phases for HILIC separation have undergone an enormous evolution since its introduction, from underivatized silica to diol, amino, amide, zwitterionic sulfobetaine and other bonded phases.^{68,69} In theory, any polar chromatographic surface can be applied for HILIC separation.

More importantly, different types of separation materials have different retention characteristics and separation properties. Previous applications have already proved that HILIC provides separation abilities for isomeric glycans similar to PGC.⁶⁹⁻⁷¹ Further optimization of stationary phases and improvement in column technology will lead to additional separation possibilities for isomeric glycans.

Rudd et al. established a database approach called GlycoBase⁴³ (<http://glycobase.nibr.ie/>) for analysis of oligosaccharide structures based on 2-AB labeled glycans and HILIC separation. The verification of structural glycan identity was accomplished by serial exoglycosidase digestions. The retention of each individual glycan is referenced to the elution of an appropriately labeled glucose ladder (a mixture of oligosaccharides), wherein the glucose unit (GU) values are assigned to the corresponding chromatographic peaks. The availability of such a

database and online tools for matching of masses and retention times will be important in the development of reliable LC-MS methods for analysis of glycans from various biological sources. Alley et al. recommended the HILIC-based measurement techniques as reference methodology for the quantification of glycans in the biopharmaceutical industry.⁶⁷

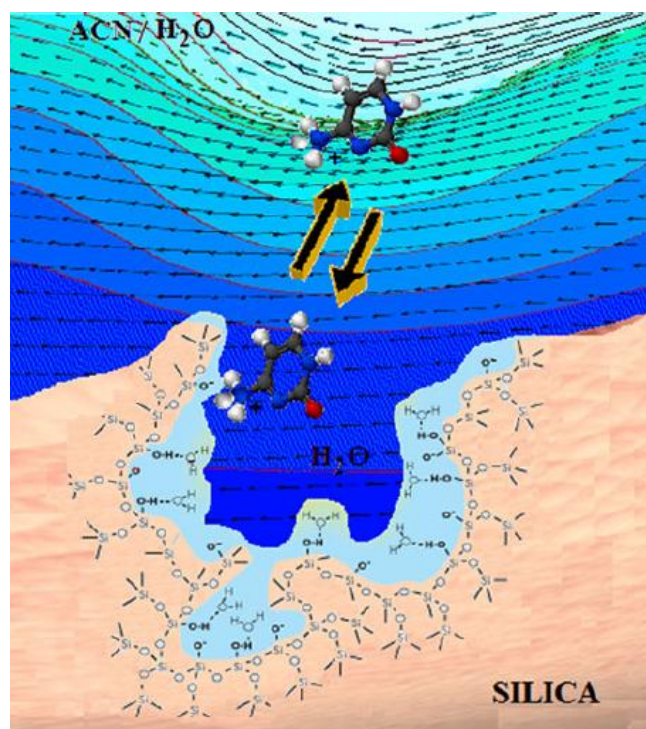


Figure 1.4 Schematic of the separation mechanism in a HILIC (Silica stationary phase) system.⁶⁸

Mass spectrometry

Mass spectrometry has been indispensable in proteomics and is extremely useful for glycomics as well, which can solve problems in both structural analysis and quantitative analysis.⁷² Nowadays, a wide range of mass spectrometers are available for users' choice based on their specific interest.⁷³ Typically, the majority of high-throughput glycomics analysis is

based on the tentative assignment of spectra on the basis of known biosynthetic pathways and expected glycan structures, which are often confirmed through secondary techniques such as exoglycosidase digestion and other techniques.⁷⁴ Moreover, MS-based glycomics also can provide comparative quantitation with the awareness of proper techniques.

Fourier Transform Cyclotron Resonance (FT-ICR) Mass Spectrometry

Although structural glycan analysis is challenging due to their non-linear nature and the branching and linkage possibilities, the number of compositions of N-glycans is limited based on what is observed in nature. Accurate masses obtained from a high resolving power mass spectrometer can rapidly provide glycan composition such as the number of Hex, HexNAc, NeuAc, and dHex (fucose) even in complicated mixtures,⁷⁵ followed by the validation of these assignments with tandem MS. FT-ICR mass spectrometers satisfy these requirements, providing high mass measurement accuracy (MMA <5 ppm) and high resolving power (RP=100, 000 at $m/z=400$).⁷⁶ Resolving power is the ability of the mass spectrometer to separate ions with similar m/z , and in FT-ICR mass spectrometers it is proportional to the amount of time the analytes are measured. MMA is the measure of how accurately a mass spectrometer can measure masses. FT-ICR mass spectrometers are capable of acquiring accurate mass by taking advantage of the m/z dependence of a gas phase ion in a magnetic field.⁷⁷

The FT-ICR mass analyzer cell (ICR cell) is located in the center of a superconductive magnet, which provides homogeneous magnetic field strengths of 3.0 T (Tesla) up to 21.0 T (Bruker, 2010). Once the ions are introduced into the ICR cell, they are exposed to the magnetic field and forced into their cyclotron motion due to the Lorentz force.⁷⁸ With the applying of an RF voltage to the two excitation plates, the ions are excited in order to increase the radius of cyclotron motion. This will cause phase coherence of ions with the same m/z , and as the ion

packet passes the detection plates, a current is generated, which is then measured over a given time period, producing a sinusoidal time domain. The time domain is a combination of signals of different ion packets that must be de-convoluted by performing a Fourier transform into a frequency spectrum, which can be subsequently converted into a mass spectrum⁷⁹ (**Figure 1.5**). In an FT-ICR, the resolving power is proportional to the magnetic field strength (B_0) and the time of acquisition⁸⁰, as shown in the following equation:

$$\text{Resolving Power} = \frac{m}{\Delta m} = \frac{1.274 \times 10^7 B_0 T_{acq} r_n}{m/z}$$

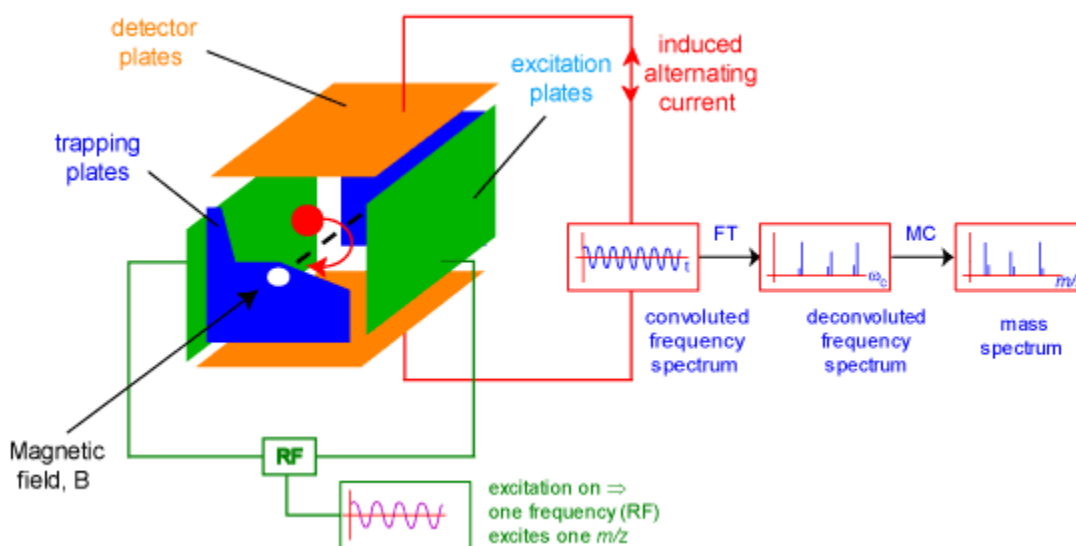
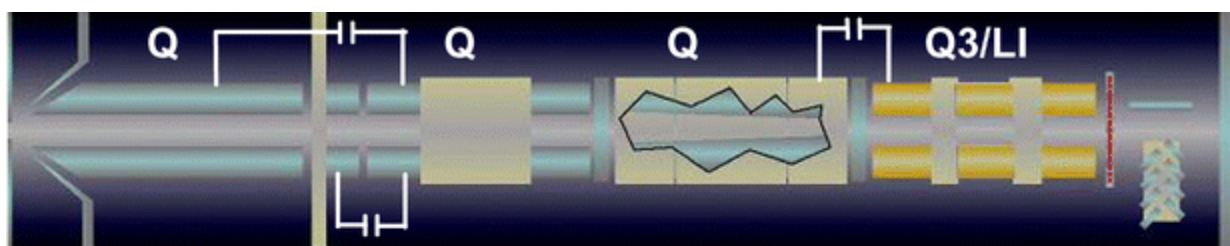


Figure 1.5 Schematic of FT-ICR-MS showing the ion trapping, detection and signal generation.⁸¹

Q-Trap Mass Spectrometry

Linear ion traps (LITs) have been widely used as stand-alone mass spectrometers with MS capabilities or ion accumulation devices coupled with other mass detectors, such as Fourier

transform ion cyclotron resonance (FT-ICR), time-of-flight (TOF) and quadrupole (Q). The combination of triple quadrupole MS and LIT technology in the form of an instrument configuration QqLIT, known as Q-Trap (AB Sciex), is particularly interesting due to its various operation modes. As the system is based on a triple quadrupole platform where Q3 can be operated either in the normal RF/DC mode or in the LIT mode,⁸² it retains the classical triple quadrupole scan functions such as selected reaction monitoring (SRM), neutral loss (NL), and precursor ion scan while also providing access to sensitive ion trap experiments⁸³ (**Figure 1.6**).



Mode of operation	Q1	Q2	Q3
Q1 Scan	Resolving (Scan)	RF-only	RF-only
Q3 Scan	RF-only	RF-only	Resolving (Scan)
Product Ion Scan (PI)	Resolving (Fixed)	Fragment	Resolving (Scan)
Precursor Ion Scan (PC)	Resolving (Scan)	Fragment	Resolving (Fixed)
Neutral Loss Scan (NL)	Resolving (Scan)	Fragment	Resolving (Scan Offset)
Selected Reaction Monitoring mode (SRM)	Resolving (Fixed)	Fragment	Resolving (Fixed)
Enhanced Q3 Single MS (EMS)	RF-only	No fragment	Trap/Scan
Enhanced Product Ion (EPI)	Resolving (Fixed)	Fragment	Trap/Scan
MS ³	Resolving (Fixed)	Fragment	Isolation/fragment trap/scan
Time Delayed fragmentation (TDF)	Resolving (Fixed)	Trap/No fragment	Fragment/trap/Scan
Enhanced Resolution Q3 Single MS (ER)	RF-only	No fragment	Trap/Scan
Enhanced Multiply Charged (EMC)	RF-only	No fragment	Trap/Scan

Figure 1.6. Schematic diagram of the Q-Trap (AB SCIEX) and description of the different triple-quadrupole and trap operation modes.⁸³

Selected reaction monitoring (SRM), also called multiple reaction monitoring (MRM), emerged as a principle technique that allows detection and quantitation of analytes with excellent specificity and sensitivity in complex mixtures.⁸⁴ In an SRM experiment, the Q1 and Q3 analyzers are used as static mass filters, to monitor a selected precursor ion which generates a particular fragment ion, whereas Q2 serves as a collision cell. This specific pair of m/z values associated with the precursor and fragment ions selected is referred to as a “transition”. Multiple transitions can be monitored over time, yielding a set of chromatographic traces with the retention time and signal intensity for a specific transition. The simultaneous detection of precursor and fragment ions ensures the specificity of the analytes while co-eluting interferences are filtered out very effectively. Also, the non-scanning nature of this operation mode gives an increased sensitivity by one or two orders of magnitude compared with conventional “full scan” techniques. Moreover, it results in a linear response over a wide dynamic range up to five orders of magnitude, which can be crucial for quantitative studies with low abundant analytes in highly complex mixtures.

Extensive panels with up to a few hundred SRM transitions are used routinely in many laboratories. In SRM mode, the instrument repeatedly cycles through a list of transitions spending a defined time, the dwell time, on each transition. Hence, the number of transitions measured per cycle and the dwell time are mutually dependent on a fixed cycle time. Higher dwell times give better signal-to-noise.⁸⁵ However, the cycle time is constrained by the peak width in order to get enough data points (>8) across the chromatographic peak. A successful approach to increase the number of transitions without sacrificing the dwell time for each transition is to restrict the acquisition of particular transitions to a window around the elution time of the corresponding transition by scheduling the experiment, such as the scheduled SRM.

In these experiments, each transition is acquired only during a time window around its expected elution time, which can be derived from previous experiments or predicted. Therefore, a much higher number of transitions (5~20 folds)⁸⁶ can be monitored within a single LC-MS experiment.

Overall, selectivity, sensitivity, dynamic range and adaptation to the sample complexity make SRM technique a promising candidate for quantitative glycomics.

Quantitative glycomics

The correlation between protein glycosylation and many biological processes and diseases has increased the demand of reliable and sensitive monitoring of the changes in structure and abundance of glycans.⁸⁷ MS-based techniques have been widely used for quantitative proteomics,⁸⁸ and many of them have been successfully adapted for glycomic analysis.⁸⁹

Label-free approaches

The general workflow for glycomics involves glycan release from samples, derivatization and detection by MALDI/ESI-MS. In mass spectrometric quantitation methods, it is usually assumed that the measured signal has a linear response to the amount of material in the sample for the entire range of amounts being studied. The label-free approaches enables facile and efficient profiling of glycans from any sample since there is no need for additional steps for sample preparation.⁹⁰ However, it is also well-known that those methods suffer from limited normalization ability for the compensation of instrument variability, matrix effect, and ionization efficiency for different analytes. Under such circumstances, internal standards are applied to reduce the run to run variances for relative quantitation, and incorporation of stable isotope labels seems to be the most popular strategy in the field.

Stable isotope labeling approaches

Many of the stable isotopic labeling of glycans can be accomplished through derivatization. Alvarez-Manilla et al. developed the tools for relative quantitation of glycans by isotopic permethylation using $^{12}\text{CH}_3\text{I}$ or $^{13}\text{CH}_3\text{I}$.⁹¹ Similarly, Orlando and colleagues introduced QUIBL (quantization by isobaric labeling) as another isotopic permethylation approach that utilizes $^{13}\text{CH}_3\text{I}$ and $^{12}\text{CH}_2\text{DI}$ so that the two species can be differentiated by high resolution MS (typically over 25,000 $\Delta\text{M}/\text{M}$) such as FT-ICR.⁹² A potential issue unique to the permethylation labeling approaches is that large errors can be introduced by small variation in labeling efficiency due to the large number of labeling sites. For instance, a 0.1% change in the labeling efficiency would result in 5% error when it comes to the glycan with 50 sites of permethylation.⁹³

On the other hand, isotopic labeling introduced onto the reducing end can effectively avoid this issue through reductive amination. Hayakawa and coworkers introduced the method for quantitative analysis of carbohydrate by using isotope tag of tetradeuterium-labeled (d4-PA) and d0-PA.⁹⁴ Similarly, both (d4) 2-AA⁹⁵ and 2- $^{13}\text{C}_6$ -AA reagents are available for relative quantitation. Furthermore, Zaia et al. described a series of synthesized tags (+0, +4, +8, +12)⁹⁶ for the direct comparison of multiple samples simultaneously in mass spectrometric glycomics.⁹⁷ Although reductive amination is effective, additional steps for purification are necessary to remove excess reaction reagents, which may introduce differential sample loss and give extra error for quantitation. Hence, new labeling reagents with ^{13}C isotopes were investigated for quantitative analysis of glycan hydrazones by Muddiman.⁹⁸ When using hydrazone formation, the product can be directly applied for MS analysis due to the lack of salts necessary in the reaction mixture.

It has been well noticed that for relative quantitation, the earlier in the work flow that the stable isotope label is introduced and the samples mixed, the better the chance to minimize the contribution of handling and work-up to overall variability. For this purpose, Yang et al. introduced the ^{18}O labeling into N-glycan reducing end by endoglycosidase release in ^{18}O -water,⁹⁹ which was known as “GREOL” for relative glycan quantitation.

In proteomics field, the *in vivo* labeling strategy “SILAC” is considered as a golden standard for relative quantitation,¹⁰⁰ since metabolic labeling provides the earliest possible introduction of stable isotope labels into the sample. Analogously, Orlando and colleagues provided the method of metabolic implementation of stable isotope labels into glycans through the hexosamine biosynthetic pathway, by employing amide- ^{15}N -Gln media to culture cells.¹⁰¹ An advantage of this method is that the “light” and “heavy” cells are mixed together immediately after cell harvest, thereby both cells are subjected to identical handling, digestion, purification and preparation steps. This strategy can be potentially applied for quantitative comparison of glycans expressed in organisms or cells subjected to different biological conditions.

LC-MS based techniques

Currently, MALDI- and ESI-MS have been effectively used in the quantitation of glycans derived from glycoconjugates. When the measurement is acquired from mass spectra, it is common that glycans are not observed as a single peak in mass spectrometry, but as a cluster of peaks, because of the presence of small amounts of stable heavy isotopes in nature (e.g., 1.11% ^{13}C). Notably, with the mixing of stable isotope labeled species, overlapping of isotopic patterns can be observed if the labeling does not give sufficient mass shift from the unlabeled analyte.^{99,101} Hence, a deconvolution strategy is needed for data processing and accurate

quantitative analysis. In addition, the MS only approaches are not sufficient to distinguish different isomers, thus efforts in tandem MS is often implemented.⁹¹

LC-MS has recently been considered as a choice for high throughput glycomic analysis due to the development of various separation techniques, especially for the separation of glycan isomers. With LC-MS, the quantity of glycans is measured by calculating the height or the area of the corresponding peaks in the ion chromatograms. The advantage of using the height of the peak as the measure of quantity is the simplicity and robustness of determination. The peak height is a good measure of quantity if the peak width does not vary between samples, and if the signal is strong with little noise. In contrast, the peak area is a better measurement when there is substantial noise because many more data points are used, but it is much more sensitive to interference from other peaks.¹⁰² It is worth noting that some of the isotope labeling may give some retention shift from their non-labeled counterparts, such as in case of deuterium.⁹⁴ This situation may not be ideal for quantitation due to the change of mobile phase composition. An alternative for this could be using ¹³C labeling instead.¹⁰³

Important study objects

Human serum

In the past decade, the understanding of the importance of glycosylation changed with evolved diseases.^{104,105} Earlier studies have aimed to monitor altered glycosylation pattern of a specific glycoprotein for diagnostic fingerprint. However, it has been difficult to correlate disease progression with particular glycoproteins of interest due to the dynamic nature of this post-translational modification and its pleiotropic regulation.¹⁰⁶ Hence, a comprehensive investigation of the glycan change in a tissue or body fluid may be more informative than

characterizing glycans on individual glycoproteins. In particular, human serum contains hundreds individual glycoproteins secreted by or leaking from different body tissues making it a great candidate for biomarker discovery.¹⁰⁷

Previous studies of the serum glycosylation patterns revealed that changes of glycans can be associated with age,¹⁰⁸ sex,¹⁰⁹ pregnancy and various diseases¹¹⁰⁻¹¹² including liver, pancreatic, prostate, ovarian, breast, lung and stomach cancers. Thus, global glycomics of whole human serum glycoproteins can lead to the identification of disease-related glycosylation changes that represent potentially useful biomarkers for the early diagnosis, monitoring, and treatment of common diseases. Driven by such facts, many groups have been put great efforts into the investigation of this subject. Recent advances include improvement of protocols for liberating N-glycans from serum glycoproteins,¹¹³ development of retrosynthetic glycan libraries to profile and classify the human serum N-glycans,¹¹⁴ and annotation of a serum N-glycan library for rapid identification of structures.¹¹⁵ Future studies of human serum glycomics demand for the development of high-throughput LC-MS approaches for large scale sample analysis, which can provide thorough information of the glycan changes, structurally and quantitatively. The sensitivity, reproducibility, reliability and robustness of those methods are essential in order to yield diagnostically or prognostically useful information with glycomic profiling of small aliquots of blood serum.¹¹⁶

Monoclonal antibody

Monoclonal antibodies (mAbs) are widely used as diagnostic and research reagents as well as in human therapy. MAbs are glycoproteins belonging to the immunoglobulin (Ig) superfamily including IgG, IgM, IgA, IgE, and IgD, which are secreted by B cells to identify and neutralize foreign organisms or antigens.¹¹⁷ The global market for therapeutic mAbs was about

\$44.6 billion in 2011, and it is expected to exceed \$58 billion in 2016 in anticipation of the rollout of at least eight new therapeutic mAb products during the forecast period.

As of today's market, there are over 20 FDA approved antibody therapeutics which are of the IgG subclasses (IgG1, IgG2, IgG3 and IgG4),¹¹⁸ containing structurally and/or functionally distinct domains. Among those four subclasses, IgG1 is often the preferred isotype due to its ability to elicit effector function and high intrinsic stability.¹¹⁹ From a structural standpoint, IgGs are tetrameric glycoproteins with molecular weights about 150 kDa, which are composed of two light heavy chains (near 50 kDa) and two light chains (near 25 kDa). N-glycosylation usually occurs on ASN-297 in the fragment crystallizable (Fc) part on each of the heavy chains (**Figure 1.7**), which are asymmetrical and may even result in hemiglycosylated IgG, i.e., antibodies with one glycosylated heavy chain and another unglycosylated.¹¹⁷

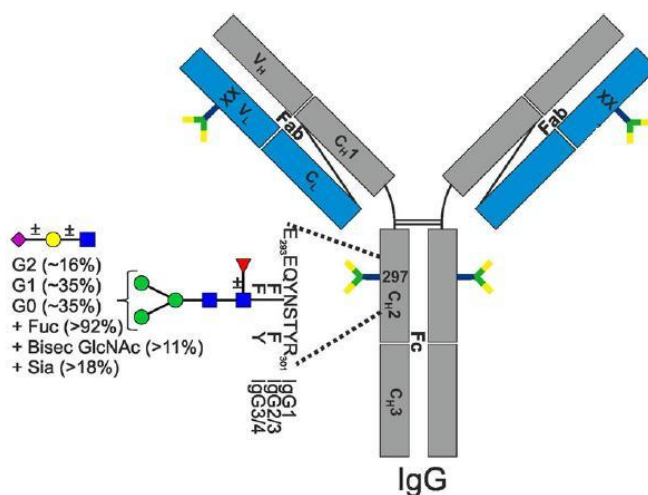


Figure 1.7 Glycosylation of IgG.

The heterogeneity of IgG glycosylation can be caused by different host cell lines, growth and expression conditions, and media compositions.¹²⁰ Although glycans only represent an average of 2~3% of the total antibody mass, many studies have shown that variations of

glycosylation of the Fc domain also influence effector function of the mAbs therapeutic products.¹²¹⁻¹²³ Hence, the monitoring of IgG glycosylation is not only necessary for the quality control,^{67,116,124} but also able to offer opportunities for Fc engineering and mAb optimization, leading to clinical benefits for patients.

Glycosylation analysis of IgGs has been carried out with (i) intact glycoprotein, (ii) enzymatically digested glycopeptides, and (iii) chemically or enzymatically released glycans based LC-MS techniques.¹²⁵⁻¹²⁷ Analysis at the glycopeptides level is the most favorable approach due to the conservation of site heterogeneity of glycosylation. However, the analysis on the released glycan level is currently the most adopted approach for obtaining sensitive and comprehensive glycosylation information from complex biological samples.¹²⁸ Although glycosylation analysis of IgGs has been extensively studied for decades, most of the previous studies are focused on structural characterization rather than quantitation.¹¹⁷ Therefore, there is still a demand for fast and reliable quantitative approaches with chromatographic separation of all the isomeric glycoforms from IgGs.

Synopsis of completed research

Quantitative analysis of N-linked glycans is often hindered by the lack of consistent strategies across laboratories, the heterogeneity of N-glycan structures, the lack of appropriate internal standards, and high-throughput quantitative approaches. This dissertation describes the development of novel strategies for quantitative analysis of N-glycans, which can be easily incorporated to the general glycomics workflow.

Chapter 2 describes in detail an isotopic labeling method using ¹⁸O-water during the enzymatic release of N-glycans from the peptide backbone by PNGase F for relative

quantitation. For PNGase F deglycosylation, the C-N bond of glycosylated asparagine side chain is cleaved and a β -glycosylamine is formed initially. The β -glycosylamine is not stable and spontaneously hydrolyzes to a hydroxyl. Thus, the ^{18}O labeling can be incorporated onto the reducing end of the released N-glycans using ^{18}O -water without altering the analysis procedure. With the analysis of N-glycans from Fetuin, it is shown that the labeling efficiency is above 95% by using ^{18}O -water (97 atom %) and the ^{18}O labeled reducing terminus are stable during following sample preparation and derivatization, such as permethylation. The incorporation of ^{18}O labeling only gives a 2 Da mass shift in MS. Therefore, some of the isotopic peaks from the unlabeled species and the ^{18}O -labeled species will overlap with each other. Accordingly, an in-house developed mathematic approach is used to facilitate the relative quantitation by high-resolution FT-ICR MS detection. This method can improve quantitation accuracy by eliminating the difference in permethylation efficiency when samples are treated separately in a parallel manner, since the labeling is achieved prior to the permethylation step.

The ^{18}O labeling method provides an alternative for relative quantitation of N-glycans. However, the challenge exists in the lack of effective separation techniques to differentiate isomeric glycoforms after permethylation. Quantitation of these individual glycans is important because changes in the abundance of these isomers are often associated with significant biomedical events. For instance, previous studies have shown that the altered ratio of α 2-3 to α 2-6 linked sialic acid (SA) plays an important role in cancer biology, yet traditional glycomic profiling cannot readily distinguish those linkage isomers. In **Chapter 3**, we present an LC-SRM approach that is capable of quantitating the individual SA linkage isomers. N-glycan derivatization is conducted by reductive amination with applying the newly reported labeling reagent ProA, which can enhance the MS detection compared to 2-AB. With optimization, the

LC method is able to separate sialylated N-glycan isomers differing in α 2-3 and α 2-6 linkages using a novel superficially porous particle (Fused-Core™) Penta-HILIC column. SRM detection by a Q-Trap MS detector provides the relative quantitation of each sialic acid linkage isomers, and minimizes interferences from the co-eluting glycans that are problematic for UV/Fluorescence based quantitation. With this approach, the relative quantitation of each sialic acid linkage isomer is obtained from a straightforward LC-MS experiment.

The developed LC-SRM method in **Chapter 3** is capable of quantitating the relative ratio of each SA linkage isomers within a given composition. However, it also reveals that the MS response changes with the composition of the glycan. The SILAC approach has been considered as the “gold standard” for comparative quantitative proteomic analysis, not only because it compensates the MS detection variability, but also it eliminates the inconsistency during the sample handling, digestion, purification and separation steps. In this note, an *in vivo* labeling strategy for glycomics studies has been reported as IDAWG, which is analogous to the SILAC approach used for proteomics. The utility of the IDAWG technology has been demonstrated by the analysis of N-glycans released from proteins of murine embryonic stem cells grown in both the presence of light and amide-¹⁵N-Glutamine (Gln). **Chapter 4** describes relative quantitation of human IgG N-glycans using ¹⁵N-labeled mAb reference by LC-SRM. Notably, ¹⁵N-labeled mAb are harvested from cell culture production and purified by protein G affinity chromatography. To serve as internal standards, equal amounts of the ¹⁵N-labeled mAb reference is spiked into the human serum samples so that the heavy and light species are mixed together; thereby both samples are subjected to the exact sample experimental conditions during the IgG extraction, N-glycan release, derivatization and clean-up steps. It is notable that for relative glycomics, a glycoprotein internal standard is advantageous in comparison to a free glycan

because any variability in the PNGase F cleavage reaction cannot be taken into account using a free oligosaccharide. Moreover, the glycoprotein can be subjected to the protein G affinity chromatography which allows for variability in every step of sample preparation to be accounted for.

It has been widely accepted that the use of isotopically labeled internal standards remains the best solution for quantitative analysis as these standards ideally match the chemical behavior of their analytes, both in chromatography and mass spectrometry. However, it is extremely difficult to generate a universal internal standard pool for all the glycans due to their complexity. For instance, the ^{15}N -labeled mAb present a smaller variety of N-glycans compared to the human serum IgGs. Therefore, quantitative analysis was performed using a single labeled N-glycan as a reference standard for all the other measured glycans without their heavily labeled counterparts in **Chapter 4**. The results reveal that the quantitation accuracy by using a single labeled reference is comparable to the relative quantitation of light-heavy pairs of each structure, which gives the confidence of quantitative analysis of complex glycomic samples.

The development of glycomics increasingly requires high through-put and consistent detection and quantitation of glycans from complex sample pools, which is only partially achieved by current glycomics approaches. Considering the glycan biosynthetic pathway, a glycome is composed of limited number of glycan structures due to the availability of glycotransferases and the restriction of glycosylation machinery, which makes it possible to build a set of database for all the analytes of interest. Taking advantage of SRM to enhance both sensitivity and selectivity, and predictable retention times by HILIC separation according to “-OH” numbers, **Chapter 5** describes the development of a targeted glycomic approach by scheduled SRM coupled with HILIC separation for highly sensitive and consistent identification

and quantitation of diverse glycans from various biological samples. In this proof-of-principle study, it adopts a highly curated structural database for N-glycans from the Complex Carbohydrate Research Center (CCRC), and the retention time model is built according to the “-OH” groups for each given glycan composition and/or structure. The capability of this strategy to identify diverse glycans is demonstrated by detection of 115 different glycans and isomers from human serum sample. With the application of a single internal standard for samples, the maximum error observed is under 20% (with 109 out of 115 glycans) for relative quantitation with a dynamic range over 5 orders of magnitude.

The **Appendices** contain supplemental material, where numerous details, calculations, analysis processes, and data tables are presented. **Appendices A-D** contain supporting information for **Chapters 2, 3, 4** and **5**, respectively.

References

- (1) Zaia, J. *Chem Biol* **2008**, *15*, 881.
- (2) Varki, A. *Cell* **2006**, *126*, 841.
- (3) Alvarez-Manilla, G.; Warren, N. L.; Atwood, J., 3rd; Orlando, R.; Dalton, S.; Pierce, M. *J Proteome Res* **2010**, *9*, 2062.
- (4) Freeze, H. H.; Schachter, H. **2009**.
- (5) Schachter, H.; Freeze, H. H. *Biochim Biophys Acta* **2009**, *1792*, 925.
- (6) Hart, G. W.; Copeland, R. J. *Cell* **2010**, *143*, 672.
- (7) Marino, K.; Bones, J.; Kattla, J. J.; Rudd, P. M. *Nature Chemical Biology* **2010**, *6*, 713.
- (8) Pabst, M.; Altmann, F. *Proteomics* **2011**, *11*, 631.

- (9) Matsui, T.; Takita, E.; Sato, T.; Kinjo, S.; Aizawa, M.; Sugiura, Y.; Hamabata, T.; Sawada, K.; Kato, K. *Glycobiology* **2011**, *21*, 994.
- (10) Harvey, D. J. *Proteomics* **2005**, *5*, 1774.
- (11) Tretter, V.; Altmann, F.; Marz, L. *European Journal of Biochemistry* **1991**, *199*, 647.
- (12) Ruhaak, L. R.; Zauner, G.; Huhn, C.; Bruggink, C.; Deelder, A. M.; Wuhler, M. *Anal Bioanal Chem* **2010**, *397*, 3457.
- (13) *Essentials of Glycobiology*; 2nd ed.; Varki, A.; Cummings, R.; Esko, J., Eds.; Cold Spring Harbor Laboratory Press, 2009.
- (14) Ciucanu, I.; Costello, C. E. *J Am Chem Soc* **2003**, *125*, 16213.
- (15) Harkomori, S. *J Biochem* **1964**, *55*, 205.
- (16) Ciucanu, I.; Kerek, F. *Carbohydr Res* **1984**, *131*, 209.
- (17) Gunnarsson, A. *Glycoconjugate J* **1987**, *4*, 239.
- (18) Kang, P.; Mechref, Y.; Klouckova, I.; Novotny, M. V. *Rapid Commun Mass Spectrom* **2005**, *19*, 3421.
- (19) Wilm, M. *Mol Cell Proteomics* **2011**, *10*, M111 009407.
- (20) Zaia, J. *Mass Spectrom Rev* **2004**, *23*, 161.
- (21) Walker, S. H.; Lilley, L. M.; Enamorado, M. F.; Comins, D. L.; Muddiman, D. C. *J Am Soc Mass Spectrom* **2011**, *22*, 1309.
- (22) Mechref, Y.; Kang, P.; Novotny, M. V. *Rapid Commun Mass Spectrom* **2006**, *20*, 1381.
- (23) Reinhold, V. N.; Reinhold, B. B.; Costello, C. E. *Anal Chem* **1995**, *67*, 1772.
- (24) Reinhold, V. N.; Sheeley, D. M. *Anal Biochem* **1998**, *259*, 28.
- (25) Sheeley, D. M.; Reinhold, V. N. *Anal Chem* **1998**, *70*, 3053.
- (26) Viseux, N.; de Hoffmann, E.; Domon, B. *Anal Chem* **1998**, *70*, 4951.

- (27) Weiskopf, A. S.; Vouros, P.; Harvey, D. J. *Anal Chem* **1998**, *70*, 4441.
- (28) Varki, A. *Glycobiology* **1992**, *2*, 25.
- (29) Anumula, K. R. *Anal Biochem* **2006**, *350*, 1.
- (30) Harvey, D. J. *J Chromatogr B Analyt Technol Biomed Life Sci* **2011**, *879*, 1196.
- (31) Lamari, F. N.; Kuhn, R.; Karamanos, N. K. *J Chromatogr B Analyt Technol Biomed Life Sci* **2003**, *793*, 15.
- (32) Yoshino, K.; Takao, T.; Murata, H.; Shimonishi, Y. *Anal Chem* **1995**, *67*, 4028.
- (33) Lattova, E.; Snovida, S.; Perreault, H.; Krokhin, O. *J Am Soc Mass Spectrom* **2005**, *16*, 683.
- (34) Bigge, J. C.; Patel, T. P.; Bruce, J. A.; Goulding, P. N.; Charles, S. M.; Parekh, R. B. *Anal Biochem* **1995**, *230*, 229.
- (35) Prater, B. D.; Anumula, K. R.; Hutchins, J. T. *Anal Biochem* **2007**, *369*, 202.
- (36) Hase, S.; Ikenaka, T.; Matsushima, Y. *Biochem Biophys Res Commun* **1978**, *85*, 257.
- (37) Klein, A.; Lebreton, A.; Lemoine, J.; Perini, J. M.; Roussel, P.; Michalski, J. C. *Clin Chem* **1998**, *44*, 2422.
- (38) Evangelista, R. A.; Guttman, A.; Chen, F. T. *Electrophoresis* **1996**, *17*, 347.
- (39) Sigma-Aldrich 2013; Available from: <http://www.sigmaaldrich.com/life-science/proteomics/post-translational-analysis/glycosylation/glycoprofile-labeling-kits-for-glycan-analysis.html>.
- (40) Ludger 2013; Available from: <http://www.selectscience.net/product-news/New-LudgerTag%E2%84%A2-2AB-and-2AA-Glycan-Labeling-Kits-with-Non-Toxic-Reductant/?&artID=26997>.
- (41) Prozyme 1998; Available from: <http://www.prozyme.com/documents/gkk-404.pdf>.

- (42) Royle, L.; Campbell, M. P.; Radcliffe, C. M.; White, D. M.; Harvey, D. J.; Abrahams, J. L.; Kim, Y. G.; Henry, G. W.; Shadick, N. A.; Weinblatt, M. E.; Lee, D. M.; Rudd, P. M.; Dwek, R. A. *Anal Biochem* **2008**, *376*, 1.
- (43) Campbell, M. P.; Royle, L.; Radcliffe, C. M.; Dwek, R. A.; Rudd, P. M. *Bioinformatics* **2008**, *24*, 1214.
- (44) Waters. Available from:
http://www.waters.com/waters/promotionDetail.htm?id=134654015&locale=en_US.
- (45) Klapoetke, S.; Zhang, J.; Becht, S.; Gu, X.; Ding, X. *J Pharm Biomed Anal* **2010**, *53*, 315.
- (46) Dwek, R. A. *Chem Rev* **1996**, *96*, 683.
- (47) Dwek, R. A.; Edge, C. J.; Harvey, D. J.; Wormald, M. R.; Parekh, R. B. *Annu Rev Biochem* **1993**, *62*, 65.
- (48) Hua, S.; An, H. J.; Ozcan, S.; Ro, G. S.; Soares, S.; DeVere-White, R.; Lebrilla, C. B. *Analyst* **2011**, *136*, 3663.
- (49) Delaney, J.; Vouros, P. *Rapid Commun Mass Spectrom* **2001**, *15*, 325.
- (50) Alley, W. R., Jr.; Madera, M.; Mechref, Y.; Novotny, M. V. *Anal Chem* **2010**, *82*, 5095.
- (51) Hu, Y.; Desantos-Garcia, J. L.; Mechref, Y. *Rapid Commun Mass Spectrom* **2013**, *27*, 865.
- (52) Ritamo, I.; Rabina, J.; Natunen, S.; Valmu, L. *Anal Bioanal Chem* **2013**, *405*, 2469.
- (53) Doyle, C. A.; Vickers, T. J.; Mann, C. K.; Dorsey, J. G. *J Chromatogr A* **2000**, *877*, 41.
- (54) Costello, C. E.; Contado-Miller, J. M.; Cipollo, J. F. *J Am Soc Mass Spectrom* **2007**, *18*, 1799.
- (55) Walker, S. H.; Carlisle, B. C.; Muddiman, D. C. *Anal Chem* **2012**, *84*, 8198.

- (56) Hase, S. *Methods Mol Biol* **1993**, *14*, 69.
- (57) Ruhaak, L. R.; Deelder, A. M.; Wuhrer, M. *Anal Bioanal Chem* **2009**, *394*, 163.
- (58) Fan, J. Q.; Kondo, A.; Kato, I.; Lee, Y. C. *Anal Biochem* **1994**, *219*, 224.
- (59) Pabst, M.; Altmann, F. *Anal Chem* **2008**, *80*, 7534.
- (60) Packer, N. H.; Lawson, M. A.; Jardine, D. R.; Redmond, J. W. *Glycoconj J* **1998**, *15*, 737.
- (61) Wilson, N. L.; Robinson, L. J.; Donnet, A.; Bovetto, L.; Packer, N. H.; Karlsson, N. G. *J Proteome Res* **2008**, *7*, 3687.
- (62) Broberg, A. *Carbohydr Res* **2007**, *342*, 1462.
- (63) Kawasaki, N.; Ohta, M.; Hyuga, S.; Hashimoto, O.; Hayakawa, T. *Anal Biochem* **1999**, *269*, 297.
- (64) Mauko, L.; Lacher, N. A.; Pelzing, M.; Nordborg, A.; Haddad, P. R.; Hilder, E. F. *J Chromatogr B Analyt Technol Biomed Life Sci* **2012**, *911*, 93.
- (65) Alpert, A. J. *J Chromatogr* **1990**, *499*, 177.
- (66) Hemstrom, P.; Irgum, K. *J Sep Sci* **2006**, *29*, 1784.
- (67) Alley, W. R., Jr.; Mann, B. F.; Novotny, M. V. *Chem Rev* **2013**, *113*, 2668.
- (68) Buszewski, B.; Noga, S. *Anal Bioanal Chem* **2012**, *402*, 231.
- (69) Zauner, G.; Deelder, A. M.; Wuhrer, M. *Electrophoresis* **2011**, *32*, 3456.
- (70) Thomsson, K. A.; Karlsson, N. G.; Hansson, G. C. *J Chromatogr A* **1999**, *854*, 131.
- (71) Wuhrer, M.; de Boer, A. R.; Deelder, A. M. *Mass Spectrom Rev* **2009**, *28*, 192.
- (72) Wuhrer, M. *Glycoconj J* **2013**, *30*, 11.
- (73) Zaia, J. *OMICS* **2010**, *14*, 401.
- (74) Rakus, J. F.; Mahal, L. K. *Annu Rev Anal Chem (Palo Alto Calif)* **2011**, *4*, 367.

- (75) Chu, C. S.; Ninonuevo, M. R.; Clowers, B. H.; Perkins, P. D.; An, H. J.; Yin, H.; Killeen, K.; Miyamoto, S.; Grimm, R.; Lebrilla, C. B. *Proteomics* **2009**, *9*, 1939.
- (76) Xian, F.; Hendrickson, C. L.; Marshall, A. G. *Anal Chem* **2012**, *84*, 708.
- (77) Marshall, A. G.; Hendrickson, C. L. *Annu Rev Anal Chem (Palo Alto Calif)* **2008**, *1*, 579.
- (78) Marshall, A. G.; Hendrickson, C. L.; Jackson, G. S. *Mass Spectrom Rev* **1998**, *17*, 1.
- (79) Comisarow, M. B.; Marshall, A. G. *Chem Phys Lett* **1974**, *25*, 282.
- (80) Scigelova, M.; Hornshaw, M.; Giannakopoulos, A.; Makarov, A. *Mol Cell Proteomics* **2011**, *10*, M111 009431.
- (81) Bristol, U.; Available from: <http://www.chm.bris.ac.uk/ms/images/>.
- (82) Hager, J. W. *Rapid Commun Mass Sp* **2002**, *16*, 512.
- (83) Hopfgartner, G.; Varesio, E.; Tschoppat, V.; Grivet, C.; Bourgoigne, E.; Leuthold, L. A. *J Mass Spectrom* **2004**, *39*, 845.
- (84) Lange, V.; Picotti, P.; Domon, B.; Aebersold, R. *Mol Syst Biol* **2008**, *4*.
- (85) Pace, N.; Schreiber, A.; Available from: <http://www.absciex.com/Documents/Downloads/Literature/mass-spectrometry-Multiple-Reaction-1282310.pdf>.
- (86) Stahl-Zeng, J.; Lange, V.; Ossola, R.; Eckhardt, K.; Krek, W.; Aebersold, R.; Domon, B. *Molecular & Cellular Proteomics* **2007**, *6*, 1809.
- (87) Mechref, Y.; Hu, Y.; Desantos-Garcia, J. L.; Hussein, A.; Tang, H. *Mol Cell Proteomics* **2013**.
- (88) Bantscheff, M.; Lemeer, S.; Savitski, M. M.; Kuster, B. *Anal Bioanal Chem* **2012**, *404*, 939.
- (89) Orlando, R. *Methods Mol Biol* **2013**, *951*, 197.

- (90) Wada, Y. *Methods Mol Biol* **2013**, 951, 245.
- (91) Alvarez-Manilla, G.; Warren, N. L.; Abney, T.; Atwood, J., 3rd; Azadi, P.; York, W. S.; Pierce, M.; Orlando, R. *Glycobiology* **2007**, 17, 677.
- (92) Atwood, J. A., 3rd; Cheng, L.; Alvarez-Manilla, G.; Warren, N. L.; York, W. S.; Orlando, R. *J Proteome Res* **2008**, 7, 367.
- (93) Orlando, R. *Methods Mol Biol* **2010**, 600, 31.
- (94) Yuan, J.; Hashii, N.; Kawasaki, N.; Itoh, S.; Kawanishi, T.; Hayakawa, T. *J Chromatogr A* **2005**, 1067, 145.
- (95) Hitchcock, A. M.; Yates, K. E.; Shortkroff, S.; Costello, C. E.; Zaia, J. *Glycobiology* **2007**, 17, 25.
- (96) Bowman, M. J.; Zaia, J. *Anal Chem* **2007**, 79, 5777.
- (97) Bowman, M. J.; Zaia, J. *Anal Chem* **2010**, 82, 3023.
- (98) Walker, S. H.; Budhathoki-Uprety, J.; Novak, B. M.; Muddiman, D. C. *Anal Chem* **2011**, 83, 6738.
- (99) Zhang, W.; Wang, H.; Tang, H.; Yang, P. *Anal Chem* **2011**, 83, 4975.
- (100) Ong, S. E.; Foster, L. J.; Mann, M. *Methods* **2003**, 29, 124.
- (101) Orlando, R.; Lim, J. M.; Atwood, J. A., 3rd; Angel, P. M.; Fang, M.; Aoki, K.; Alvarez-Manilla, G.; Moremen, K. W.; York, W. S.; Tiemeyer, M.; Pierce, M.; Dalton, S.; Wells, L. *J Proteome Res* **2009**, 8, 3816.
- (102) Zhang, G.; Ueberheide, B. M.; Waldemarson, S.; Myung, S.; Molloy, K.; Eriksson, J.; Chait, B. T.; Neubert, T. A.; Fenyo, D. *Methods Mol Biol* **2010**, 673, 211.
- (103) Xia, B.; Feasley, C. L.; Sachdev, G. P.; Smith, D. F.; Cummings, R. D. *Anal Biochem* **2009**, 387, 162.

- (104) Adamczyk, B.; Tharmalingam, T.; Rudd, P. M. *Biochim Biophys Acta* **2012**, *1820*, 1347.
- (105) Lebrilla, C. B.; An, H. J. *Mol Biosyst* **2009**, *5*, 17.
- (106) Bosques, C. J.; Raguram, S.; Sasisekharan, R. *Nat Biotechnol* **2006**, *24*, 1100.
- (107) Klein, A. *Adv Clin Chem* **2008**, *46*, 51.
- (108) Vanhooren, V.; Dewaele, S.; Libert, C.; Engelborghs, S.; De Deyn, P. P.; Toussaint, O.; Debacq-Chainiaux, F.; Poulain, M.; Glupczynski, Y.; Franceschi, C.; Jaspers, K.; van der Pluijm, I.; Hoeijmakers, J.; Chen, C. C. *Exp Gerontol* **2010**, *45*, 738.
- (109) Ding, N.; Nie, H.; Sun, X.; Sun, W.; Qu, Y.; Liu, X.; Yao, Y.; Liang, X.; Chen, C. C.; Li, Y. *Age Ageing* **2011**, *40*, 568.
- (110) Kirmiz, C.; Li, B.; An, H. J.; Clowers, B. H.; Chew, H. K.; Lam, K. S.; Ferrige, A.; Alecio, R.; Borowsky, A. D.; Sulaimon, S.; Lebrilla, C. B.; Miyamoto, S. *Mol Cell Proteomics* **2007**, *6*, 43.
- (111) Tessitore, A.; Gaggiano, A.; Ciccirelli, G.; Verzella, D.; Capece, D.; Fischietti, M.; Zazzeroni, F.; Alesse, E. *Int J Proteomics* **2013**, *2013*, 125858.
- (112) Ruhaak, L. R.; Miyamoto, S.; Lebrilla, C. B. *Mol Cell Proteomics* **2013**, *12*, 846.
- (113) Kita, Y.; Miura, Y.; Furukawa, J.; Nakano, M.; Shinohara, Y.; Ohno, M.; Takimoto, A.; Nishimura, S. *Mol Cell Proteomics* **2007**, *6*, 1437.
- (114) Kronewitter, S. R.; An, H. J.; de Leoz, M. L.; Lebrilla, C. B.; Miyamoto, S.; Leiserowitz, G. S. *Proteomics* **2009**, *9*, 2986.
- (115) Aldredge, D.; An, H. J.; Tang, N.; Waddell, K.; Lebrilla, C. B. *J Proteome Res* **2012**, *11*, 1958.
- (116) Novotny, M. V.; Alley, W. R., Jr. *Curr Opin Chem Biol* **2013**.

- (117) Zauner, G.; Selman, M. H.; Bondt, A.; Rombouts, Y.; Blank, D.; Deelder, A. M.; Wuhrer, M. *Mol Cell Proteomics* **2013**, *12*, 856.
- (118) Patel, R.; Johnson, K.; Andrien, B.; Tamburini, P. *American Journal of Biochemistry and Biotechnology* **2013**, *9*, 206.
- (119) Buss, N. A.; Henderson, S. J.; McFarlane, M.; Shenton, J. M.; de Haan, L. *Curr Opin Pharmacol* **2012**, *12*, 615.
- (120) Jang, K.-S.; Kim, Y.-G.; Gil, G.-C.; Park, S.-H.; Kim, B.-G. *Analytical biochemistry* **2009**, *386*, 228.
- (121) Abes, R.; Teillaud, J. *Pharmaceuticals* **2010**, *3*, 146.
- (122) Strohl, W. R. *Curr Opin Biotechnol* **2009**, *20*, 685.
- (123) Chan, A. C.; Carter, P. J. *Nat Rev Immunol* **2010**, *10*, 301.
- (124) Alley, W. R., Jr.; Novotny, M. V. *Annu Rev Anal Chem (Palo Alto Calif)* **2013**, *6*, 237.
- (125) Huhn, C.; Selman, M. H.; Ruhaak, L. R.; Deelder, A. M.; Wuhrer, M. *Proteomics* **2009**, *9*, 882.
- (126) Dalpathado, D. S.; Desaire, H. *Analyst* **2008**, *133*, 731.
- (127) Morelle, W.; Michalski, J. C. *Nat Protoc* **2007**, *2*, 1585.
- (128) Kolarich, D.; Jensen, P. H.; Altmann, F.; Packer, N. H. *Nat Protoc* **2012**, *7*, 1285.

CHAPTER 2

A NOVEL METHOD FOR RELATIVE QUANTITATION OF N-GLYCANS BY ISOTOPIC LABELING USING ^{18}O -WATER ¹

¹ Tao, S. and Orlando, R. To be submitted to *Journal of Biomolecular Techniques*.

Abstract

Quantitation is an essential aspect of comprehensive glycomics study. Here, a novel isotopic labeling method is described for N-glycan quantitation using ^{18}O -water. The incorporation of the ^{18}O labeling to the reducing end of N-glycans can be simply and efficiently achieved during PNGase F release. This process gives a mass difference of 2 Da from the N-glycans released in regular ^{16}O -water. The sample analysis was carried out on a Fourier transform ion cyclotron resonance (FT-ICR) mass spectrometer in selected ion monitoring (SIM) mode. Also, a new mathematical calculation method was developed to determine the $^{18}\text{O}/^{16}\text{O}$ ratios from isotopic peaks. Application of this method to several standard glycoproteins and human serum demonstrated that this method can facilitate the relative quantitation of N-glycans over a linear dynamic range of two orders, with high accuracy and reproducibility.

Introduction

Glycosylation, a ubiquitous post-translational modification (PTM), can significantly affect numerous biological processes, such as protein stability and activity, recognition by antibodies, susceptibility to proteases, and binding specificity.¹ Previous studies indicate that changes in glycosylation are associated with many common human health issues, including cancer, inflammation, neurodegenerative disease, and congenital disorder of glycosylation (CDG).² In order to identify disease-related glycosylation changes and discover potentially useful biomarkers³ for diagnostic and prognostic processes, many researchers have devoted great effort to glycosylation characterization. In recent decades, the study of glycomics has undergone a rapid development as a result of advances in analytical techniques. Particularly, mass

spectrometry (MS) has become a highly informative analytical tool to provide structure and quantitative measures for glycomics due to its high sensitivity, resolution and mass accuracy.⁴⁻⁶

For glycan characterization with MS, permethylation of released oligosaccharide is one of the most prevalent sample derivatizations, since it offers significant benefits for both structural and quantitative analysis. Permethylation converts all of the highly polar -OH, -COOH and NH- groups into non-polar derivatives. This change in polarity enables both acidic and neutral structures to be analyzed in positive-ion mode while also stabilizing the sialic acid residues and leads to more uniform ionization.⁷ Permethylated glycans also have more predictable fragmentation patterns in MS/MS.⁸

Furthermore, permethylation can also introduce various stable isotopic labeling approaches with different methylation reagents for quantitative glycomics, such as $^{12}\text{CH}_3\text{I}/^{13}\text{CH}_3\text{I}$, $^{13}\text{CH}_3\text{I}/^{12}\text{CH}_2\text{DI}$, etc. Alvarez-Manilla *et al.* reported the $^{12}\text{CH}_3\text{I}/^{13}\text{CH}_3\text{I}$ labeling method for relative quantitation of glycans with a coefficient of variation that was 13% on average.⁹ However, this approach may not be appropriate for extremely complex samples since it increases the spectral complexity due to the various methylation sites.¹⁰ Recently, Orlando *et al.* developed a quantitation method by isobaric labeling (QUIBL), which generates isobaric pairs of permethylated glycans with $^{13}\text{CH}_3\text{I}/^{12}\text{CH}_2\text{DI}$.¹⁰ Since the mass difference between those isobaric pairs is so small that it can only be differentiated at high resolution, QUIBL can successfully achieve relative quantitation without causing any difficulty to match the heavy/light pairs. Moreover, it enables the relative quantitation of individual glycans in isomeric mixtures. However, when it comes to application, as with other labeling methods utilizing permethylation, there are several potential issues generated during permethylation which may cause inaccurate quantitation. Namely, samples treated separately may have different yield. Another issue to

permethylation is that large errors can be introduced by a small variation in labeling efficiency, due to the large number of methylation sites of each glycan.¹¹ To overcome those limitations, an *in vivo* labeling method for glycomics called Isotopic Detection of Amino sugars With Glutamine (IDAWG).¹² However, the limitation of this *in vivo* labeling strategy is that it can be only applied to cells grown in culture.

As a common stable isotope, ¹⁸O has been widely used for different applications. In proteomics, ¹⁸O stable isotope labeling can be used for relative quantitation with mass spectrometers.^{13,14} In glycoproteomics, ¹⁸O labeling is usually applied for identification of the N-glycosylation sites on the protein.¹⁵ Also, ¹⁸O labeling is involved in oligosaccharide structural analysis to determine the reducing end.^{16,17}

Here, we have devised a simple isotope labeling procedure to incorporate ¹⁸O labeling into the reducing end of N-glycans during PNGase F release, which gives 2 Da mass shift for the heavily labeled species and can be utilized for N-glycan relative quantification without altering the sample workflow.

Experimental Section

Materials. Bovine fetuin (F) and human serum were purchased from Sigma-Aldrich. ¹⁸O-water (97 atom %) was purchased from Sigma-Aldrich. Trypsin (TPCK treated) was purchased from Sigma-Aldrich. PNGase F (Glycerol free) was purchased from New England Biolabs (NEB). Iodomethane (CH₃I, reagent plus grade) was purchased from Sigma. C18-Sep-Pak columns were purchased from J. T. Baker. All other chemicals were of analytical grade.

Protein digestion. Fetuin (200 µg) was dissolved in 200 µL 50mM Ammonium Bicarbonate (AmBic) and human serum (200 µL aliquot) was mixed with 200 µL AmBic, then

both samples were heated at 100 °C for 5 minutes to denature the proteins. After cooling to room temperature, samples were digested at 37 °C for 16~18 hours with an appropriate amount of Trypsin (50 µg Trypsin for 1 mg glycoprotein sample).

N-glycan release and ¹⁸O labeling. Each of the samples were divided into two equal aliquots then dried using a speed-vac centrifuge. One aliquot was re-dissolved in 100 µL H₂¹⁸O, and the other aliquot was re-dissolved in 100 µL H₂¹⁶O. Equal amounts of PNGase F were added into both aliquots (PNGase F from NEB was dried up and then re-dissolved in either H₂¹⁸O or H₂¹⁶O before use and 20 IUB milliunits of PNGase F for 1 mg glycoprotein). The release of N-glycans was carried out at 37 °C for 16~18 hours.

N-glycan isolation and ¹⁸O/¹⁶O-labeling N-glycan mixture preparation. N-glycans were separated from peptides by reverse-phase liquid chromatography. Each of the PNGase F digested samples were loaded onto a C18-Sep-Pak column, which had been pre-equilibrated in 5% acetic acid, and the N-glycans were eluted from the column with 4 mL 5% acetic acid. The following ¹⁸O-labeled/¹⁶O N-glycan mixtures at various ratios of 10:1, 5:1, 3:1, 1:1, 1:3, 1:5, 1:10 were prepared for N-glycans from the fetuin samples. For N-glycans from the human serum samples, ¹⁸O-labeled/¹⁶O N-glycans were mixed at a ratio of 1:1. The solutions of mixture were immediately frozen with dry ice and acetone and lyophilized to dryness.

¹⁸O-labeled/¹⁶O N-glycan mixture permethylation. The N-glycan permethylation for each mixture was performed as described previously.⁹ Briefly, each of the dried N-glycan mixtures was stirred to dissolve in 200 µL DMSO, then 200 µL freshly prepared base (200 mg NaOH in 1 mL dry DMSO) and 150 µL dry CH₃I was added. After stirring vigorously for 10 min followed by sonicating for another 10 min, the methylation reaction was stopped by adding

2 mL H₂O. The permethylated N-glycan mixtures were then extracted with dichloromethane and dried under N₂ gas.

Permethylated sample clean-up. The permethylated N-glycan mixtures were cleaned by reverse-phase chromatography. Each sample was dissolved in 200 µL 50% methanol and loaded onto a C18-Sep-Pak column which had been washed with 3 mL methanol and pre-equilibrated in 5% acetic acid. After washing 5 times with Nanopure H₂O, the permethylated N-glycans were eluted with 2 mL 85% acetonitrile and dried under N₂ gas.

MS analysis of the permethylated ¹⁸O/¹⁶O-labeling N-glycan mixture. The cleaned sample mixtures were dissolved in 100 µL 50% methanol in 1 mM NaOH and analyzed independently, in triplicate. The MS analysis was carried out on a hybrid linear ion trap Fourier transform ion cyclotron resonance (FT-ICR) mass spectrometer (LTQ-FT, Thermo Scientific) by direct infusion. Each glycan mixture was infused into the LTQ-FT at a flow rate of 1 µL/min. For relative quantitation of interested N-glycans, the MS scan was performed in Selected Ion Monitoring (SIM) mode by FT-ICR mass spectrometer. In SIM mode, each individual glycan was monitored at its monoisotopic peak with an isolation width of 10 m/z at 100,000 resolution.

The overall experimental procedure is shown in **Figure 2.1**.

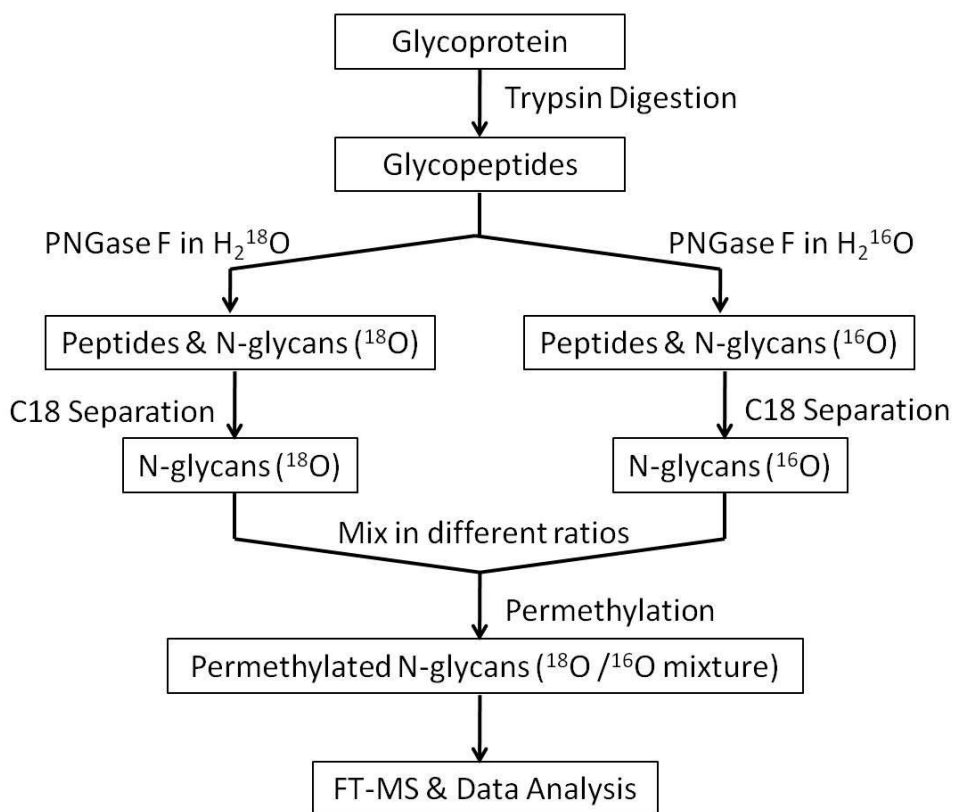


Figure 2.1. Workflow for relative quantitation of N-glycans using ^{18}O labeling. N-glycans released in ^{18}O -water gives ^{18}O labeling on the reducing end. Sample mixtures are made before permethylation derivatization.

Results and Discussions

^{18}O incorporation during PNGase F deglycosylation. PNGase F ((peptide-N4-(N-acetyl- β -glucosaminyl) asparagine amidase F) is an amidase that cleaves the glycan-asparagine amino bond of glycosylated asparagines side chain, which gives the intact release of N-glycans and deglycosylated peptides. During this process, the asparagine residue is converted to aspartic acid, while the N-glycans are released as β -glycosylamine initially. Under the enzymatic deglycosylation condition (pH=7), the β -glycosylamine is spontaneously hydrolyzed to a

hydroxyl and ammonia is liberated.¹⁸ Thus, the ¹⁸O-labeling can be incorporated to the reducing end of the released N-glycans during hydrolysis (**Figure 2.2**).

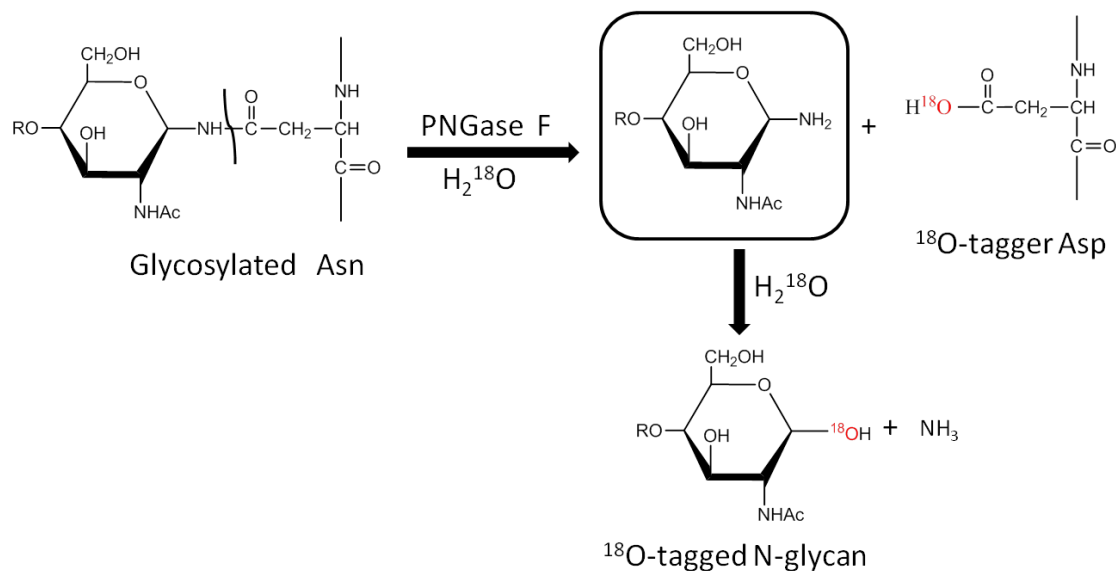


Figure 2.2. ^{18}O incorporation during PNGase F deglycosylation. The C-N bond of glycosylated asparagine side chain is cleaved and a β -glycosylamine is formed initially. The β -glycosylamine is not stable and spontaneously hydrolyzes to a hydroxyl with ^{18}O .

Calculation of $^{18}\text{O}/^{16}\text{O}$ ratio. Water- ^{18}O (97 atom %) was used to introduce the ^{18}O labeling onto the reducing end of the release N-glycans for relative quantification. For N-glycan separation, regular H_2O was applied to elute N-glycans from the C18-Sep-Pak column, which may cause the loss of ^{18}O labeling during mutarotation (ring opening and closing).¹⁹

The incorporation of ^{18}O labeling gives a 2 Da mass shift in MS (**Figure 2.3A, B**), which causes some of the isotopic peaks from the unlabeled species to overlap with peaks from the ^{18}O -labeled species. For calculation of the under-labeling ratio (UL), the percentage (p) of the first

two isotopic peaks divided by the summed intensity of all the isotopic peak distribution of the regular ^{16}O -N-glycan was determined.

$$p = \frac{R1+R2}{\sum_{i=1}^n Ri} \quad \text{(Equation 2.1)}$$

$$UL = \frac{(U1+U2)/p}{\sum_{i=1}^n Ui + \sum_{i=1}^n Li} \quad \text{(Equation 2.2)}$$

Here, p is the percentage of the summed intensity of the first two isotopic peaks divided by the summed intensity of all the isotopic peaks; Ri is the intensity of the i th isotopic peak of the regular ^{16}O -N-glycan; Ui is the intensity of the i th isotopic peak of under-labeling N-glycans; Li is the intensity of the i th isotopic peak of ^{18}O -labeled N-glycans; UL is the under-labeling ratio.

For the ^{16}O and ^{18}O mixture,

$$\begin{cases} X + Y = \sum_{i=1}^n Mi \\ X + Y * UL = (M1 + M2)/p \end{cases}$$

So,
$$Y/X = \frac{\sum_{i=1}^n Mi - (M1+M2)/p}{(M1+M2)/p - \sum_{i=1}^n Mi * UL} \quad \text{(Equation 2.3)}$$

Here, X stands for the signal intensity of the ^{16}O -N-glycan; Y stands for the signal intensity of the ^{18}O -N-glycan; Mi is the relative intensity of the i th peak from the ^{16}O and ^{18}O N-glycan mixture; Y/X is the ratio of $^{18}\text{O}/^{16}\text{O}$.

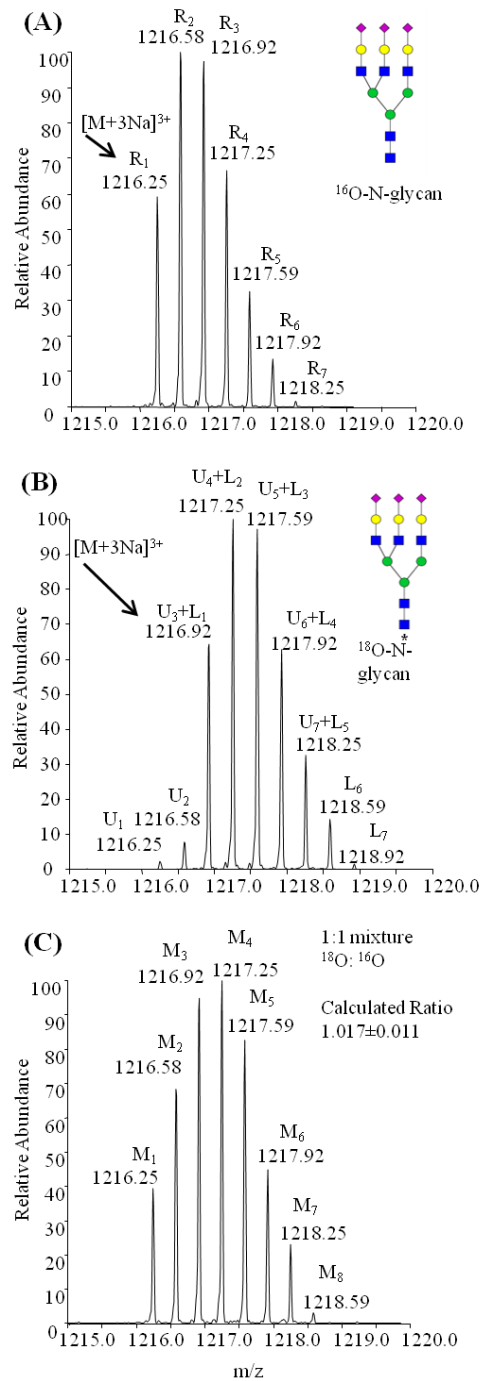


Figure 2.3. FT-ICR spectra of permethylated triantennary glycans from fetuin in SIM mode. (A) Regular ^{16}O -N-glycan; (B) ^{18}O -labeled N-glycan; (C) 1:1 mixture of regular ^{16}O -N-glycan and ^{18}O -labeled N-glycan.

Standard N-glycan analysis using ^{18}O labeling. To demonstrate the ^{18}O labeling method for relative quantitation, including the under-labeling ratio and the mathematical calculation of $^{18}\text{O}/^{16}\text{O}$ ratio, one of the triantennary glycans from fetuin was examined at the sample ratio of 1:1. The FT-ICR spectra are shown in **Figures 2.3A** and **Figure 2.3B**, for a regular ^{16}O -N-glycan and an ^{18}O -labeling N-glycan, respectively. With the mathematical calculation method described above, the under-labeling ratio (UL) was 0.056 (Example for mathematical calculation of $^{18}\text{O}/^{16}\text{O}$ ratio, **Appendix A**). The average ratio obtained by applying this method to a standard 1:1 mixture was 1.017 ± 0.011 for the triantennary fetuin glycans.

To evaluate the linearity of response obtained by the ^{18}O labeling method, seven standard mixtures were prepared by combining fetuin glycans of $^{18}\text{O}/^{16}\text{O}$ ratios at 10:1, 5:1, 3:1, 1:1, 1:3, 1:5, 1:10 (**Figure S2.1, Appendix A**). For the most abundant peaks from fetuin sample, the maximum error was below 15%. Specifically, when the sample mixture ratio was 1:1, the maximum error was below 8% for all the analyzed N-glycans from fetuin, which showed the remarkable quantitation accuracy as an isotopic labeling method. However, the standard deviations and errors became larger as the ratio increased to 10:1 or decreased to 1:10 due to the bias of measuring of the ^{16}O peaks from the under labeling ^{18}O labeled N-glycans based on the MS spectra. The linearity of response was evaluated with seven peaks from fetuin (**Figure 2.4A**). All seven peaks were measured at each $^{18}\text{O}/^{16}\text{O}$ ratio, separately. The average of those seven peaks at each ratio was calculated and compared to the theoretical ratio to generate linearity determination (**Figure 2.4B**).

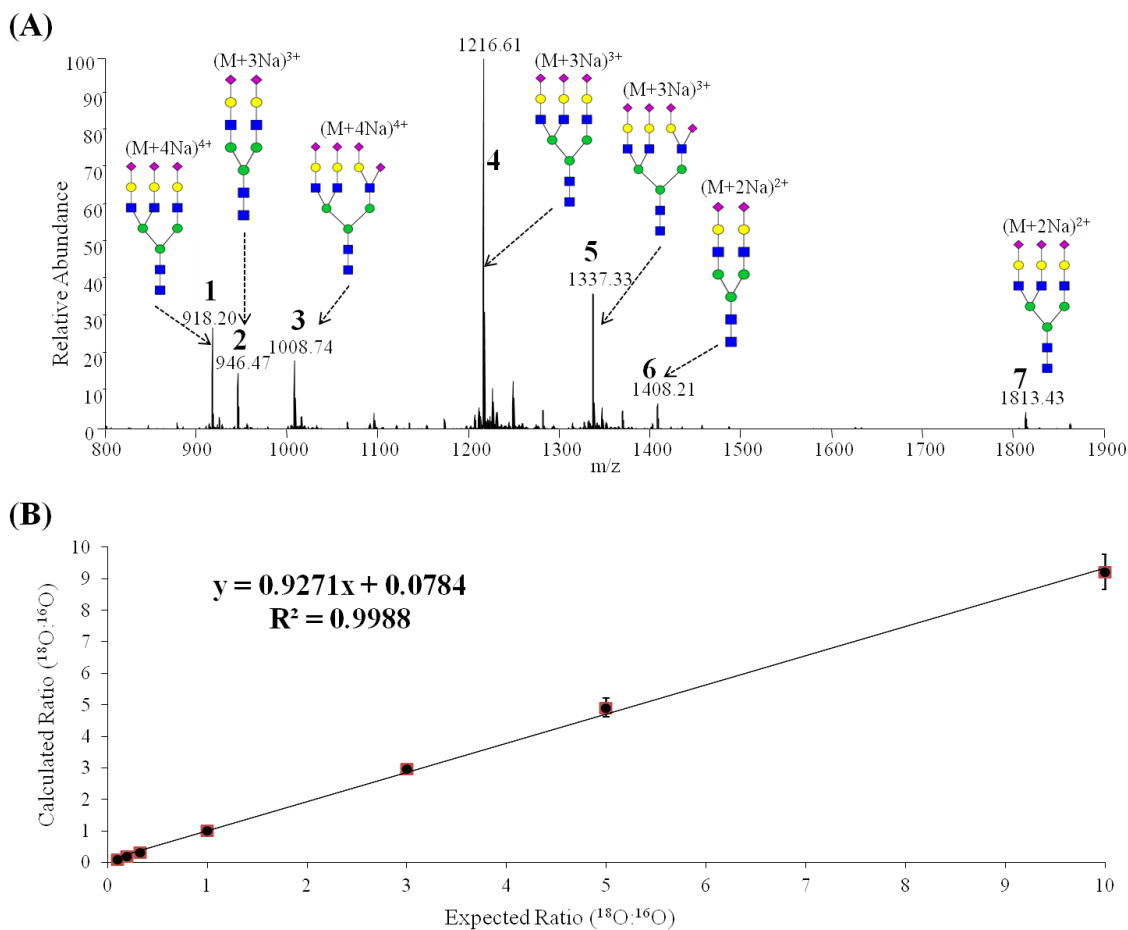


Figure 2.4. Dynamic range determination with fetuin N-glycans. (A) Full MS spectrum of ^{16}O -N-glycans; (B) For each ratio, seven N-glycan peaks were measured individually and averaged to give the calculated ratio. The error bar represents the standard deviation among those seven N-glycan peaks. A plot of the expected ratio to that obtained experimentally yielded a straight line ($R^2=0.9988$) was observed with the comparison of the calculated $^{18}O/^{16}O$ ratios with their expected ratios.

Selected Ion Monitoring (SIM) mode for quantitation. SIM is a mass spectrometry scanning mode in which only a limited mass-to-charge ratio range is transmitted/detected by the instrument, as opposed to the full spectrum range. This mode of operation typically results in

significantly increased sensitivity. For relative quantitation, data were acquired in two different modes: Full MS scan mode with mass range of 500-2000 m/z at 100,000 resolution; and SIM mode of monoisotopic peak of analyte with an isolation width of 10 m/z at 100,000 resolution. **Figure 2.5A** shows the zoom-in spectrum of full MS scan for the triantennary N-glycan from fetuin with ^{18}O labeling. **Figure 2.5B** shows the spectrum of SIM scan for the same N-glycan. Obviously, the background noise (indicated in ellipse in **Figure 2.5A**) was decreased with the SIM scan mode (**Figure 2.5B**). The background noise might cause an overestimation of the under-labeling ratio (UL); therefore leading to errors in the $^{18}\text{O}/^{16}\text{O}$ ratios. For example, the UL calculated with the full MS scan mode was 0.083 (**Figure 2.5A**), which gave a $^{18}\text{O}/^{16}\text{O}$ ratio of 1.145 (14.5% error) for a 1:1 sample mixture. The UL calculated for the same glycan with the SIM mode was 0.056, which gave $^{18}\text{O}/^{16}\text{O}$ ratio of 1.012 (1.2% error) for the same sample mixture. For a 1:10 sample mixture, the background in full MS scan mode led to an error of 13.19 (31.9%). However, the maximum error was below 15% over a linear dynamic range of two orders of magnitude when it was operated in SIM mode. Therefore, data acquisition in the SIM mode works better for relative quantitation on the LTQ-FT mass spectrometer.

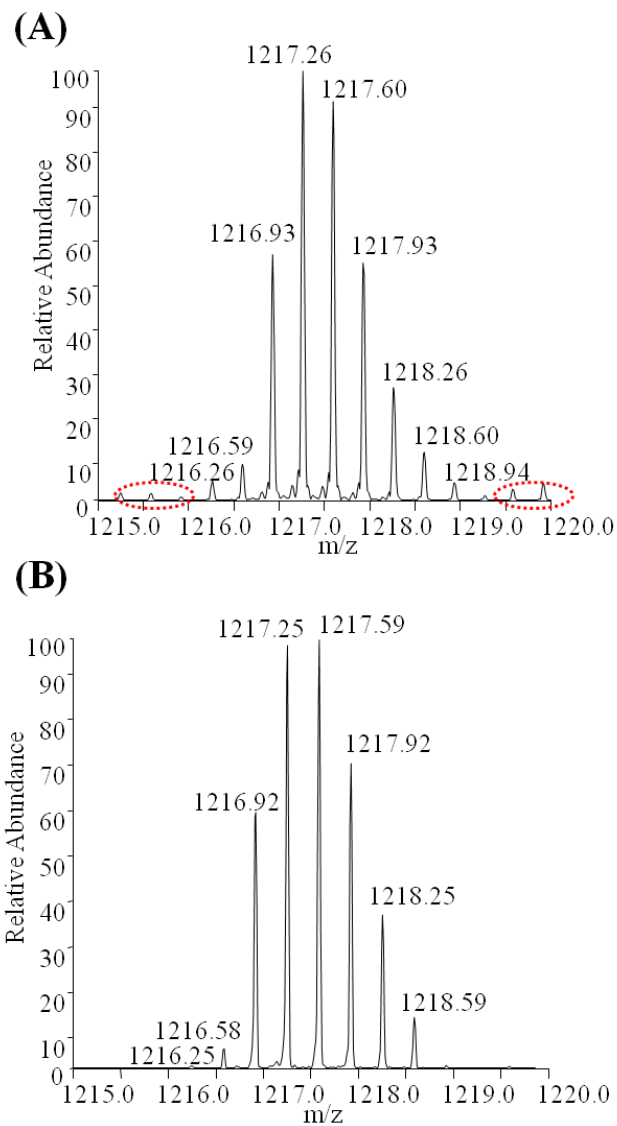


Figure 2.5. Comparison of quantitation in full MS scan mode and SIM mode. (A) Zoom-in spectrum of triantennary ¹⁸O-labeled N-glycan within full MS scan; **(B)** Triantennary ¹⁸O-labeled N-glycan in SIM mode.

^{18}O -labeling application to human serum N-glycans. Studies have shown that human serum N-glycome profiling is widely investigated as a potential biomarker for human diseases²⁰⁻²² and the quantitative assay of comparing the profile of disease and control cases could be crucial for diagnosis.²³ Here, we evaluated the ^{18}O labeling scheme for relative quantitation with N-glycans from human serum. Specifically, the ^{16}O -N-glycans released by PNGase F in regular H_2O and ^{18}O -labeled N-glycans released by PNGase F in ^{18}O - H_2O from the same amount of human serum sample were well mixed to give a theoretical ratio of 1:1. Then the mixture was derivatized by permethylation and then analyzed by an FT-ICR mass spectrometer in triplicate. The full MS spectrum acquired from the mixture of ^{16}O -N-glycans and ^{18}O -labeled N-glycans from human serum at 1:1 ratio is shown in **Figure 2.6**.

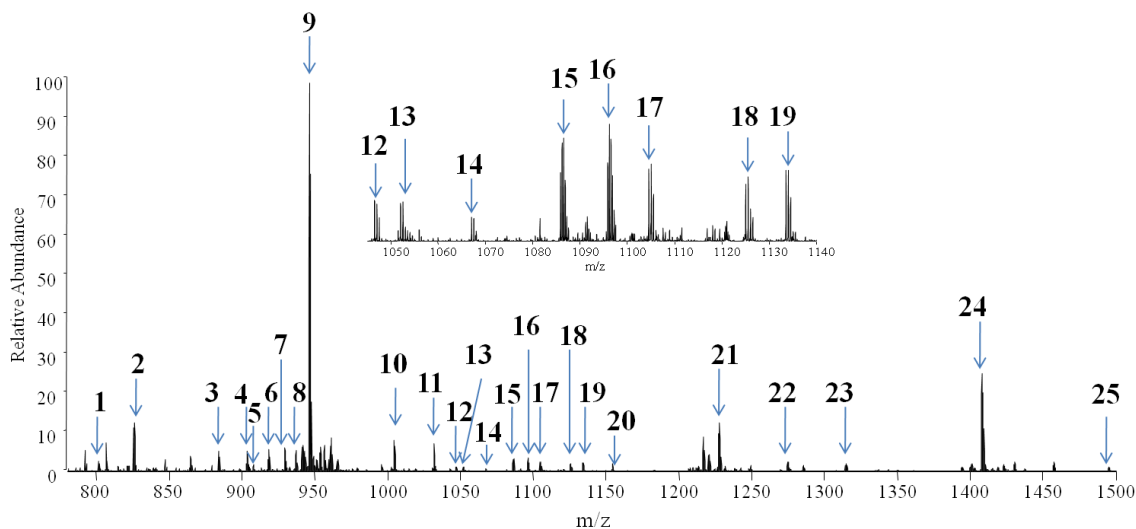


Figure 2.6. Full MS scan of human serum N-glycan mixture ($^{18}\text{O}/^{16}\text{O}=1:1$). 25 of the identified peaks were labeled out for the quantitative analysis.

The calculated $^{18}\text{O}/^{16}\text{O}$ ratios were obtained with the mathematical method described above and shown in **Table 2.1**. With comparison to the theoretical ratio from sample preparation,

the maximum observed error was 7.5% among the 25 analyzed N-glycan peaks, and the average error was 2.7%. With the incorporation of the ^{18}O isotope during PNGase F release of N-glycans, the heavily labeled species can be mixed with the light species prior to the derivatization procedure. Both samples will be subjected to permethylation with identical conditions. Therefore, the variances caused by different permethylation efficiency can be eliminated, which results in the increased accuracy and precision for relative quantitation.

Table 2.1. Quantitation of human serum N-glycans by ¹⁸O labeling method.

Peak	Charge state	N-glycan composition	Calculated ratio (Average±SD)	Expected ratio	Error (%)
1	[M+2Na] ²⁺	HexNAc ₂ Hex ₅	1.009±0.014	1	0.9
2	[M+3Na] ³⁺	HexNAc ₄ NeuAc ₁ Hex ₅	1.066±0.019	1	6.6
3	[M+3Na] ³⁺	Deoxyhex ₁ HexNAc ₄ NeuAc ₁ Hex ₅	1.004±0.019	1	0.4
4	[M+4Na] ⁴⁺	HexNAc ₅ NeuAc ₃ Hex ₆	1.028±0.041	1	2.8
5	[M+3Na] ³⁺	Deoxyhex ₂ HexNAc ₅ Hex ₅	1.012±0.006	1	1.2
6	[M+3Na] ³⁺	HexNAc ₅ NeuAc ₁ Hex ₅	1.005±0.021	1	0.5
7	[M+2Na] ²⁺	Deoxyhex ₁ HexNAc ₄ Hex ₃	1.015±0.021	1	1.5
8	[M+3Na] ³⁺	HexNAc ₆ Hex ₆	1.005±0.011	1	0.5
9	[M+3Na] ³⁺	HexNAc ₄ NeuAc ₂ Hex ₅	0.997±0.007	1	0.3
10	[M+3Na] ³⁺	Deoxyhex ₁ HexNAc ₄ NeuAc ₂ Hex ₅	0.996±0.007	1	0.4
11	[M+2Na] ²⁺	Deoxyhex ₁ HexNAc ₄ Hex ₄	1.054±0.015	1	5.4
12	[M+2Na] ²⁺	HexNAc ₄ Hex ₅	1.075±0.012	1	7.5
13	[M+2Na] ²⁺	Deoxyhex ₁ HexNAc ₅ Hex ₃	0.988±0.007	1	1.2
14	[M+2Na] ²⁺	HexNAc ₅ Hex ₄	1.031±0.011	1	3.1
15	[M+3Na] ³⁺	Deoxyhex ₁ HexNAc ₅ NeuAc ₂ Hex ₅	0.989±0.019	1	1.1
16	[M+3Na] ³⁺	HexNAc ₅ NeuAc ₂ Hex ₆	0.959±0.018	1	4.1
17	[M+2Na] ²⁺	HexNAc ₃ NeuAc ₁ Hex ₅	0.960±0.008	1	4.0
18	[M+2Na] ²⁺	HexNAc ₄ NeuAc ₁ Hex ₄	0.987±0.015	1	1.3
19	[M+2Na] ²⁺	Deoxyhex ₁ HexNAc ₄ Hex ₅	1.045±0.021	1	4.5
20	[M+2Na] ²⁺	Deoxyhex ₁ HexNAc ₅ Hex ₄	0.963±0.017	1	3.7
21	[M+3Na] ³⁺	HexNAc ₄ NeuAc ₁ Hex ₅	1.048±0.002	1	4.8
22	[M+3Na] ³⁺	Deoxyhex ₁ HexNAc ₅ NeuAc ₃ Hex ₆	0.980±0.022	1	2.0
23	[M+2Na] ²⁺	Deoxyhex ₁ HexNAc ₄ NeuAc ₁ Hex ₅	1.040±0.020	1	4.0
24	[M+2Na] ²⁺	HexNAc ₄ NeuAc ₂ Hex ₅	1.042±0.004	1	4.2
25	[M+2Na] ²⁺	Deoxyhex ₁ HexNAc ₄ NeuAc ₂ Hex ₅	1.008±0.004	1	0.8

Conclusions

This work presented a novel labeling method for N-glycan quantitation using ^{18}O -water. The ^{18}O labeling was efficiently incorporated into the reducing end of N-glycans during PNGase F release without altering the sample workflow. This method could improve quantitation accuracy by eliminating the difference in permethylation efficiency when samples are treated separately in a parallel manner. Also, a new mathematical calculation method for $^{18}\text{O}/^{16}\text{O}$ ratio measurement was developed to resolve the problem caused by the isotopic peak overlapping. This method was successfully applied to quantitate N-glycans released from standard glycoproteins and from human serum. Lastly, the ^{18}O labeling is expected to be applicable to oligosaccharides, such as O-glycans, since the ^{18}O labeling could also be incorporated into the reducing end during mutarotation.^{19,24,25}

Acknowledgements

This work was supported by NIH/NCRR grant # P41RR018502.

References

- (1) Varki, A. *Glycobiology* **1993**, *3*, 97.
- (2) HH, F. *Glycobiology* **2001**, *11*, 129R.
- (3) Kim, Y.-G.; Jeong, H.-J.; Jang, K.-S.; Yang, Y.-H.; Song, Y.-S.; Chung, J.; Kim, B.-G. *Analytical Biochemistry* **2009**, *391*, 151.
- (4) Jang, K.-S.; Kim, Y.-G.; Gil, G.-C.; Park, S.-H.; Kim, B.-G. *Analytical Biochemistry* **2009**, *386*, 228.
- (5) Zaia, J. *Chemistry & Biology* **2008**, *15*, 881.

- (6) Harvey, D. J.; Royle, L.; Radcliffe, C. M.; Rudd, P. M.; Dwek, R. A. *Analytical Biochemistry* **2008**, *376*, 44.
- (7) Kang, P.; Mechref, Y.; Klouckova, I.; Novotny, M. V. *Rapid Commun Mass Spectrom* **2005**, *19*, 3421.
- (8) DM, S.; VN, R. *Anal Chem.* **1998**, *70*, 3053.
- (9) Alvarez-Manilla, G.; Warren, N. L.; Abney, T.; Atwood, J.; Azadi, P.; York, W. S.; Pierce, M.; Orlando, R. *Glycobiology* **2007**, *17*, 677.
- (10) Atwood, J. A.; Cheng, L.; Alvarez-Manilla, G.; Warren, N. L.; York, W. S.; Orlando, R. *Journal of Proteome Research* **2008**, *7*.
- (11) Orlando, R. *Methods Mol Biol* **2010**, *600*, 31.
- (12) Orlando, R.; Lim, J.-M.; Atwood, J. A.; Angel, P. M.; Fang, M.; Aoki, K.; Alvarez-Manilla, G.; Moremen, K. W.; York, W. S.; Tiemeyer, M.; Pierce, M.; Dalton, S.; Wells, L. *Journal of Proteome Research* **2009**, *8*, 3816.
- (13) Ye, X.; Luke, B.; Andresson, T.; Blonder, J. *BRIEFINGS IN FUNCTIONAL GENOMICS AND PROTEOMICS* **2009**, *8*, 136.
- (14) Mirza, S. P.; Greene, A. S.; Olivier, M. *J Proteome Res.* **2008**, *7*, 3042.
- (15) Liu, Z.; Cao, J.; He, Y.; Qiao, L.; Xu, C.; Lu, H.; Yang, P. *Journal of Proteome Research* **2009**, *9*, 227.
- (16) Viseux, N.; Hoffmann, E. d.; Domon, B. *Anal. Chem.* **1997**, *69*, 3193.
- (17) Que ´me ´nera, B.; De ´sire ´, C. d.; Debrauwerb, L.; Rathahaob, E. *Journal of Chromatography A* **2003**, *984*, 185.
- (18) Rasmussen, J. R.; Davis, J. *J. Am. Chem. Soc* **1992**, *114*, 1124.
- (19) Mutenda, K. E.; Matthiesen, R. *Methods in Molecular Biology* **2006**, 367.

- (20) Kirmiz, C.; Li, B.; An, H. J.; Clowers, B. H.; Chew, H. K.; Lam, K. S.; Ferrige, A.; Alecio, R.; Borowsky, A. D.; Sulaimon, S.; Lebrilla, C. B.; Miyamoto, S. *Molecular & Cellular Proteomics* **2007**, *6*, 43.
- (21) Kronewitter, S. R.; Leoz, M. L. A. d.; Peacock, K. S.; McBride, K. R.; An, H. J.; Miyamoto, S.; Leiserowitz, G. S.; Lebrilla, C. B. *Journal of Proteome Research* **2010**, *9*, 4952.
- (22) Stanta, J. L.; Saldova, R.; Struwe, W. B.; Byrne, J. C.; Leweke, F. M.; Rothermund, M.; Rahmoune, H.; Levin, Y.; Guest, P. C.; Bahn, S.; Rudd, P. M. *Journal of Proteome Research* **2010**, *9*, 4476.
- (23) Kam, R. K. T.; Poon, T. C. W.; Chan, H. L. Y.; Wong, N.; Hui, A. Y.; Sung, J. J. Y. *Clinical Chemistry* **2007**, *53*, 1254.
- (24) rner, R. K.; Limberg, G.; Christensen, T. M. I. E.; Mikkelsen, J. D.; Roepstorff, P. *Anal. Chem.* **1999**, *71*, 1421.
- (25) Mutenda, K. E.; rner, R. K.; Christensen, T. M. I. E.; Mikkelsen, J.; Roepstorffa, P. *Carbohydrate Research* **2002**, *337*, 1217.

CHAPTER 3

AN LC-SRM APPROACH FOR THE SEPARATION AND QUANTITATION OF SIALYLATED N-GLYCANS LINKAGE ISOMERS ²

²Tao, S., Huang, Y., Boyes, B. and Orlando, R. Submitted to *Analytical Chemistry*, 06/06/2014.

Abstract

The study of N-linked glycans is among the most challenging bio-analytical tasks because of their complexity and variety. The presence of glycoform families that differ only in branching and/or linkage position makes the identification and quantitation of individual glycans exceedingly difficult. Quantitation of these individual glycans is important because changes in the abundance of these isomers are often associated with significant biomedical events. For instance, previous studies have shown that the ratio of α 2-3 to α 2-6 linked sialic acid (SA) plays an important role in cancer biology. Consequently, quantitative methods to detect alterations in the ratios of glycans based on their SA linkages could serve as a diagnostic in oncology, yet traditional glycomic profiling cannot readily differentiate between these linkage isomers. Here, we present an LC-selected reaction monitoring (SRM) approach that we demonstrate is capable of quantitating the individual SA linkage isomers. The LC method is capable of separating sialylated N-glycan isomers differing in α 2-3 and α 2-6 linkages using a novel superficially porous particle (Fused-Core™) Penta-HILIC column. SRM detection provides the relative quantitation of each SA linkage isomer, and minimizes interferences from co-eluting glycans that are problematic for UV/Fluorescence based quantitation. With our approach, the relative quantitation of each SA linkage isomer is obtained from a straightforward LC-MS experiment.

Introduction

Glycosylation is one of the most common and complex protein post-translational modifications. The glycosylation pattern of proteins depends on multiple factors, including enzyme activity, nucleotide sugar availability, kinetics of glycoconjugate transport, and cell type/stage. Alterations in glycan structures are associated with various pathologies such as

cancer and inflammation¹ and thus the detection of these changes offers the potential of being used for diagnostic and prognostic purposes.

A family of acidic 9-carbon sugars, which are known as sialic acids (SAs),² have attracted great attention due to the recognition of their biological functions.³ Previous studies have shown that the degree of sialylation affects the half-lives of many circulating glycoproteins and plays critical roles in a variety of biological processes, such as cell-cell communication, cell matrix interaction, adhesion, and protein targeting.⁴ Usually, SAs are found as terminal sugars on many of the oligosaccharides attached to proteins or lipids. In mammalian cells, the most common SAs are N-acetylneuraminic acid (Neu5Ac) and N-glycolylneuraminic acid (Neu5Gc), of these only the former is present in normal human cells.⁵⁻⁶ The structural diversity of SAs arises not only from different types of SAs but also from their linkage to the underlying glycan residues. Typically, SAs can be attached to a galactose (Gal) residue via α 2-3 or α 2-6 linkages or attached to N-acetylgalactosamine (GalNAc) via an α 2-6 linkage.⁷ In addition, SAs can also be attached to another SA residue via an α 2-8 linkage.⁸ These linkage configurations are regulated by the transferring enzymes, sialyltransferases (STs).

There are approximately 20 different STs, which can be classified into four groups according to the linkages they attach SAs to the glycan residue, including ST3Gal, ST6Gal (α 2,6-ST), ST6GalNAc, and ST8Sia (α 2,8-ST).⁸ The abbreviated key for this ST nomenclature is the linkage position (i.e., 3, 6, 8) followed by the monosaccharide onto which the SA is transferred (i.e., Gal, GlcNAc, SA). In other words, ST3Gal would be the term for a transferase that attached a sialic acid via an α 2-3 linkage to a galactose residue. Among the STs, ST6Gal-1 is probably the most studied due to its biological significance and its relationship to cancer. Evidence shows that the proteins on the cell surface undergo an increased level of α 2-6 linked

sialylation on galactose residues during tumor progression,⁹ which is correlated to the increased expression of ST6Gal-1.¹⁰⁻¹³ Hence, the altered ratio of α 2-3/2-6 can be used as an indicator for diagnostic purpose.

Mass spectrometry (MS) has been an enabling technology in glycomics.¹⁴⁻¹⁵ Although mass spectrometry can provide extensive information on structure and quantity, MS glycomics profiling has difficulty quantitating linkage isomers, such as those resulting from SA α 2-3/2-6 linkages, particularly when multiple species are present.¹⁶ Several groups have proposed techniques to overcome this issue with quantitation of SA linkage isomers. To differentiate these linkage isomers, Mechref, *et al.* has described the formation of diagnostic ions by tandem MS of permethylated oligosaccharides specific to SA with α 2-6 linkage.¹⁷ Novotny, *et al.* has reported a method that involves the selective amination of α 2-6 linked SAs, which causes the α 2-3 linked SAs to undergo spontaneous lactonization. Followed by permethylation, the α 2-6 linked SA gives a mass shift of 13 Da over SA attached via α 2-3 linkage, which can be easily distinguished by MS.¹⁶ These methods require extensive chemical derivatization for sample preparation.

Liquid chromatography (LC) is a useful addition to the MS-based glycomics techniques due to its ability to separate glycan isomers and thus offers great potential for the characterization/quantitation of individual glycans. Various separation techniques have demonstrated the ability to resolve isomeric N-glycans, both in their native and derivatized forms, using normal-phase,¹⁸ porous graphitized carbon (PGC)¹⁹ and reversed-phase²⁰ liquid chromatography. Recently, Hincapie has reported the separation of isomeric sialylated N-glycans by hydrophilic interaction liquid chromatography (HILIC) combined with a linkage specific derivatization.²¹ In this work, the derivatization of SAs is not only essential to identify the isomers due to the linkage specific reactions, but also important to separate the linkage

specific subpopulations of those highly sialylated N-glycans by HILIC. The routine chromatographic separation of SA linkage isomers has not currently been achieved without linkage specific chemistry.

Here, we present an LC-selected reaction monitoring (SRM) approach that enables quantitation of the individual SA linkage isomers. We have developed a chromatographic method capable of separating the sialylated N-glycan α 2-3 and α 2-6 linkage isomers using a novel superficially porous particle (Fused-Core™) Penta-HILIC column. Exoglycosidase digestion confirmed the identity of each N-glycan isomer from a standard glycoprotein. Quantitation of the linkage isomers is provided by interfacing the LC to a Q-Trap MS detector that was operated in SRM mode, which minimized interferences from the co-eluting glycans that caused problems with UV/Fluorescence based quantitation. This straightforward LC-MS experiment provides the relative quantitation of each SA linkage isomer.

Experimental Section

Materials. Bovine fetuin, human serum, trypsin (TPCK treated) and procainamide hydrochloride were purchased from Sigma. Ammonium bicarbonate, ammonium formate, formic acid (for LC-MS) and sodium cyanoborohydride were purchased from Fluka. PNGase F (Glycerol free) was purchased from New England Biolabs (NEB). Sialidase S (recombinant from *Streptococcus pneumonia* expressed in E. coli) was purchased from Prozyme. Acetonitrile (ACN, HPLC grade) was purchased from Fisher. Octadecyl (C18) disposable extraction columns were purchased from J.T.Baker. PD MiniTrap G-10 was purchased from GE Healthcare. Other reagents were analytical grade.

N-glycan Release and Purification. Bovine fetuin (200 μg) was dissolved in 200 μL of 50 mM ammonium bicarbonate, pH=7.8. For human serum, a 50 μL aliquot was mixed with 50 mM ammonium bicarbonate, pH=7.8. Both sample solutions were heated at 100 $^{\circ}\text{C}$ for 5 minutes to denature the protein. Trypsin digestion was carried out at 37 $^{\circ}\text{C}$ overnight with an adjusted enzyme amount (a 10 μL aliquot for fetuin or 100 μL aliquot for serum of a 1 $\mu\text{g}/\mu\text{L}$ trypsin in the buffer solution). The trypsin was then deactivated by heating at 100 $^{\circ}\text{C}$ for 10 min. For N-glycan release, an 1 μL aliquot and 4 μL aliquot of PNGase F (used as received from NEB at 500,000 U/mL) was added to the fetuin sample and the human serum sample, respectively. After incubation at 37 $^{\circ}\text{C}$ overnight, the released N-glycans were separated from peptides and undigested proteins by reverse-phase liquid chromatography with a C18 SPE column. Specifically, the PNGase F digests were loaded onto a C18-Sep-Pac, which had been pre-equilibrated in 5% acetic acid. The column was washed with 3 mL of 5% acetic acid, the N-glycans were present in the flow-through, which was collected, frozen and lyophilized to dryness.

Procainamide (ProA) Labeling of free N-glycans. The labeling of the glycans was carried out by following Klapoetke's procedure²² with a modification for the sialylated glycans.²³ The labeling solution was prepared fresh with 108 mg/mL procainamide hydrochloride and 63 mg/mL Na[BH₃(CN)] in dimethyl sulfoxide (DMSO) / acetic acid at a ratio of 7:3 by volume. A 20 μL aliquot of the labeling solution was added to the fetuin sample and 40 μL to the serum sample. The mixtures were incubated at 37 $^{\circ}\text{C}$ overnight in darkness. Excess labeling reagent was removed using the MiniTrap G-10 size exclusion columns following the user's guide with this product. The fraction containing the fluorescently labeled N-glycans was lyophilized and stored at -20 $^{\circ}\text{C}$ pending analysis.

HILIC separation of ProA labeled N-glycans. This study utilized a Nexera UFLC (Shimadzu) LC system and Halo Penta-HILIC columns (Advanced Materials Technology, 2.1 mm x 15 cm, 2.7 μ m particle size, Wilmington, DE). The separation was carried out at a flow rate of 0.4 mL/min at 60 $^{\circ}$ C with a mobile phase A consisting of 95% H₂O/ACN with 50 mM ammonium formate (adjusted to pH 4.4 with formic acid) and mobile phase B being pure ACN. A linear gradient of 78% mobile phase B to 48% mobile phase B in 75 min was utilized. The UV absorbance signal for the ProA tag was detected at a wavelength of 300 nm. In most cases, the absorbance detector was operated in series with the MS detector. A small ID (50 μ m PEEK-Sil) tube connected the flow cell to the MS interface. One fiftieth of the sample dissolved in 78% ACN was injected for each experiment. With the fetuin sample, fractions were collected based on individual peaks observed from UV detector. After drying in a Speed-vac (Thermo/Savant), the fractions were stored at -20 $^{\circ}$ C pending exoglycosidase study to determine the isomer linkages of SAs.

SRM detection of chromatographically resolved isomers. MS analysis was performed on a 4000 Q-Trap (AB SCIEX) mass spectrometer. An initial LC-MS experiment, where ions were detected across the 700-2000 m/z range, was performed on each sample to determine the most abundant molecular ion species for each glycan. These values, listed in **Table 3.1**, were used as the precursor ions for the SRM experiments. MS/MS experiments performed on the ProA-labeled N-glycans revealed that each of these glycans produced an intense fragment ion at m/z 441.4, which corresponded to the GlcNAc derivatized with the ProA tag. This fragment ion was used in the SRM experiment for all of the labeled N-glycans. As a side note, the high abundance of this fragment ion was expected because of the high gas-phase basicity associated with the tertiary amine on the ProA tag. A series of experiments was performed and led to the

conclusion that a collision energy (CE) of 70 V and declustering potential (DP) of 40 V were optimal. The dwell time was set at 100 ms with unit resolution in both Q1 and Q3 mass selectors.

Exoglycosidase digestion for SA linkage identification with fetuin N-glycans. To confirm the separation of SA linkage isomers, fractions collected from the fetuin sample were digested with sialidase S, an exoglycosidase that specifically releases α 2-3 linked SA residues. For this digestion, each of the dried fractions was dissolved in 14 μ L Nanopure water, then 4 μ L of 5x Reaction Buffer B (as received) and 2 μ L of sialidase S (at 5 U/mL) were added to the mixture to give a total volume of 20 μ L. The digestions were carried out at 37 °C for 2 h. After digestion, each reaction solution was frozen and lyophilized to dryness and then re-dissolved in 78% ACN/H₂O for LC/MS analysis with the same experimental conditions described above.

Results and Discussions

Fetuin N-glycan separation with the Penta-HILIC columns. Fetuin is a standard glycoprotein that has a variety of well-characterized glycoforms consisting predominantly of bi-, tri-, and tetra-antennary N-glycans with variable degrees of sialylation.²⁴⁻²⁶ The HILIC separation of the ProA-labeled N-glycans from fetuin contained 21 abundant chromatographically resolved peaks (**Figure 3.1A**). Comparing the observed masses from the LC-MS experiment to those reported previously,²⁷⁻²⁸ glycan compositions could be assigned for each peak (**Table 3.1**). For example, the m/z value obtained over peak 1 corresponds with a bi-antennary N-glycan with two SAs, which is abbreviated as Bi-2SA. LC-MS analysis identified 8 unique compositions in 21 chromatographic peaks. Four compositions (Bi-2SA, Tri-2SA, Tri-3SA and Tri-4SA) are found in 13 individual peaks, which are represented in blue, red, green and grey, respectively in the SRM traces (**Figure 3.1B**). It is noteworthy that there are some

minor peaks in blue and red underneath the most abundant green peaks, which presumably result from the loss of SAs by in-source fragmentation. A reasonable explanation for the observation of multiple peaks with the same composition was that the SA α 2-3/ α 2-6 linkage isomers were being resolved with the HILIC separation. To confirm our hypothesis, each of these peaks was collected and further characterized by exoglycosidase digestion with subsequent LC-MS analysis.

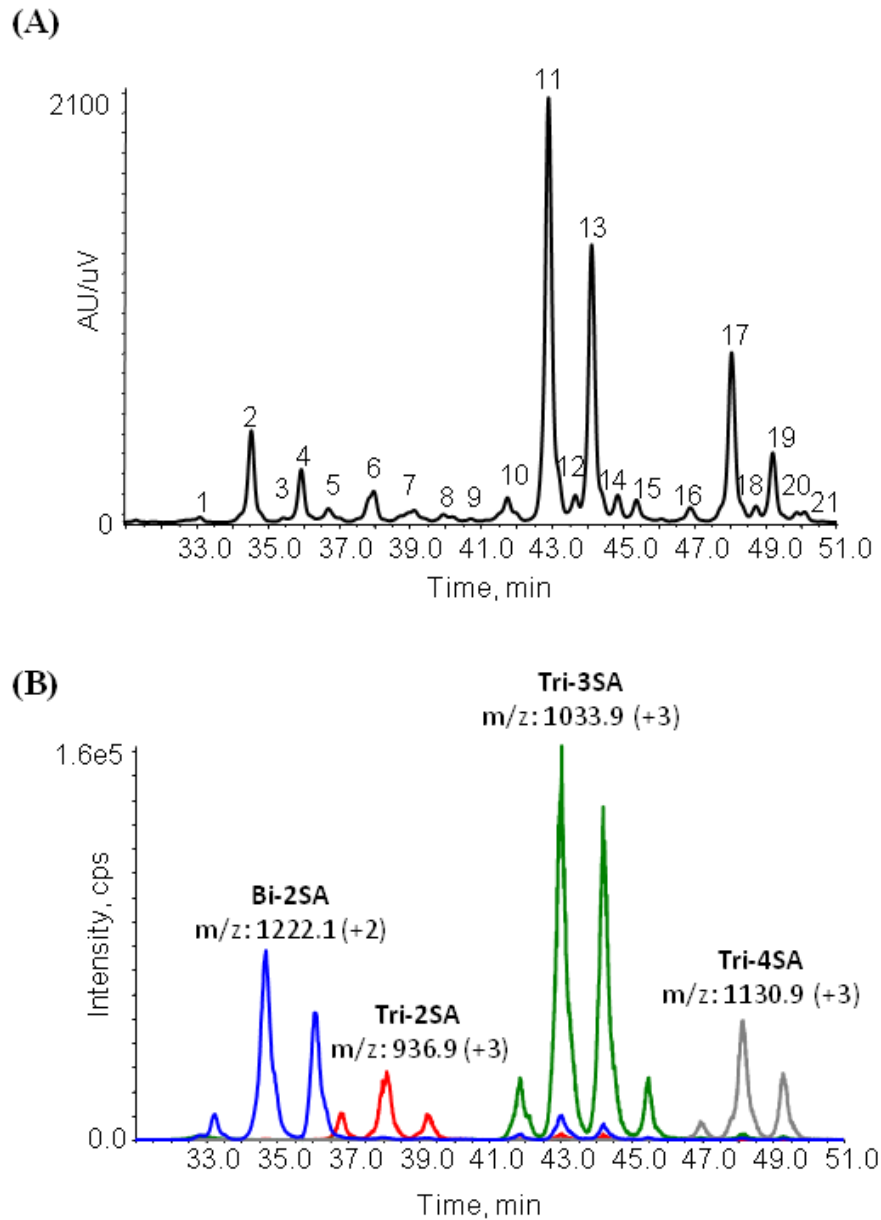


Figure 3.1. Major ProA-labeled N-glycans from fetuin. (A) UV trace of the fetuin sample denoting the peak/fraction number. Fractions were collected for peaks 1 through 21 and subjected individually to exoglycosidase digestion, LC-SRM analysis. (B) LC-SRM traces for the major N-glycan compositions from the same fetuin sample, indicating the Bi-2SA (blue), Tri-2SA (red), Tri-3SA (green) and Tri-4SA (grey).

Table 3.1. N-glycans Detected in the Fetuin Sample.

Group	Observed m/z (charge)	Theoretical m/z (charge)	Composition	Peak No.
I	1222.1 (+2)	1222.06 (+2)	Bi-2SA	1, 2, 4
II	1259.2 (+2)	1259.08 (+2)	Tri-SA	3
III	936.9 (+3)	936.75 (+3)	Tri-2SA	5, 6, 8
IV	1367.8 (+2)	1367.60 (+2)	Bi-3SA	7, 9
V	1033.9 (+3)	1033.78 (+3)	Tri-3SA	10, 11, 13, 15
VI	1155.9 (+3)	1155.49 (+3)	Tetra-3SA	12, 14
VII	1130.9 (+3)	1130.81(+3)	Tri-4SA	16, 17, 19
VIII	1252.9 (+3)	1252.52 (+3)	Tetra-4SA	18, 20, 21

A series of exoglycosidase digestion studies were performed to identify if the multitude of chromatographic peaks from glycans with the same apparent composition indeed resulted from different linkage isomers. Each of the isolated fetuin fractions was subjected to digestion with Sialidase S, which should exclusively cleave α 2-3 linked SA from the non-reducing termini. Each digested fraction was analyzed by LC-SRM using the same LC gradient as the original separation and the SRM transitions listed in **Table S3.1**. LC-SRM analysis of the earliest eluting Bi-2SA glycoform after exoglycosidase digestion revealed that the original peak at 33.2 min had disappeared and was replaced by a new peak at 24.3min (**Figure 3.2B**). The SRM data indicated that the glycan in this new peak corresponded to a bi-antennary structure with no SAs. This result indicates that both of the SAs on this N-glycan have attachment through α 2-3 linkages.

Analysis of the second Bi-2SA fraction after digestion once again revealed the disappearance of the original peak, the appearance of a new peak at 31.5min (**Figure 3.2C**), and the mass of the new glycan corresponding to a Bi-SA structure. Consequently, the N-glycan present in this fraction was found to have one SA attached through an α 2-3 linkage (released by sialidase S digestion) and one SA attached through an α 2-6 linkage (resistant to sialidase S digestion). The glycan in the last Bi-2A fraction was not affected by the Sialidase S digestion (**Figure 3.2D**), which indicating that both SAs are attached via α 2-6 linkages. Combined these results indicate that each of the fractions contains a different SA linkage isomer(s) and the three fractions correspond to Bi-2SA(3,3), Bi-2SA(3,6) and Bi-2SA(6,6) listed in order from the shortest to longest retention time. Similar experiments were conducted on the fractionated Tri-2SA, Tri-3SA, and Tri-4SA N-glycans and the SA linkage identifications also demonstrated the retention pattern of the SA α 2-3 isomer eluting before the corresponding an α 2-6 isomer. The three isomeric structures observed from the Tri-2SA N-glycans corresponded to Tri-2SA(3,3), Tri-2SA(3,6) and Tri-2SA(6,6) in the order of the shortest to longest retention time (**Figure S3.1**). The 4 isomeric structures detected from the Tri-3SA N-glycan corresponded to Tri-3SA(3,3,3), Tri-3SA(3,3,6), Tri-3SA(3,6,6) and Tri-3SA(6,6,6) (**Figure S3.2**). The Tri-4SA N-glycans have more SAs than their antenna, and the fourth SA has been found to be attached to the non-reducing end GlcNAc through α 2-6 linkage.²⁴ The exoglycosidase digestions revealed that the SA linkage sites for glycans eluting in these peaks were Tri-4SA(3,3,3,6), Tri-4SA(3,3,6,6) and Tri-4SA(3,6,6,6) (**Figure S3.3**), where the italicized numbers indicate the linkage of the SA not attached to the terminal Gal residue. These experiments clearly demonstrate that the glycans are being resolved based on the ratio of their SA α 2-3 to α 2-6 linkages.

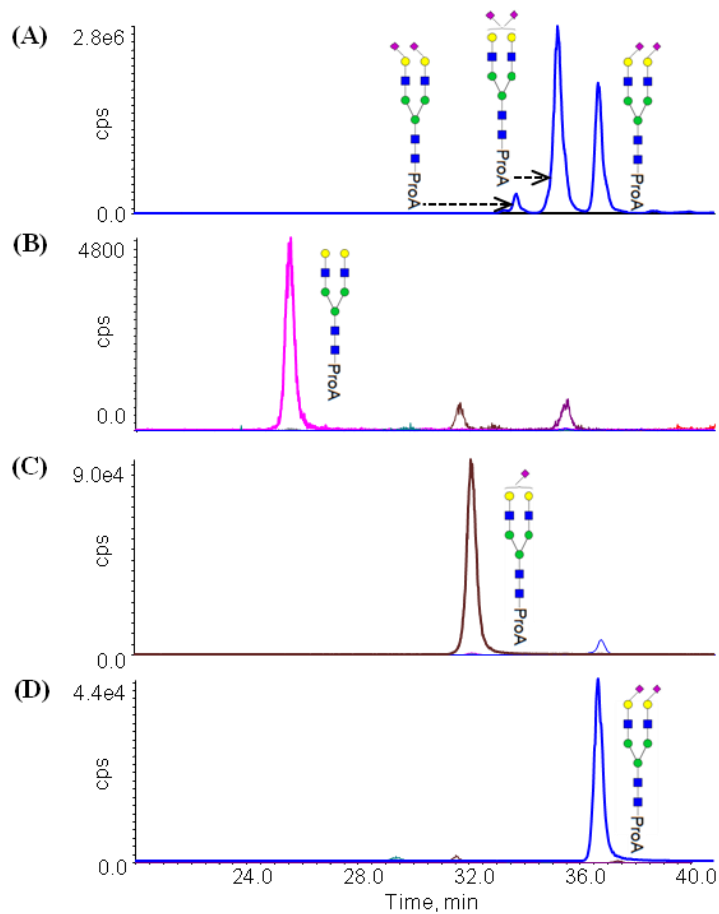


Figure 3.2. Sialidase S digestions for Bi-2SA fractions by SRM detection. (A) LC-SRM trace for Bi-2SA (m/z at 1222.1) from analysis of the fetuin N-glycans. LC-SRM analysis illustrates (B) the disappearance of the blue peak (Bi-2SA) and the appearance of the pink peak (Bi-0SA) after Sialidase S digestion for the first fraction; (C) the disappearance of the blue peak (Bi-2SA) and the appearance of the brown peak (Bi-SA) after Sialidase digestion for the second fraction; and (D) no change of the blue peak (Bi-2SA) after Sialidase S digestion for the third fraction. **Figures B-D** contain SRM traces for all three possible glycans resulting from this treatment, i.e., the Bi-0SA, Bi-SA and Bi-2SA, however the low levels make these difficult to see in all of the figures.

Another conclusion from these results is that the substitution of an α 2-3 linked SA with an α 2-6 linked SA on biantennary glycans (Bi-SA and Bi-2SA) increases the retention time by a constant value, in this case, approximately 1.4 min. The shift in retention time with such substitution for triantennary glycans (Tri-2SA, Tri-3SA and Tri-4SA) is about 1.1 min under the described experimental conditions. It is possible that the shift in glycan retention by the isomeric substitution is altered by the overall retention of the glycan, which is determined by the overall size of the glycan (number of sugar units).

Even with the ability to resolve α 2-3/ α 2-6 linkage isomers, many of these fractions likely contain multiple glycoforms. For instance, there are two branching isomers that correspond to the composition Bi-2SA(3,6) found in the second LC fraction. One of these has the α 2-6 linked SA on the antennae originating on the 6 branch of the core pentasaccharide, while the other has the α 2-6 linked SA on the antennae originating on the 3 branch (**Figure 3.3A**). Since both of these structures have been reported attached to fetuin, it does not appear that the chromatographic conditions here are capable of resolving these two branching isomers. Analogous discussions can be made concerning the three possible Tri-2SA(3,3) branching isoforms (**Figure 3.3B**). Many of the other compositions have the potential to have multiple branching isomers, in particular the compositions indicated by Tri-2SA(3,6), Tri-2SA(6,6), Tri-3SA(3,3,6), Tri-3SA(3,6,6) and all 3 of the Tri-4SA combinations, which if present, are not resolved with these conditions. The triantennary structures of fetuin are also known to have Gal β 1-3/Gal β 1-4 linkage isomers.^{24, 29} The chromatographic conditions in the current study do not appear to resolve these linkage isomers. Further study will be required to define conditions that may allow resolution of these additional linkage isomers either. Despite these limitations, the ability to resolve glycans based on their SA α 2-3/ α 2-6 linkages offers the potential to quickly

isolate/quantitate these linkage isomers. This capacity is expected to advance biomedical research as it will facilitate the study of disease conditions wherein the ratio of α 2-3 to α 2-6 SA linkages is expected to change.

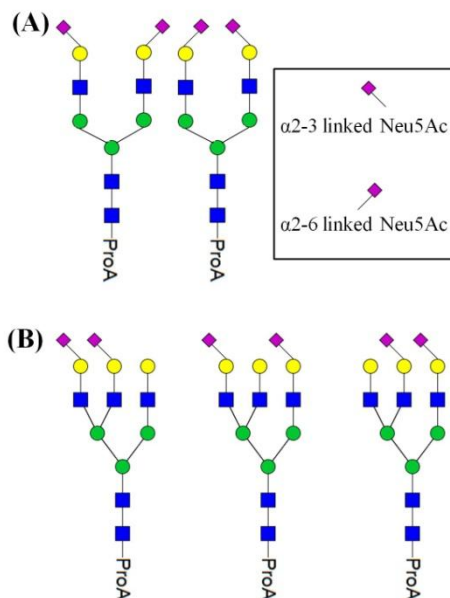


Figure 3.3. Branching isoforms. (A) Two isomeric structures for Bi-2SA(3,6) glycans; (B) Three isomeric structures for Tri-2SA(3,3) glycans.

UV and SRM quantitation of isomeric N-glycans with different SA linkages from fetuin. The ProA tag of N-glycans added through reductive amination chemistry gives nonselective labeling on the reducing end in a 1:1 ratio, which makes it possible to achieve quantitation by UV absorbance or fluorescence detection. However, the UV/fluorescence quantitation requires that all the peaks are resolved from each other in order to obtain individual peak area measurement, which can be challenging with complex glycomic samples. Alternatively, SRM has been widely employed for quantitative purposes, due to its excellent selectivity, sensitivity, and ability to quantitate individual components in complex mixtures.

However, with the SRM approach each glycan may have a different response because of changes in parameters such as the precursor charge states/adducts, ionization/fragmentation efficiencies, etc. For example, in positive ion mode, the ionization efficiency may decrease with increasing number of SA residues. In the fetuin sample, the 3 isomers of Bi-2SA, 3 isomers of Tri-2SA, 4 isomers of Tri-3SA and 3 isomers of Tri-4SA were well-resolved from other detectable glycans. Thus, the relative ratio of each structure could be obtained without bias from UV detection, which enabled the exploration of the SRM detection response for each of these glycans.

The relative quantity of each resolvable species was calculated by dividing the peak area, obtained either by UV or SRM detection, obtained for each glycan, with the sum of the peak areas from all identifiable glycans. The standard deviations from triplicate measurements were less than 1% for the results using UV and SRM detection, indicating the high reproducibility of both detection methods. However, the relative quantities obtained by UV detection are different from those obtained by SRM (**Figure 3.4**). For example, the relative quantity of Bi-2SA(3,6) was 7.8% with UV detection, while it was 14.5% by SRM detection. Conversely, the relative ratio of Tri-3SA(3,3,6) was 34.5% by UV detection but only 26.2% by SRM detection. In general, the relative quantities of Bi-2SA and Tri-2SA by SRM detection would result in overestimation of the amounts, and the relative ratios of Tri-3SA and Tri-4SA would be underestimated. In order to determine whether the measurement differences between the UV and SRM detection were significant, standard T-tests were performed. For those 13 individual glycans, 11 glycans were found at $p < 0.001$. The results indicated that there were statistically significant differences between the UV and SRM detection for the relative quantitation of individual structure across different glycan compositions. The values obtained from UV detection were assumed to be correct because (1) UV detection should not be affected by glycan

structure/composition and (2) MS analysis of each chromatographic peak demonstrated that each contained a single glycan specie. A possible explanation is that the MS response in positive ion mode decreases with the addition of negatively charged SA residues. Another explanation is that the SRM response decreases with increasing MW of the glycan, which could result from decreased ionization efficiency, ion transmission, and/or fragmentation efficiency. Yet another possibility is that the organic/aqueous composition of the chromatographic solvent changes during the gradient elution, and that ionization efficiency is dependent on the composition at elution for each component. Of course, there are multiple other explanations, all of which may be correct, but the important point is simply that the SRM response changes with the composition of the glycan.

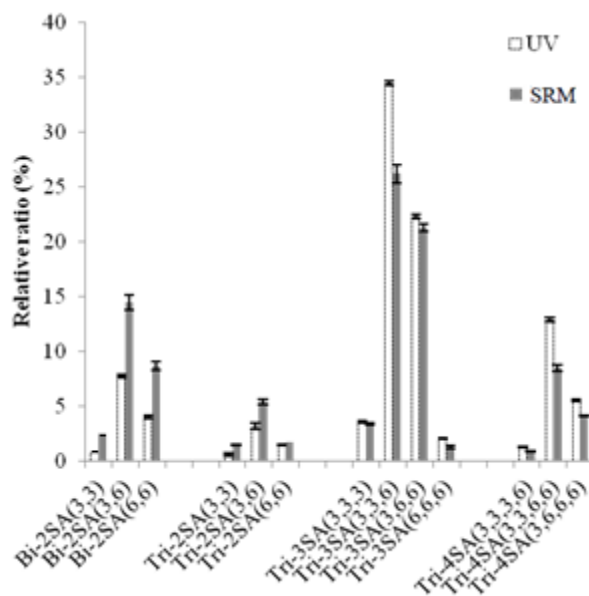


Figure 3.4. Relative quantitation of the major glycan linkage isomers of fetuin by UV and LC-SRM detection. The response for each glycoform is relative to the summed response for all identified glycans.

The SRM responses for isomeric glycans were then evaluated by comparing the relative quantitation of isomeric structures for glycans of a given composition. For instance, the relative ratios of each Bi-2SA isomers were calculated from the total amount of all the three isomers for both UV absorbance and SRM detection, and so forth. Comparisons of the relative responses for each of the glycan to the other glycans having the same compositions demonstrate that the relative quantitation obtained by SRM detection are in very good agreement with those obtained by UV detection (**Figure 3.5**), which suggests that there is negligible differences in the SRM responses for linkage isomers. T-tests were again used to determine the significance of these differences and various levels of significance were tested. With the same 13 glycans, only 2 glycans were found at $p < 0.05$ and none of them was found at $p < 0.001$. Hence, reliable relative quantitation of individual isomers can be achieved by comparing the SRM responses to other N-glycans with the same composition.

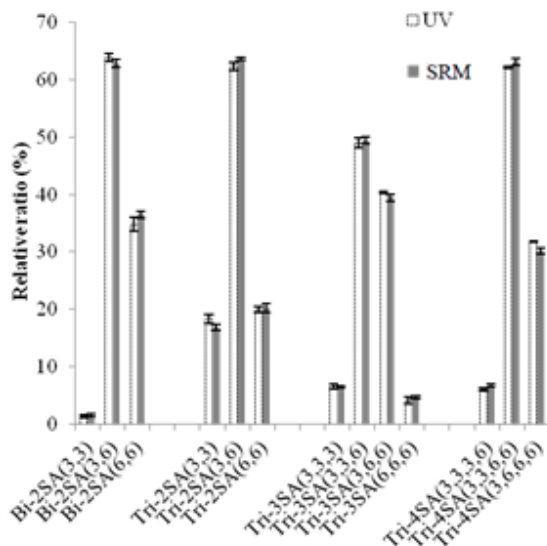


Figure 3.5. Relative quantitation of the major glycan linkage isomers of fetuin with UV and LC-SRM detection. The response for each glycoform is relative to the summed response for all glycoforms with the same composition.

SRM quantitation of SA linkage isomers from human serum. Human serum has received considerable attention in the glycomic field as a rich source of structurally and functionally diverse glycoproteins,³⁰⁻³⁴ which are potential biomarkers for numerous conditions. The released glycan pool from human serum contains over 120 different N-glycan structures;³⁵ consequently, many glycans co-elute. For instance, the Q1 MS full scan showed that the Bi-SA glycan (m/z at 1076.5) and the Man 9 glycan (m/z at 1052.0, which represents the glycan composition of Man9GlcNAc2) are co-eluting at retention time of 30.5 min with the LC conditions used in this study (**Figure 3.6**). However, due to the difference of their molecular weights, these two glycans produce two different SRM traces, enabling quantitation of both species. The use of MS detection also adds a level of confidence in the identity of the species being quantitated, as well as indicating peaks that result from overlapping glycans, where the quantitative results will be suspect. For the human serum sample, identity of the SA linkage isomers was determined based on a combination of mass and retention time. The relative quantity of the individual glycan isomers was calculated relative to the SRM response for glycans with the same composition, as shown in **Table 3.2**. The ability to chromatographically resolve SA linkage isomers coupled with SRM detection permits the identification and relative quantitation of N-glycan SA α 2-3/2-6 linkage isomers.

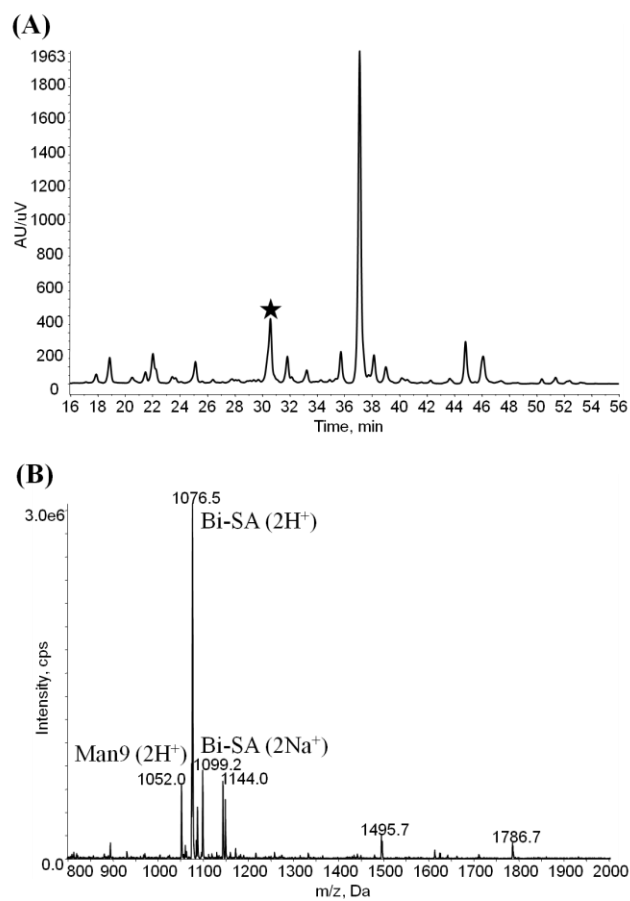


Figure 3.6. (A) UV Chromatogram for detection of ProA-labeled N-glycans from human serum; (B) MS spectrum for the selected peak (indicated by the star), showing the co-elution of several different glycans. Man9 corresponds to the high mannose glycan with a composition of Man9GlcNAc2.

Table 3.2. SRM quantitation of sialylated N-glycan linkage isomers from human serum.

m/z	Glycan	RT (min)	Relative Ratio (%)	
			Average	STD
1076.50	Bi-SA(3)	29.2	9.11	1.64
	Bi-SA(6)	30.6	90.9	1.56
1222.20	Bi-2SA(3,3)	33.3	0.59	0.22
	Bi-2SA(3,6)	34.8	21.3	2.96
	Bi-2SA(6,6)	36.2	78.2	2.91
1259.08	Tri-SA(3)	33.8	67.2	4.31
	Tri-SA(6)	34.8	32.7	4.38
937.05	Tri-2SA(3,3)	37.9	2.62	0.88
	Tri-2SA(3,6)	39.2	54.5	6.88
	Tri-2SA(6,6)	40.2	46.5	3.70
1034.10	Tri-3SA(3,3,3)	42.5	0.62	0.19
	Tri-3SA(3,3,6)	43.7	16.8	3.81
	Tri-3SA(3,6,6)	44.8	61.6	1.63
	Tri-3SA(6,6,6)	46.0	20.8	2.96
1155.49	Tetra-3SA(3,3,3)	44.3	3.07	0.54
	Tetra-3SA(3,3,6)	45.6	36.2	4.15
	Tetra-3SA(3,6,6)	46.7	50.0	2.21
	Tetra-3SA(6,6,6)	47.8	10.7	2.41

Conclusions

A novel hydroxylated Fused-CoreTM silica material has high utility for HILIC separation of reducing terminus labeled N-linked glycans. With the developed method, baseline separation was achieved for N-glycan isomers with α 2-3/2-6 SA linkages, which facilitated the structure identification and quantitation of each isomer via LC-SRM analysis. The current method has been used for relative quantitation of SA linkage isomers of individual glycoproteins, and for N-glycans from human serum. Resolution and quantitation of these glycans may assist in early diagnosis of certain pathologies, based on previous observations of altered α 2-3 and α 2-6 SA linkage quantities.

Acknowledgements

Research reported in this publication was supported by the National Institute of General Medical Sciences of the National Institutes of Health under Award Numbers P41RR018502 (RO), R41GM104631-01 (RO) and R44GM093747-02 (BB). The content is solely the responsibility of the authors and does not necessarily represent the official views of the National Institutes of Health.

References

- (1) Marino, K.; Bones, J.; Kattla, J. J.; Rudd, P. M., *Nat Chem Biol* **2010**, *6* (10), 713-23.
- (2) Chen, X.; Varki, A., *ACS Chem Biol* **2010**, *5* (2), 163-76.
- (3) Varki, A., *Proc Natl Acad Sci U S A* **2010**, *107 Suppl 2*, 8939-46.
- (4) Schauer, R., *Glycoconj J* **2000**, *17* (7-9), 485-99.
- (5) Chou, H. H.; Takematsu, H.; Diaz, S.; Iber, J.; Nickerson, E.; Wright, K. L.; Muchmore, E. A.; Nelson, D. L.; Warren, S. T.; Varki, A., *Proc Natl Acad Sci U S A* **1998**, *95* (20), 11751-6.
- (6) Malykh, Y. N.; Schauer, R.; Shaw, L., *Biochimie* **2001**, *83* (7), 623-34.
- (7) Tsuji, S., *J Biochem* **1996**, *120* (1), 1-13.
- (8) Wang, P., *J. Cancer Mol.* **2005**, *1* (2), 73-81.
- (9) Lin, S.; Kemmner, W.; Grigull, S.; Schlag, P. M., *Exp Cell Res* **2002**, *276* (1), 101-10.
- (10) Pousset, D.; Piller, V.; Bureaud, N.; Monsigny, M.; Piller, F., *Cancer Res* **1997**, *57* (19), 4249-56.
- (11) Dall'Olio, F.; Chiricolo, M.; Lau, J. T., *Int J Cancer* **1999**, *81* (2), 243-7.

- (12) Wang, P. H.; Lee, W. L.; Lee, Y. R.; Juang, C. M.; Chen, Y. J.; Chao, H. T.; Tsai, Y. C.; Yuan, C. C., *Gynecol Oncol* **2003**, *89* (3), 395-401.
- (13) Recchi, M. A.; Hebbbar, M.; Hornez, L.; Harduin-Lepers, A.; Peyrat, J. P.; Delannoy, P., *Cancer Res* **1998**, *58* (18), 4066-70.
- (14) Zaia, J., *OMICS* **2010**, *14* (4), 401-18.
- (15) Wuhrer, M., *Glycoconj J* **2013**, *30* (1), 11-22.
- (16) Alley, W. R., Jr.; Novotny, M. V., *J Proteome Res* **2010**, *9* (6), 3062-72.
- (17) Mechref, Y.; Kang, P.; Novotny, M. V., *Rapid Commun Mass Spectrom* **2006**, *20* (8), 1381-9.
- (18) Maslen, S.; Sadowski, P.; Adam, A.; Lilley, K.; Stephens, E., *Anal Chem* **2006**, *78* (24), 8491-8.
- (19) Hua, S.; An, H. J.; Ozcan, S.; Ro, G. S.; Soares, S.; DeVere-White, R.; Lebrilla, C. B., *Analyst* **2011**, *136* (18), 3663-71.
- (20) Higel, F.; Demelbauer, U.; Seidl, A.; Friess, W.; Sorgel, F., *Anal Bioanal Chem* **2013**, *405* (8), 2481-93.
- (21) Tousi, F.; Bones, J.; Hancock, W. S.; Hincapie, M., *Anal Chem* **2013**, *85* (17), 8421-8.
- (22) Klapoetke, S.; Zhang, J.; Becht, S.; Gu, X.; Ding, X., *J Pharm Biomed Anal* **2010**, *53* (3), 315-24.
- (23) Melmer, M.; Stangler, T.; Schiefermeier, M.; Brunner, W.; Toll, H.; Rupprechter, A.; Lindner, W.; Premstaller, A., *Anal Bioanal Chem* **2010**, *398* (2), 905-14.
- (24) Green, E. D.; Adelt, G.; Baenziger, J. U.; Wilson, S.; Van Halbeek, H., *J Biol Chem* **1988**, *263* (34), 18253-68.

- (25) Townsend, R. R.; Hardy, M. R.; Cumming, D. A.; Carver, J. P.; Bendiak, B., *Anal Biochem* **1989**, *182* (1), 1-8.
- (26) Nakano, M.; Saldanha, R.; Gobel, A.; Kavallaris, M.; Packer, N. H., *Mol Cell Proteomics* **2011**, *10* (11), 1988-91.
- (27) Anumula, K. R.; Dhume, S. T., *Glycobiology* **1998**, *8* (7), 685-94.
- (28) Nakano, M.; Kakehi, K.; Tsai, M. H.; Lee, Y. C., *Glycobiology* **2004**, *14* (5), 431-41.
- (29) Bendiak, B.; Harris-Brandts, M.; Michnick, S. W.; Carver, J. P.; Cumming, D. A., *Biochemistry* **1989**, *28* (15), 6491-9.
- (30) Kyselova, Z.; Mechref, Y.; Al Bataineh, M. M.; Dobrolecki, L. E.; Hickey, R. J.; Vinson, J.; Sweeney, C. J.; Novotny, M. V., *J Proteome Res* **2007**, *6* (5), 1822-32.
- (31) Kirmiz, C.; Li, B.; An, H. J.; Clowers, B. H.; Chew, H. K.; Lam, K. S.; Ferrige, A.; Alecio, R.; Borowsky, A. D.; Sulaimon, S.; Lebrilla, C. B.; Miyamoto, S., *Mol Cell Proteomics* **2007**, *6* (1), 43-55.
- (32) Leiserowitz, G. S.; Lebrilla, C.; Miyamoto, S.; An, H. J.; Duong, H.; Kirmiz, C.; Li, B.; Liu, H.; Lam, K. S., *Int J Gynecol Cancer* **2008**, *18* (3), 470-5.
- (33) Chen, C. C.; Engelborghs, S.; Dewaele, S.; Le Bastard, N.; Martin, J. J.; Vanhooren, V.; Libert, C.; De Deyn, P. P., *Rejuvenation Res* **2010**, *13* (4), 439-44.
- (34) Kamiyama, T.; Yokoo, H.; Furukawa, J.; Kurogochi, M.; Togashi, T.; Miura, N.; Nakanishi, K.; Kamachi, H.; Kakisaka, T.; Tsuruga, Y.; Fujiyoshi, M.; Taketomi, A.; Nishimura, S.; Todo, S., *Hepatology* **2013**, *57* (6), 2314-25.
- (35) Aldredge, D.; An, H. J.; Tang, N.; Waddell, K.; Lebrilla, C. B., *J Proteome Res* **2012**, *11* (3), 1958-68.

CHAPTER 4

EVALUATION OF AN ^{15}N -LABELED MONOCLONAL ANTIBODY (MAB) AS AN INTERNAL STANDARD FOR QUANTITATIVE GLYCOMICS

Abstract

Monoclonal antibodies (mAbs) are currently essential biopharmaceutical products, and most FDA-approved therapeutical mAbs are Immunoglobulin (IgG) class. Numerous studies have established the fact that differential glycosylation of IgGs has a significant impact on the efficacy of these products, including target specificity, *in vivo* half-life and activity.¹ Hence, the examination of the glycan moiety of IgGs can be critical to the product quality control and can be used to further improve the therapeutic effectiveness of this class of molecules. Here, we introduced a liquid chromatography-mass spectrometry (LC-MS) based method for comparative glycomics analysis of IgG N-glycans using ^{15}N -labeled mAb as reference. The reference was produced from cell culture with metabolic incorporation of stable isotope labels into glycans, so the labeled reference and the sample can be mixed prior to all sample preparation procedures. With this approach, it can not only greatly reduce the quantitation errors caused by instrument response, but can also avoid the bias due to sample handling and processing.

Introduction

MAbs have become one of the most successful therapeutic strategies for cancer treatments by virtue of their ability to specifically targeting cancer cells while simultaneously

sparing normal tissues.²⁻⁴ MAbs and their derivatives are now key drug modalities in the pharmaceutical industry.^{5,6} The BCC Research reported that the global market for therapeutic mAb was about \$44.6 billion in 2011, and it is expected to reach \$58 billion in 2016 with a compound annual growth rate (CAGR) of 5.3% in expectation of the rollout of at least eight new therapeutic mAb products during the forecast period.

As of today's market, there are over 20 FDA approved antibody therapeutics which are of the IgG subclasses.⁷ These molecules are made up of two heavy chains and two light chains, which are held together and folded via intra and inter-chain disulfide bonds. The average molecular weight for each of the light and heavy chains is about 25 kDa and 50 kDa, respectively. Except for the peptide chains, mAbs have an additional modification with N-glycans, which are attached to ASN-297 in the fragment crystallizable (Fc) part on each of the heavy chains. Although it is a small part of the antibody molecule, the presence and composition of these glycans can greatly affect the bioactivity of mAbs. For example, the lack of core-fucoses on the N-glycans may cause drastic enhancement of antibody-mediated cellular cytotoxicity. Also, sialylation of the N-glycans determines the immunosuppressive properties of IgGs from human blood.⁸ The heterogeneity of glycans present in recombinant glycoproteins is often controlled by different host cell lines, growth and expression conditions, and media compositions.⁹ Therefore, qualitative and quantitative analysis of therapeutic glycoprotein glycans is critical for quality control of batch-to-batch variations in pharmaceutical industries.

Mass spectrometry (MS) coupled with high performance liquid chromatography (HPLC) techniques have become a prevalent tool for glycomics studies.¹⁰⁻¹² Sinha and his colleagues compared six LC-MS methods for quantitating N-glycans from recombinant IgGs, which were based on the intact protein, the Fc fragment was produced by limited proteolysis with Lys-C, the

IgG heavy chain was produced by reduction, the Fc/2 fragment was produced by limited proteolysis and reduction, and the glycosylated tryptic fragment and enzymatically released N-glycans were produced through the use of PNGase F. Despite the loss of information on the site of the protein-carbohydrate bond, the N-glycan release assay is still considered the standard for glycomics analysis.¹³

The general sample preparation workflow for the N-glycan release assay includes mAbs purification from the cell culturing medium, enzymatical release of N-glycans, and chemical derivatization (reductive amination, permethylation, etc.) before LC-MS analysis. One major drawback to this procedure is the differences that can be created from one sample to another, such as a different yield for the mAbs purification, incomplete N-glycan release, varied labeling efficiency, or sample loss during clean-up. Thus, a suitable internal standard is essential for the accuracy of quantitative glycomics analysis of mAbs. Recently, the Orlando and Wells research groups introduced an *in vivo* labeling strategy for glycomic studies of cultured cells, which was termed IDAWG (Isotopic Detection of Amino sugars With Glutamine).¹⁴ This approach introduced the ¹⁵N isotope labeling into all the amino sugars, including GlcNAc, GalNAc, and sialic acids through their biosynthetic pathway in cell culture. Hence, the labeled species can be processed together with the analyte and serve as an internal standard for quantification. Here, we explored the labeling method for mAbs from cell culture production by the same principle. With the success of labeling mAb N-glycans with ¹⁵N, the heavily labeled species has been utilized as an internal standard for comparative quantification of N-glycans by LC-MS.

Experimental Section

Materials. Human serum, trypsin (TPCK treated), ^{15}N -L-glutamine (98 atom %), ^{15}N -ammonium chloride (98 atom %) and procainamide hydrochloride were purchased from Sigma. Ammonium bicarbonate, ammonium formate, formic acid (for LC-MS) and sodium cyanoborohydride were purchased from Fluka. Acetonitrile (ACN, HPLC grade) was purchased from Fisher. PNGase F (Glycerol free) was purchased from New England Biolabs (NEB). HiTrap Protein G HP columns were purchased from GE Healthcare. Octadecyl (C18) disposable extraction columns were purchased from J. T. Baker. PD MiniTrap G-10 was purchased from GE Healthcare. Other reagents were analytical grade.

Protein G purification of ^{15}N labeled mAb from cell culture. A 25 mL sample with ^{15}N -labeled mAb in Tris solution (pH=8.0, as received from the provider) was applied to the Protein G column that had been equilibrated with 20 mM sodium phosphate buffer (pH=7.3). The column was washed 5 times with the binding buffer (20 mM sodium phosphate) and then the desired product eluted with 3 mL x3 elution buffer (0.1 M glycine-HCl, pH=2.5). The mAb sample was immediately neutralized with 1 M Tris-HCl buffer (pH=9.0) and then lyophilized to serve as an internal standard.

Protein G purification of IgG from human serum with spiked ^{15}N -mAb. The dried ^{15}N -labeled mAb from the previous step was re-dissolved in 500 μL binding buffer (20 mM sodium phosphate, pH=7.3), and an individual 50 μL aliquot of this reference was spiked into 10 μL , 25 μL , 50 μL , 100 μL and 250 μL human serum samples (referred to by the relative ratio of “5:1”, “2:1”, “1:1”, “1:2” and “1:5”, respectively) and well mixed. Additionally, two control samples which contained a 50 μL aliquot of the purified ^{15}N -mAb or 50 μL human serum only

were prepared as well. These seven samples were purified individually to extract the IgGs utilizing the Protein G column as described above.

N-glycan release and purification. The human serum IgG with ^{15}N -mAb samples were first digested with trypsin (the amount was adjusted accordingly to the sample amount; 10 μg trypsin for the 50 μL human serum sample). After incubation at 37 $^{\circ}\text{C}$ overnight, the enzyme was deactivated by heating at 100 $^{\circ}\text{C}$ for 10 min. For enzymatical release of N-glycans, a 2 μL aliquot of PNGase F was added to the 50 μL human serum, and the enzyme amount for other samples was adjusted accordingly. The reaction was carried out at 37 $^{\circ}\text{C}$ overnight and the released N-glycans were purified with a C18 SPE column. The eluates containing N-glycans were subsequently dried on a lyophilizer.

Procinamide (ProA) labeling of free N-glycans. The labeling of the glycans was carried out by following Klapoetke's procedure¹⁵ with a small modification for the sialylated glycans as described below.¹⁶ The labeling solution was freshly prepared with 108 mg/mL procainamide hydrochloride and 63 mg/mL $\text{Na}[\text{BH}_3(\text{CN})]$ in dimethyl sulfoxide (DMSO)/acetic acid at a ratio of 7:3 by volume. A 40 μL aliquot of the labeling solution was added to each of those seven samples individually. The mixtures were incubated at 37 $^{\circ}\text{C}$ overnight in darkness. To clean-up the excess labeling reagent, MiniTrap G-10 size exclusion columns were used following the user's guide. The eluate, containing fluorescently labeled N-glycans, was lyophilized and stored at -20 $^{\circ}\text{C}$ for analysis.

LC-SRM-MS quantitation of ProA labeled N-glycans. A Nexera UFLC (Shimadzu) LC system was utilized in this study. For the N-glycan separation, the Halo Penta-HILIC columns were kindly provided by Advanced Materials Technology (2.1 mm x 15 cm, 2.7 μm , Wilmington, DE). The separation was carried out at a flow rate of 0.4 mL/min at 60 $^{\circ}\text{C}$ with a

mobile phase A as 95% H₂O/ACN with 50 mM ammonium formate and mobile phase B as pure ACN. A linear gradient of 78% mobile phase B to 48% mobile phase B in 75min was applied for the LC runs. The UV signal for the ProA tag was detected at a wavelength of 300 nm. The ProA labeled sample mixtures were dissolved in 50 μ L 78% ACN, and triplicate analysis was performed for each sample with a 5 μ L injection each time.

For MS detection, a 4000 Q-Trap (AB SCIEX) mass spectrometer was operated in scheduled selected reaction monitoring (SRM) mode. The GlcNAc with the ProA tag at the reducing end was chosen as a universal transition for all the N-glycans, which gave an m/z at 441.4 for the light species and an m/z at 442.3 for the ¹⁵N-labeled reference. A collision energy (CE) of 70 V and a declustering potential (DP) of 40 V were decided to be optimal. The programmed retention time for each transition was determined by a regular SRM run (shown in **Table S4.1**) and the detection window for each transition was set as 5 min. Q1 resolution was set as “Low”, however, Q3 resolution was set as “Low”, “Unit” or “High” to investigate the effect on quantification. All the samples were analyzed in triplicate with each condition.

Results and discussions

Overall concept and experimental workflow. The concept of using the ¹⁵N-labeled mAb as a glycome reference for relative quantitation of IgG N-glycans by SRM is illustrated in **Figure 4.1**. The ¹⁵N-labeled mAb were generated by cell culture production. After purified with Protein G affinity column, the same amount of ¹⁵N-labeled mAb was spiked into different amount of human serum sample to serve as an internal standard for relative quantitation. The mixtures subsequently underwent a general glycomics workflow for sample preparation. Triplicate LC-SRM-MS experiments were carried out for each sample. The quantitation of

relative glycan abundances across different samples was based on the peak area ratios ($^{14}\text{N}/^{15}\text{N}$) of predetermined SRM transitions (**Table S4.1**). It is worth noting that the ^{13}C isotope has a small contribution to the artificial ^{15}N detection; also, the incomplete incorporation of ^{15}N might cause under-estimation of the ^{15}N sample amount within each sample. To overcome these problems, an in-house developed mathematical algorithm was used during the data analysis. Details for the mathematical method are revealed in supporting information (**Appendix C**).

^{15}N incorporation efficiency for mAb from cell culture production. The N-glycans from both human serum IgG and ^{15}N mAb were prepared as described in the experimental part. The incorporation of ^{15}N into the N-linked glycans of mAb from cell culture was investigated by comparing the FT-ICR MS spectra of the ProA labeled N-glycans released from either the regular IgG sample or the ^{15}N -labeled mAb. The spectra of the most abundant N-glycans from mAb are shown in **Figure 4.2**. For the ^{15}N -labeled mAb sample, a minor peak was observed before the monoisotopic peak for the fully ^{15}N -labeled monoisotopic specie. The under-labeling ratio was calculated based on the isotopic distribution from the experimental data (in **Appendix C**). Each of the N-glycans from the reference has four ^{15}N incorporation sites. For each site, the under-labeling ratio was only 3.83~4.47% in average, which indicated the success of the labeling strategy with the 98% ^{15}N -glycosamine.

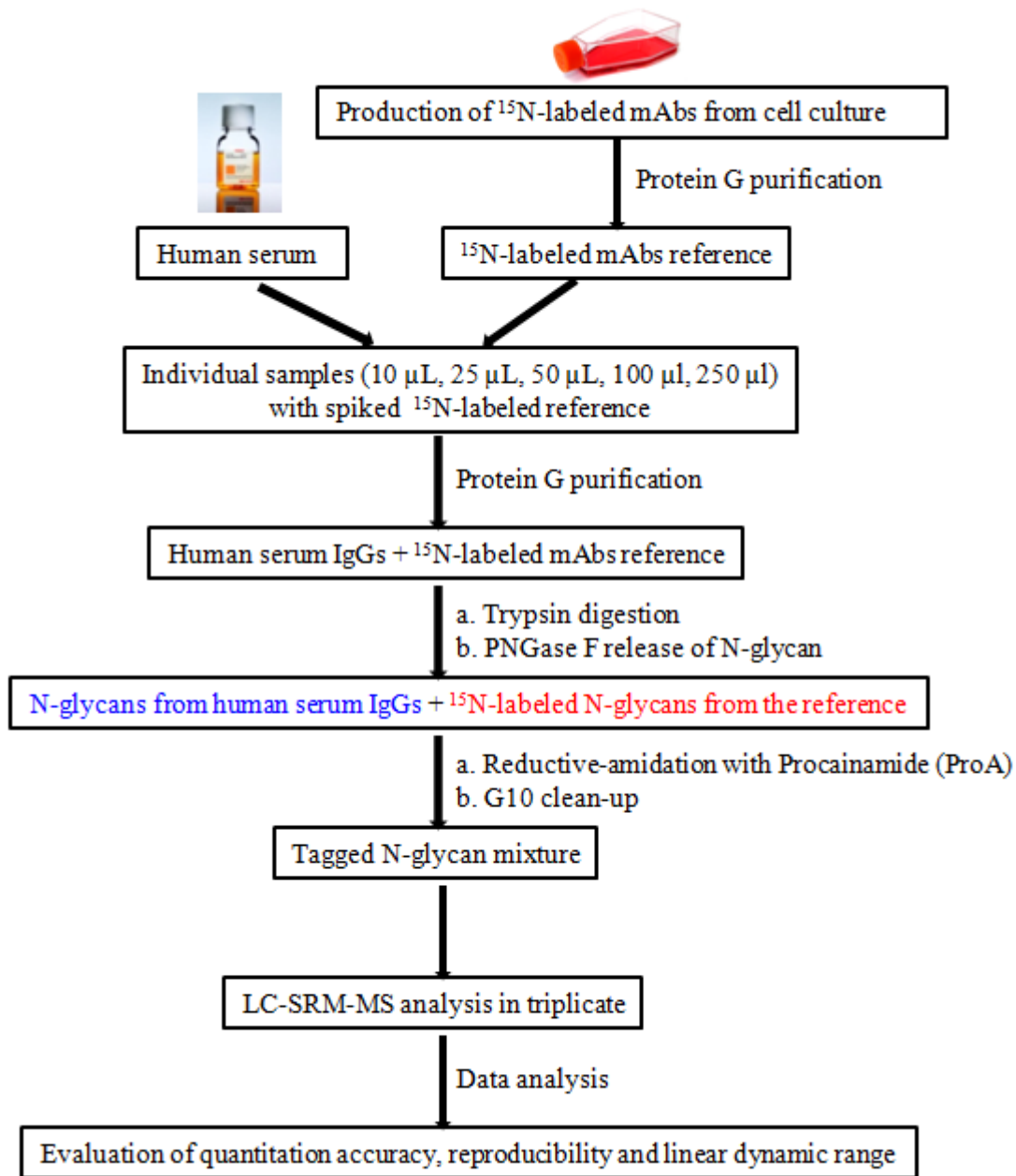


Figure 4.1. Overall conceptual workflow for the use of ¹⁵N-labeled mAb reference for SRM Quantitation. The same amount of ¹⁵N-labeled mAb was spiked into different amounts of human serum as a reference before Protein G purification to minimize the error caused by parallel sample handling processes.

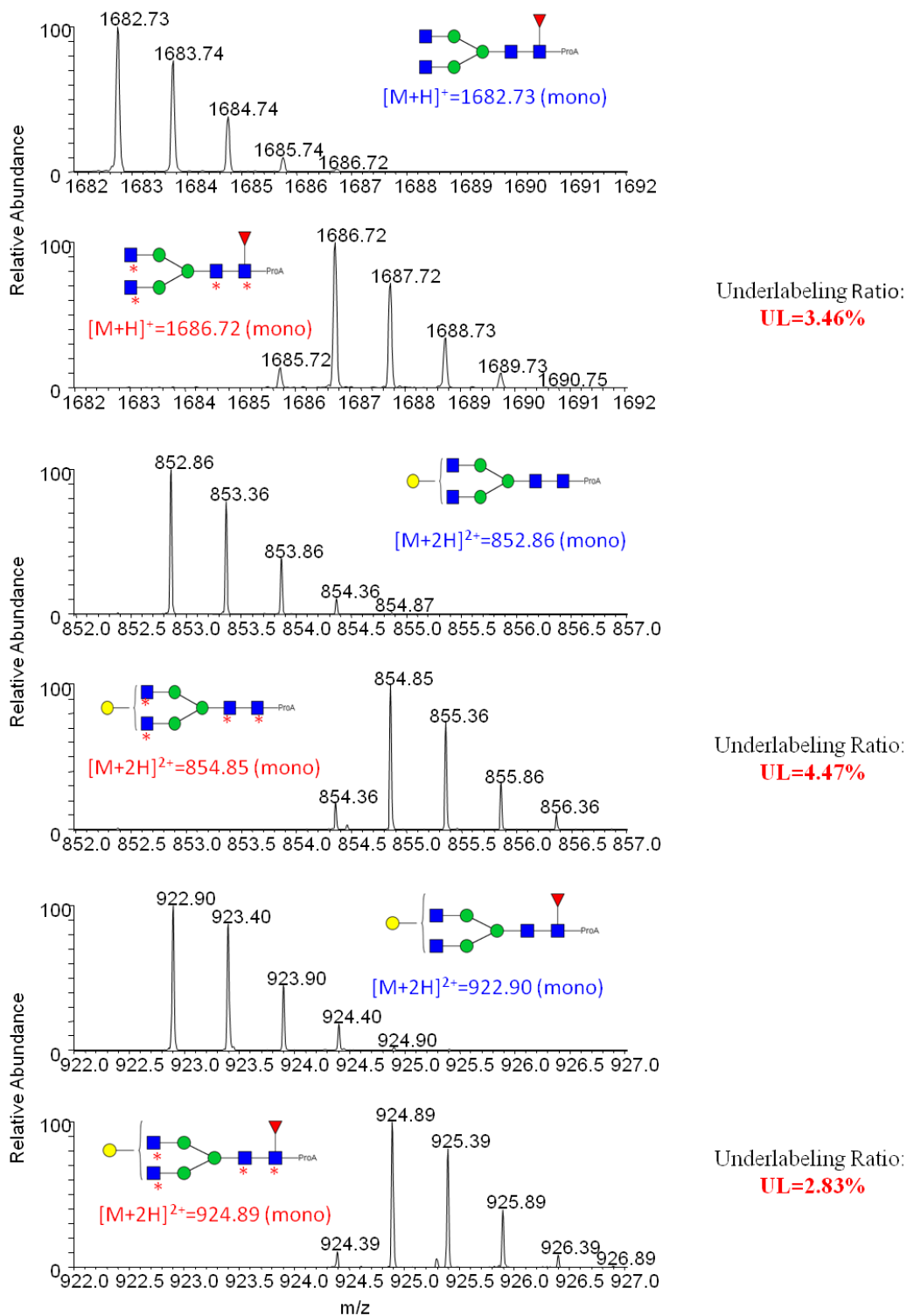


Figure 4.2. Labeling efficiency for the ¹⁵N-labeled mAb. Spectra were acquired by FT-ICR MS at the resolution of 10,000. (The “*” indicated the location of ¹⁵N incorporation.)

N-glycan profiling using LC-SRM-MS for human IgG and ^{15}N -labeled mAb. For glycan profiling, a Q1 full MS scan was carried out with HILIC separation to determine the transitions and retention time for both samples. Then the SRM experiments were conducted with the transitions listed in **Table 4.1** with the human IgG sample and the ^{15}N -mAb sample separately. The most abundant N-glycans identified from each sample is shown in **Figure 4.3** and **Figure 4.4**. For the human IgG sample, twelve major N-glycans were observed with two sets of isomers which had the same compositions. Comparison of the two samples revealed they shared five major N-glycans, which including one isomer set. For those five N-glycans in common, each of them would serve as an internal standard for the corresponding N-glycan for comparative quantification. The most abundant N-glycan F1A2 (Fuc1GalNAc4Man3Gal2) from the ^{15}N -labeled mAb would serve as an internal standard for all the other unique N-glycans from human serum IgG for comparative quantitation.

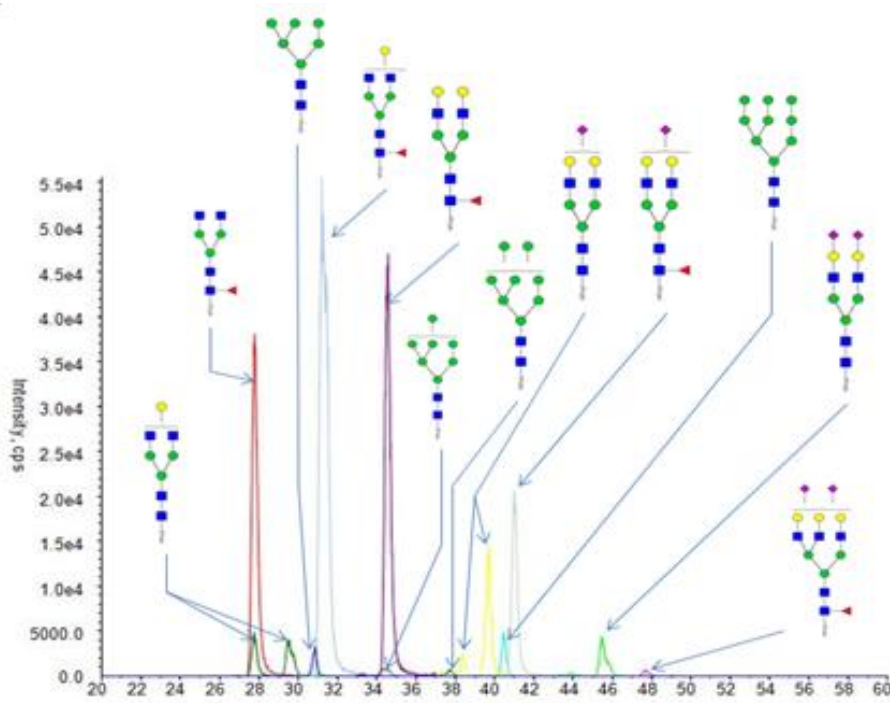


Figure 4.3. N-glycan profiling from human serum IgG.

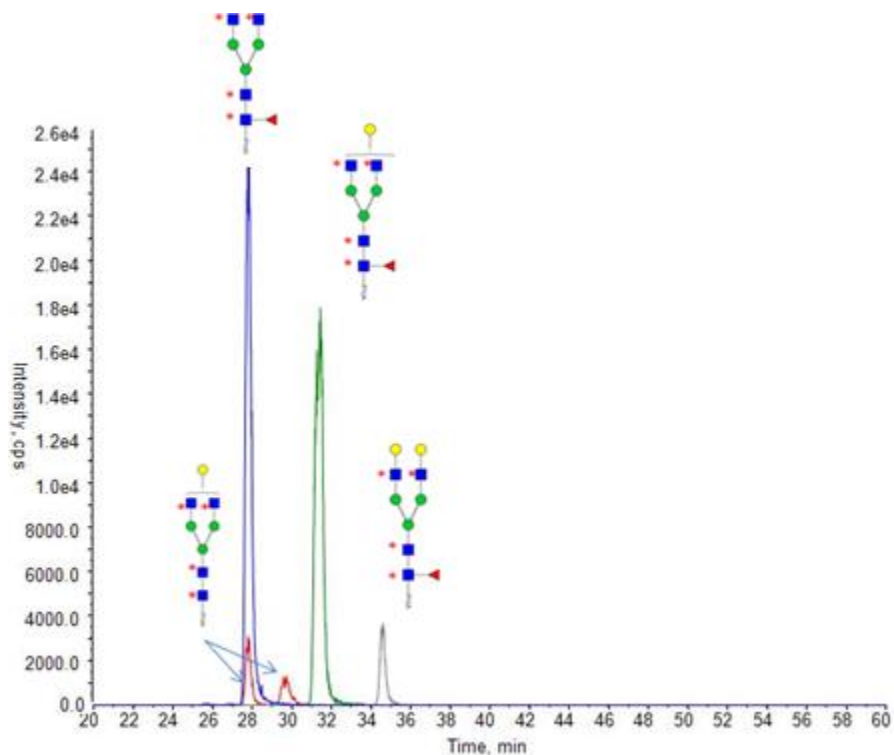


Figure 4.4. N-glycan profiling from ^{15}N -labeled mAb.

SRM quantitation of N-glycans with the ^{15}N references. Figure 4.5 exemplifies the SRM quantification of N-glycans with the ^{15}N reference. The experiments were carried out with the Q1 resolution as “Low” (1.1 Th FWHM) and the Q3 resolution as “Unit” (0.7 Th FWHM). The SRM transitions are listed in Table S4.1. Figure 4.5A shows the extracted SRM traces for glycan F1A2 at the transitions of 842.3/441.3 and 844.3/442.3. Although this sample was from pure human serum IgG, a very small amount of 844.3/442.3 (the red trace) was observed, which could be contributed by the ^{13}C isotope as an artificial ^{15}N isotope. The relative ratio of the heavy species over the total species was 1.55%. Figure 4.5B shows the extracted SRM traces for glycan F1A2 at the transitions of 842.3/441.3 and 844.3/442.3 from pure ^{15}N -labeled mAb sample. A small amount of 842.3/441.3 (the blue trace) was observed, which could be

contributed by the under-labeling species of the ^{15}N -labeled mAb. Thus, the under-labeling ratio (UL) for this N-glycan could be calculated based on the relative ratio of the under-labeling species over the total abundance of the two transitions, which gave a value of 4.74%.

Although the labeling efficiency for this approach is higher than 95%, an artificial detection of the unlabeled species becomes significant when the sample amount is much lower than the reference. *Vice versa*, the artificial detection of the labeled species becomes significant when the sample amount is much higher than the reference due to the overlapping of the isotopic peaks. This would give some error when seeking to comparatively quantitate the sample and reference by the peak areas. To solve this problem, a mathematic approach was utilized to get a more accurate calculation with those factors taken into consideration. The following equations were used to correct the abundance ratios ($^{14}\text{N}/^{15}\text{N}$).

Firstly, the ratio of ^{13}C isotopic contribution (I) to the heavy species can be calculated from the unlabeled sample only,

$$I = \frac{A_{\text{heavy}/442.3}}{A_{\text{light}/441.3} + A_{\text{heavy}/442.3}} \times 100\% \quad (\text{Equation 4.1})$$

Then, the underlabeling ratio (UL) of the ^{15}N labeling can be calculated from the labeled reference only,

$$UL = \frac{A_{\text{light}/441.3}}{A_{\text{light}/441.3} + A_{\text{heavy}/442.3}} \times 100\% \quad (\text{Equation 4.2})$$

Hence, the relative abundance of the analyte over the reference can be calculated from the mixed sample (details described in supporting material **Appendix C**),

$$R\left(\frac{^{14}\text{N}}{^{15}\text{N}}\right) = \frac{A_{\text{light}/441.3} - (A_{\text{light}/441.3})(UL) - (A_{\text{heavy}/442.3})(UL)}{A_{\text{heavy}/442.3} - (A_{\text{light}/441.3})(I) - (A_{\text{heavy}/442.3})(I)} \quad (\text{Equation 4.3})$$

$A_{\text{light}/441.3}$ and $A_{\text{heavy}/442.3}$ are the measured peak areas for unlabeled transition (light) and the ^{15}N -labeled transition (heavy) for each structure.

Figure 4.5C-G shows extracted traces for transitions of 842.3/441.3 and 844.3/442.3 from samples of 10 μL , 25 μL , 50 μL , 100 μL and 250 μL human serum spiked with the same amount of reference. To compare the abundance of each of the N-glycans across the five human serum samples, the ratio of $^{14}\text{N}/^{15}\text{N}$ was converted into a relative abundance format. This was accomplished by dividing the ratio of $^{14}\text{N}/^{15}\text{N}$ from individual analyses by a common denominator, namely the averaged ratio of $^{14}\text{N}/^{15}\text{N}$ across the triplicate analyses with the 50 μL human serum sample. Accordingly, theoretical relative ratios of 1:5, 1:2, 1:1, 2:1 and 5:1 were corresponded to 10 μL , 25 μL , 50 μL , 100 μL and 250 μL samples of human serum, respectively. For the SRM experiment, the resolution of Q1 was set as “Low”, and the resolution of Q3 was set as “Unit”. For the five N-glycans present in both human serum and ^{15}N -labeled mAb, the comparative quantitation was conducted by using the references with the same structures; for all the other N-glycans present in human serum but not in the ^{15}N -labeled mAb, the N-glycan ^{15}N -F1A2 was chosen as the reference for comparative quantitation. All the results were normalized based on the 50 μL human serum sample (**Table 4.1**). For all the 13 most abundant N-glycans in human serum, the average maximum error was 10.36% from the 250 μL serum sample. **Figure 4.6** showed that a linear dynamic range was achieved within 25 fold of sample amount with an R^2 value of 0.9995.

With the awareness of limited resolving power of quadrupole mass detector, the SRM experiments were performed with the Q3 resolution at “low”, “Unit” and “High”. However, when the Q3 resolution was set as “low”, it has difficulties to differentiate the mass/z of 441.3 (light species) and 442.3 (heavy species), which makes it impossible for relative quantitation. On

the other hand, the accuracies for relative quantitation were similar with the Q3 resolution at “Unit” or “High” (Table S4.2), though the signal intensity was about 10 folds higher with the resolution at “Unit” than “High”. Hence, the Q3 resolution set as “Unit” is more appropriate for this quantitative approach.

Table 4.1. Relative quantitation using ¹⁵N-labeled mAb reference.

N-glycans		Normalized ratio				
Simplified Representation	Composition	10 μ L	25 μ L	50 μ L	100 μ L	250 μ L
F1A2/ ¹⁵ N-F1A2	Fuc1GlcNAc4Man3	0.206	0.515	1.00	1.93	4.43
A2G1/ ¹⁵ N-A2G1 (iso1)	GlcNAc4Man3Gal1	0.207	0.497	1.00	1.88	4.63
A2G1/ ¹⁵ N-A2G1 (iso2)	GlcNAc4Man3Gal1	0.209	0.518	1.00	1.88	4.63
F1A2G1/ ¹⁵ N-F1A2G1	Fuc1GlcNAc4Man3Gal1	0.210	0.520	1.00	1.90	4.31
F1A2G2/ ¹⁵ N-F1A2G2	Fuc1GlcNAc4Man3Gal2	0.233	0.539	1.00	1.85	4.481
M7/ ¹⁵ N-F1A2	GlcNAc4Man7	0.216	0.483	1.00	2.10	5.09
M8/ ¹⁵ N-F1A2	GlcNAc4Man8	0.206	0.524	1.00	1.89	4.49
M9/ ¹⁵ N-F1A2	GlcNAc4Man9	0.179	0.467	1.00	2.02	4.98
A3G3S2/ ¹⁵ N-F1A2	GlcNAc5Man3Gal3SA2	0.199	0.515	1.00	2.17	4.71
A2G2S1/ ¹⁵ N-F1A2 (iso1)	GlcNAc4Man3Gal2SA1	0.1895	0.528	1.00	2.01	4.51
A2G2S1/ ¹⁵ N-F1A2 (iso2)	GlcNAc4Man3Gal2SA1	0.203	0.517	1.00	1.97	4.74
F1A2G2S1/ ¹⁵ N-F1A2	Fuc1GlcNAc4Man3Gal2SA1	0.199	0.468	1.00	1.86	4.42
A2G2S2/ ¹⁵ N-F1A2	GlcNAc4Man3Gal2SA2	0.203	0.516	1.00	1.97	4.74
Average		0.204	0.508	1.00	1.96	4.62
SD		0.0153	0.0225	0	0.0992	0.224

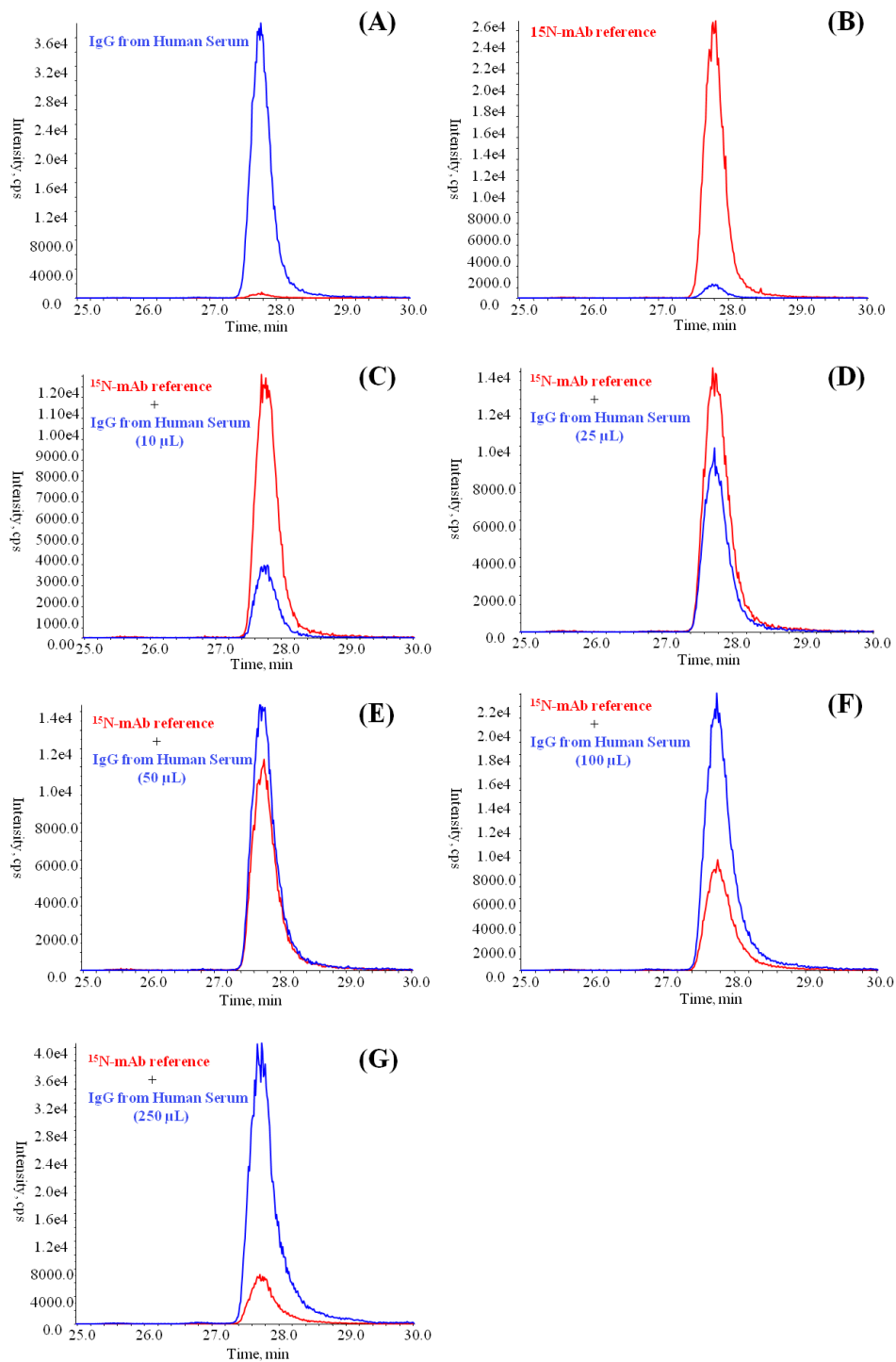


Figure 4.5. SRM quantification with the ^{15}N reference. Extracted ions with m/z at 842.3 (blue traces) and 844.3 (red traces) from different amounts of human serum IgG samples with spiked ^{15}N -labeled mAb reference.

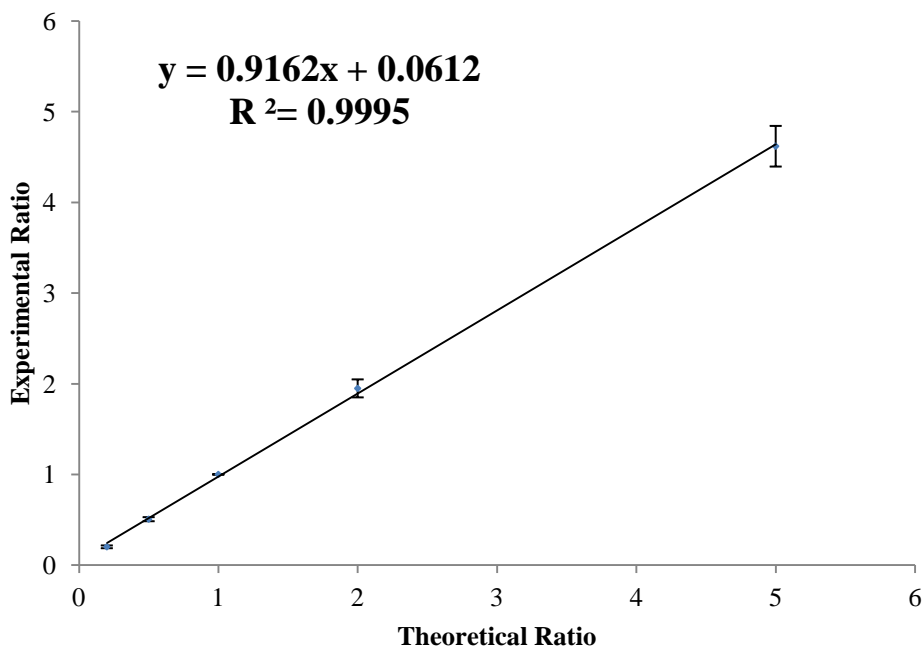


Figure 4.6. Dynamic range of quantitation with ¹⁵N-labeled mAb reference.

Comparison of the methods for quantitative glycomics with/without internal standards. Figure 4.7 shows the results of relative quantitation of the most abundant N-glycans from human serum IgG from 10 μ L, 25 μ L, 50 μ L, 100 μ L and 250 μ L samples, which are normalized with the 50 μ L sample. The red dashed lines represent results which are identical with the theoretical ratios, 0.2, 0.5, 1, 2 and 5, respectively. Without using any internal standards, it is observed that the response wasn't linear among the sample range from 10 μ L to 250 μ L samples. Furthermore, the maximal error for some N-glycans could go up to 50%. Moreover, there was a significant underestimation for the N-glycan amounts from the 250 μ L sample (Figure 4.7A). A possible explanation is that the decreased efficiency of the protein G column used for affinity purification of the IgGs from whole human serum, by re-using it over the

sample process may cause a more severe sample loss towards the 250 μL human serum due to its large amount. An alternate explanation is that the incomplete release of N-glycans by PNGase F, which might be dependent on the glycan structural differences and the amounts. Of course, each step of the sample preparation and detection may contribute to other errors. However, the results could be greatly improved by using the ^{15}N -labeled mAb as an internal standard, as shown in **Figure 4.7B**. A linear response for all the N-glycans among the different samples was observed. Additionally, the maximal error for all the quantitatively measured N-glycans was below 10%. By applying the ^{15}N -labeled mAb internal standard prior to the sample preparation, it can compensate for all the variances, such as the recovery from the affinity purification for IgGs, which could possibly be caused by each step of sample preparation. Furthermore, we theorize that using a glycoprotein as internal standard is likely to minimize the error caused by the PNGase F release efficiency.

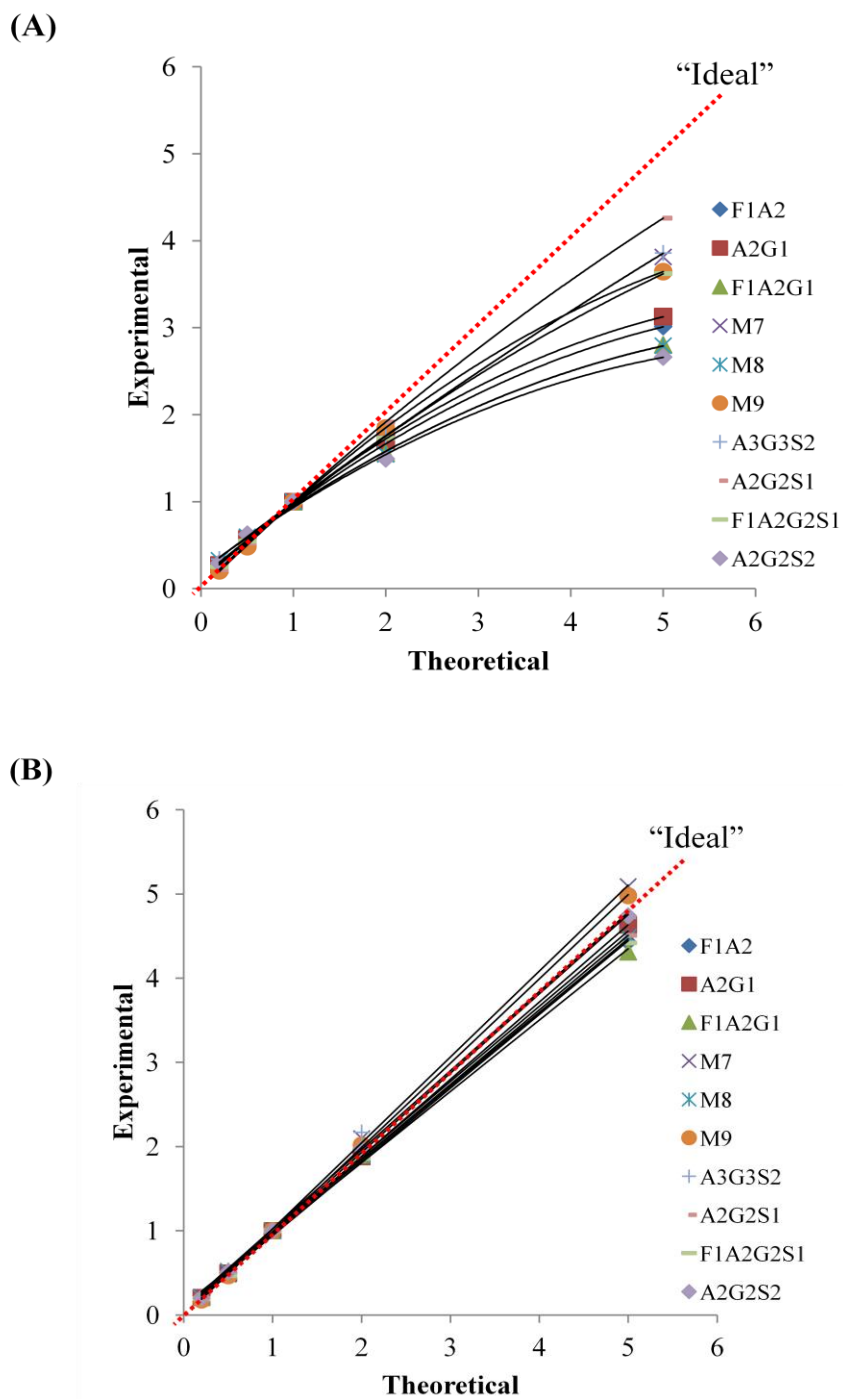


Figure 4.7. Comparison of the methods for quantitative glycomics. (A) Relative quantitation of human serum IgG N-glycans without internal standards; (B) Relative quantitation of human serum IgG N-glycans with ^{15}N -labeled mAb as an internal standard.

Conclusions

Here, we evaluated the use of ^{15}N -labeled mAb as an internal standard for quantitative glycomics. It demonstrated that increased accuracy and analytical precision in the relative quantitation of human serum IgG N-glycans can be achieved with the ^{15}N -labeled mAb reference. One of the advantages of this approach is that the sample and reference are mixed together prior to MS based glycomics, thereby subjecting glycans from both the sample and reference to the exact same experimental conditions during the protein G purification, N-glycan release, ProA labeling, and sample clean-up steps. Therefore, eliminating the discrepancies caused not only by MS detection, but also by the different losses encountered during sample handling and processing. With this study, we have confirmed that the ^{15}N -labeled mAb can provide an effective internal standard for quantitative glycomics on the glycoprotein level. Furthermore, this reference can be added to any glycoprotein sample and can be used with any glycomic work-up/analysis. Moreover, in this proof of concept study, we established that this labeling method is suited for SRM-based quantitation, providing a linear dynamic range of at least 5 orders of magnitude for quantitative glycomics.

Acknowledgements

The ^{15}N -labeled mAb reference as internal standard for quantitation was provided by GlycoScientific, LLC.

References

- (1) Lux, A.; Nimmerjahn, F. *Adv Exp Med Biol* 2011, 780, 113.
- (2) Scott, A. M.; Allison, J. P.; Wolchok, J. D. *Cancer Immun* 2012, 12, 14.

- (3) Chartrain, M.; Chu, L. *Curr Pharm Biotechnol* 2008, 9, 447.
- (4) Imai, K.; Takaoka, A. *Nat Rev Cancer* 2006, 6, 714.
- (5) Buss, N. A.; Henderson, S. J.; McFarlane, M.; Shenton, J. M.; de Haan, L. *Curr Opin Pharmacol* 2012, 12, 615.
- (6) Chames, P.; Van Regenmortel, M.; Weiss, E.; Baty, D. *Br J Pharmacol* 2009, 157, 220.
- (7) Patel, R.; Johnson, K.; Andrien, B.; Tamburini, P. *American Journal of Biochemistry and Biotechnology* 2013, 9, 206.
- (8) Huhn, C.; Selman, M. H.; Ruhaak, L. R.; Deelder, A. M.; Wuhrer, M. *Proteomics* 2009, 9, 882.
- (9) Jang, K.-S.; Kim, Y.-G.; Gil, G.-C.; Park, S.-H.; Kim, B.-G. *Analytical biochemistry* 2009, 386, 228.
- (10) Morelle, W.; Michalski, J. C. *Curr Pharm Des* 2005, 11, 2615.
- (11) Zaia, J. *OMICS* 2010, 14, 401.
- (12) Wuhrer, M. *Glycoconj J* 2013, 30, 11.
- (13) Sinha, S.; Pipes, G.; Topp, E. M.; Bondarenko, P. V.; Treuheit, M. J.; Gadgil, H. S. *J Am Soc Mass Spectrom* 2008, 19, 1643.
- (14) Fang, M.; Lim, J. M.; Wells, L. *Curr Protoc Chem Biol* 2010, 2, 55.
- (15) Klapoetke, S.; Zhang, J.; Becht, S.; Gu, X.; Ding, X. *J Pharm Biomed Anal* 2010, 53, 315.
- (16) Melmer, M.; Stangler, T.; Schiefermeier, M.; Brunner, W.; Toll, H.; Rupprechter, A.; Lindner, W.; Premstaller, A. *Anal Bioanal Chem* 2010, 398, 905.

CHAPTER 5

TARGETED GLYCOMICS BY SCHEDULED SELECTED REACTION MONITORING (SRM) COUPLED WITH HILIC SEPARATION FOR GLOBAL GLYCAN PROFILING

Abstract

The development of glycomics increasingly requires consistent detection and quantification of glycans from complex sample pools, which is only partially accomplished by current glycomics approaches. Taking the predictability of HILIC separation based on the “-OH” group numbers and the advantage of selected reaction monitoring (SRM) to achieve high sensitivity and selectivity, we report here a targeted discovery glycomic method by scheduled SRM detection coupled with HILIC separation of procainamide labeled N-glycans. In this proof-of-principle study, we validated the method by profiling N-glycans from whole human serum, which gave 115 different N-glycans with 74 unique masses. With application of a single internal standard at the beginning of the sample preparation, the maximum error observed was under 20% (for 109 out of 115 N-glycans from human serum) for comparative quantitation with a dynamic range over 5 orders of magnitude.

Introduction

In the last a couple of decades, mass spectrometry (MS) techniques coupled with liquid chromatography (LC) separation have become predominant in the field of glycomics. With the development of chromatographic and mass spectrometric techniques for glycomics, LC-MS

methods are capable of generating data on glycan pools expressed in biological systems that are rich in information. For glycan identification, the retention time of the unknown glycan is usually converted to glucose units (GU) and compared to a database of experimental values with known glycans to obtain a preliminary structure assignment.¹ For further elucidation of glycan structures, data acquired by MS and exoglycosidase array will give a near-complete characterization of the glycan structure.² A major problem of glycomic studies based on LC-MS techniques lies in the interpretation of analytical data, which is very time-consuming and highly dependent on the expertise of the researchers. Taking into consideration of the complex non-templated biosynthesis of glycans, large heterogeneity and diversity of glycan structures, large dynamic range of abundance, and relatively low response to mass spectrometers, the development of automated and highly sensitive analytical strategies capable of generating consistent structural and quantitative glycomics analysis is highly demanded.

Due to the low response of native glycans to mass spectrometers, derivatization strategies are highly recommended before LC-MS analysis, such as reducing end labeling through reductive amination. Among various reductive amination reagents, 2-AB labeling of glycans before MS has been the most widely adopted approach and thoroughly studied.^{1,3} However, procainamide (ProA) is favored in our study due to the enhancement of glycan MS response compared to the former.⁴ Moreover, the ProA labeled N-glycans are UV visible, which allows accurate quantitative measurement of individual glycans when it coupled with LC separation. Currently, N-glycan separation by liquid chromatography can be achieved by reverse-phase (RP), porous graphitized carbon (PGC) and hydrophilic interaction chromatography (HILIC). Our previous studies showed that HILIC can not only resolve N-glycans based on the compositions, but also on isomeric structures, such as difference in linkages. Furthermore,

another important characteristic of HILIC separation lies in the predictable retention times according to the size and composition of oligosaccharides.⁵⁻⁷

Recently, a targeted proteomic strategy was introduced for quantitative proteomics studies, which applies selected reaction monitoring (SRM, plural form: multiple reaction monitoring, MRM) mass spectrometry detection.⁸⁻¹⁰ Targeted proteomics by using SRM on a triple quadrupole mass spectrometer has advantages in specificity and sensitivity as well as a much greater dynamic range (over 5 orders of magnitude) over other quantitative proteomics.¹¹ However, the application of SRM to proteomics is limited to detection of samples that have a sufficient amount of information available, due to the requirement of pre-determined transitions and the enormous number of peptides/transitions from complex biological samples. Unlike a proteome, a glycome is composed of a limited number of glycan structures due to the availability of glycotransferases and the restriction of glycosylation machinery, especially when it comes to a given glycan class within certain species.^{12,13} Using SRM for glycomics analysis, the overall number for transitions can be further reduced by building them with only the compositions. More conveniently, for N-glycans, the fragment ion can be chosen from the commonly shared core structures without making efforts for individual structures. Although modern mass spectrometers are capable of detection a few hundred transitions “simultaneously” while sacrificing the dwell time for each transition to get enough data points across the chromatographic peak, a better solution is by doing scheduled SRM. With scheduled SRM, transitions of the targeted analytes are monitored only around the expected retention time, which gives higher dwell times for each transition to get better signal-to-noise (S/N) especially for low abundant analytes.¹⁴ This intelligent use of retention time not only results in more transitions (multiple transitions for a single composition to get better structure information) during the LC run, but it also gives more

reliable detection by auto-matching the retention time of each transition. Here, we aimed at developing a targeted glycomics strategy by scheduled SRM detection coupled with HILIC separation to achieve highly sensitive and consistent identification and quantification of large numbers of glycans from different systems, such as single proteins and whole serum samples.

Experimental Section

Materials. Standards used for method generation included dextran 5000 (generously provided by collaborator), bovine fetuin (“F”, Sigma), asialofetuin (“AF”, Sigma), ribonuclease B (“RB”, Sigma), egg white ovalbumin (“OV”, Worthington Biochemical Corporation) and human α 1-acid glycoprotein (“ α 1-Acid gp”, Sigma). Human serum (“HuSe”, Sigma) was used for method validation as a complex biological sample.

Instrumentation. A Nexera UFLC (Shimadzu) LC system was utilized in this study. For the N-glycan separation, the Halo Penta-HILIC columns were kindly provided by Advanced Materials Technology (2.1 mm x 15 cm, 2.7 μ m, Wilmington, DE). The SRM experiments were carried out on a 4000 Q-Trap (AB SCIEX) mass spectrometer.

N-glycan release and ProA labeling. N-glycans from 1 mg glycoproteins (F, AF, RB, OV, α 1-Acid gp) were released by PNGase F and then purified on C18 SEP columns. All the released N-glycan samples and dextran ladder were labeled with ProA with the previously described protocol. For relative quantitation, 0.2 nmol of maltopentaose reference was spiked into 20 μ L, 50 μ L, 100 μ L, 200 μ L, 500 μ L and 1000 μ L human serum sample respectively to serve as internal standard. The well-mixed samples then were subjected to the standard protocol for glycan preparation. Briefly, each sample was digested overnight at 37 $^{\circ}$ C by trypsin (10 μ g trypsin for 20 μ L human serum sample, proportionally). After deactivating trypsin by heating

samples at 100 °C for 5 min, PNGase F (0.5 µL, 2 µL, 4 µL, 8 µL, 20 µL and 40 µL) was added into the digested samples directly and N-glycan release was carried out at 37 °C overnight. The oligosaccharides (maltopentaose and released N-glycans from HuSe) were purified on C18 SEP columns. All the samples were labeled with ProA with the previously described protocol.

Human serum N-glycan discovery and quantitation with LC-SRM-MS experiments.

For scheduled SRM experiments, 318 N-glycan transitions were included in the list with predicted retention times by using the “-OH” group number model. The SRM acquisition was in positive ion mode with Q1 and Q3 at unit resolution. Collision energies (CE) were set as 70 V and declustering potential (DP) was set as 40 V for N-glycans. Other parameter settings: curtain gas, 25 units; spray voltage, 5500 V; temperature, 450 °C; ion source gas flow rates 1 and 2 both at 25 units; collision gas, 4 units.

Each of the ProA labeled human serum N-glycan samples were re-dissolved with 10 µL H₂O, and then 30 µL acetonitrile (ACN) was added to bring up the sample to 75% ACN/ H₂O for the HILIC separation under the following conditions: (i) columns: 2 x 15 cm Penta-HILIC; (ii) mobile phase A: 94.9% H₂O/5% ACN/0.1% formic acid with 100 mM ammonium formate (pH=4.3); mobile phase B: 100% ACN; (iii) gradient: 0-4min, 70% B-69% B; 4-100 min, 69%-64.5% B; 100-175 min, 64.5%-53.5% B; 175 min-180 min, 53.5% B-20% B; 180 min-195 min, 20%B; 195 min-196 min, 20% B-70%B; 196 min-220 min, 70% B. (iv) flow rate: 400 µL/min; (v) column temperature: 60 °C; (vi) UV wavelength: 300 nm. (vii) injection volume: 10 µL. All the samples were analyzed in triplicate for quantitation.

Results and discussions

Generation of scheduled SRM method. Step 1: Construction of SRM transitions

(Q1) A highly curated structural database for N-glycans was adopted from the Complex Carbohydrate Research Center at University of Georgia (GlycomeDB, <http://glycomics.ccrcc.uga.edu/qrator/>).¹⁵ Among those 888 approved N-glycans, 204 unique masses were determined by eliminating the N-glycans with NeuGc since it has been widely accepted that Neu5Gc cannot be synthesized in normal humans. In addition, our previous studies proved that N-glycans containing multiple sialic acids (SAs, such as Neu5Ac) can be highly resolved within the Halo-HILIC columns based on the number of α 2-3/ α 2-6 linkages. With such consideration, it was predetermined that 2 transitions were set for each of the N-glycans with 1 SA, 3 transitions were set for each of the N-glycans with 2 SAs, 4 transitions were set for each of the N-glycans with 3 SAs and 5 transitions were set for each of the N-glycans with 4 SAs (the highest number of SAs within structures from the database). Therefore, there were 318 transitions in total for the “human N-glycans”.

It is worth noting that multiple charged ions can be produced in ESI for an analyte. The full MS analysis of N-glycans showed that the most intense ion for each glycan is highly dependent on their molecular weights. The charge state of the most abundant ion for each glycan was determined experimentally as follows: singly charged ions for glycans with molecular weight (MW) less than 1500 Da; doubled charged ions for glycans with MW between 1500~2800 Da and triply charged ions for glycans with MW between 2800~5000 Da (as the highest MW in the database, with the modification of the ProA tag). Therefore, the Q1 m/z values were selected based on the molecular weights of the glycan compositions of interest and their corresponding charge states.

Step 2: Determination of the fragment ion (Q3). For proteomics, unique fragment ions (Q3) for each peptide were usually applied to achieve high specificity. However, the MS/MS data for every single glycan structure is limited due to the sample availability and sometimes it is impossible to find a unique fragment ion for the individual glycan of interest. Hence, the conserved fragment ion that are common in all the N-glycans was chosen as the Q3 marker ion. MS/MS experiments were performed on neutral and acidic glycans (**Figure 5.1**) with optimized collision energy to give the best signal for the targeted fragment ion (m/z at 400.7). Also, ion source optimization was carried out to decrease in-source decay for ProA-N-glycans which gave the declustering potential (DP) at 40 V (data not shown).

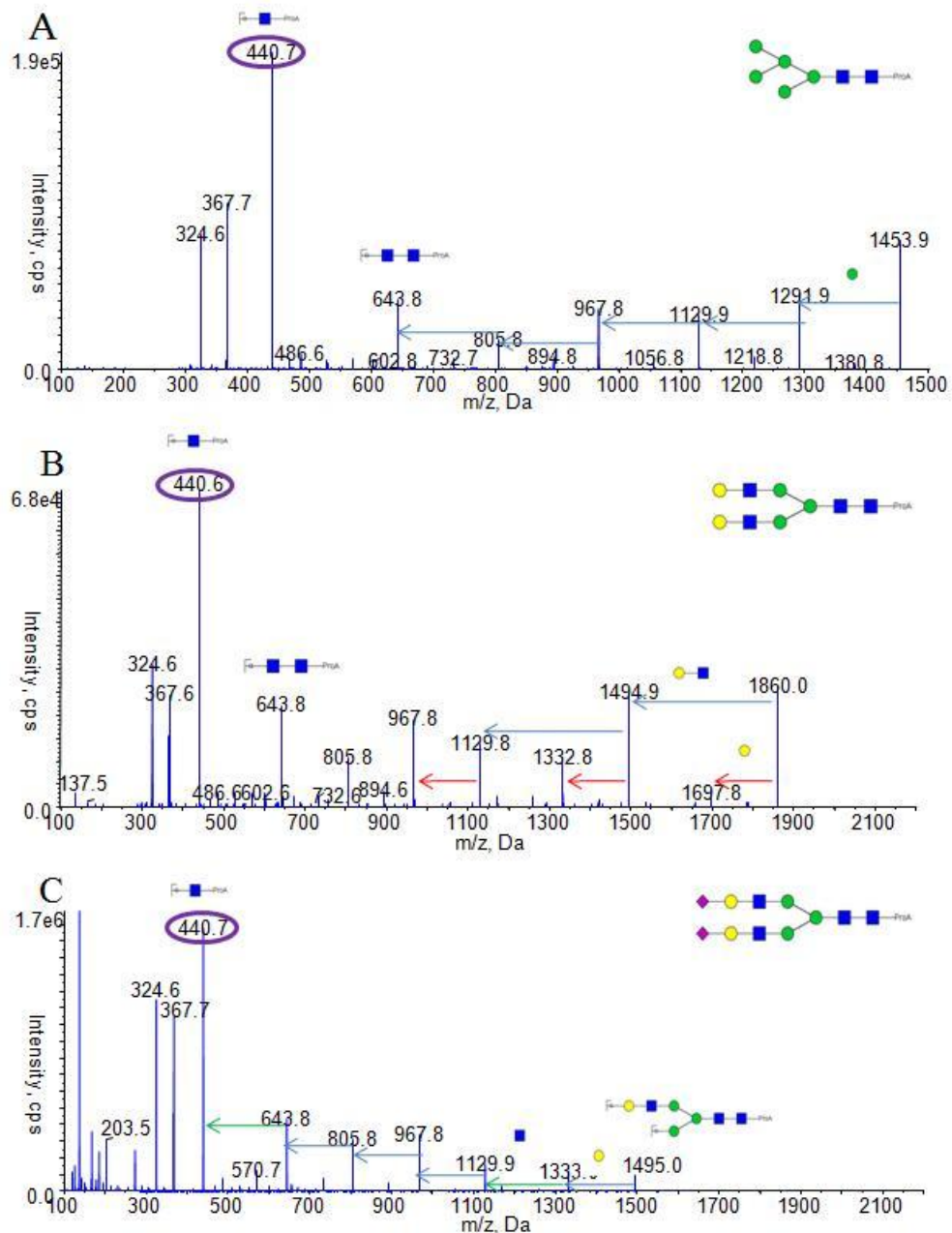


Figure 5.1. Fragmentation pathway for N-glycans on the 4000 Q-Trap mass spectrometer.

Collision energy was optimized for the best signal of the fragment with m/z at 440.7.

Step 3: Retention time prediction model for N-glycans (RT)

a. Oligosaccharides separation on multiple Penta-HILIC columns

ProA labeled dextran ladder was separated on two Penta-HILIC columns (15 cm) in series with segmented gradient: 0-4min, 70% B-69% B; 4-100 min, 69%-64.5% B; 100-175 min, 64.5%-53.5% B. The separation of the dextran ladder revealed that the retention time of oligosaccharides on the HILIC column was predominantly driven by the number of –OH groups (**Figure 5.2**) and a fourth-order polynomial distribution curve was fitted to the dextran ladder and used to correlate the number of –OH groups to retention times. The retention time can be calculated according to their respective number of “-OH” groups by the following equation:

$$y = 0.0000591751x^4 - 0.0123553000x^3 + 0.8786634696x^2 - 21.5532351061x + 179.1335320888 \quad \text{(Equation 5.1)}$$

where y is the retention time and x is the number of “-OH” groups.

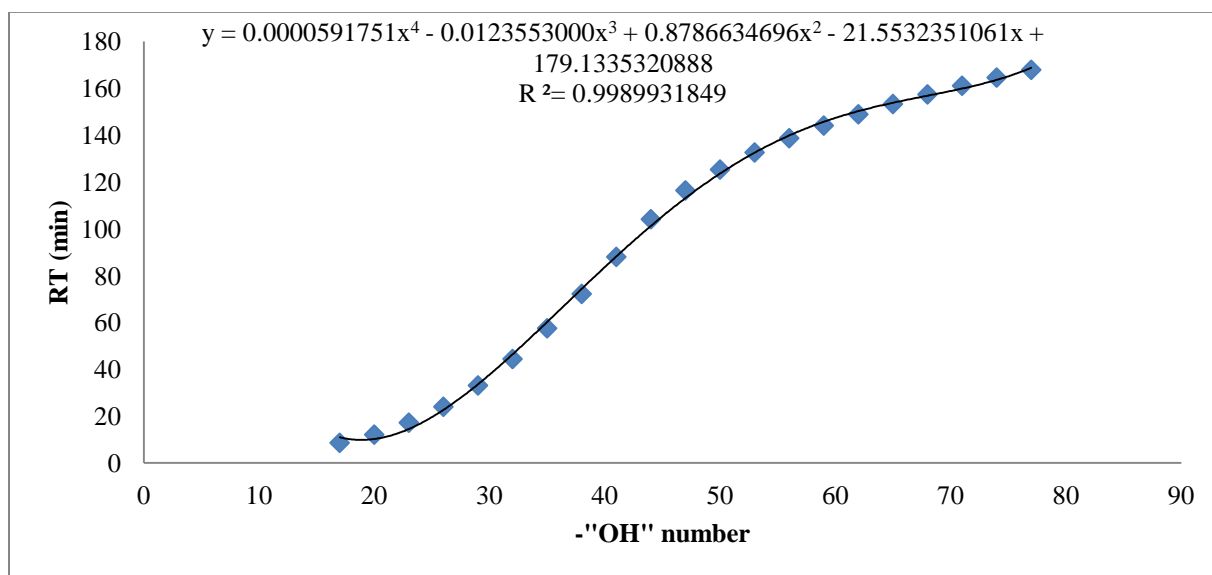


Figure 5.2. HILIC retention times of dextran ladder against the number of “-OH” groups.

b. Equivalent “-OH” number determination for monosaccharides with other functional groups

Each of the hexoses (Man, Glc and Gla) possesses 5 –OH groups and the Fuc has 4 –OH groups. However, other functional groups from monosaccharides such as HexNAc (GlcNAc and GalNAc) and sialic acid (Neu5Ac), the –NHAc, and –COOH may contribute differently to the retention on HILIC in terms of the “-OH” numbers. Furthermore, the equivalent “-OH” numbers for glycans different in α 2-3 and α 2-6 linked Neu5Ac needed to be adjusted as well. Hence, the equivalent “-OH” numbers for HexNAc, Neu5Ac/ α 2-3 and Neu5Ac/ α 2-6 were determined experimentally by using well characterized samples (AF, F, RB, OV, and α 1-Acid gp) as control. Firstly, retention time data for 96 identified N-glycans from the known samples were obtained on the HILIC column under the conditions described in **Step 3a**. Secondly, for HexNAc, the best fit for the equivalent “-OH” number was determined to be 4.0 (step size: 0.1, range 3-5) by comparing the experimental retention times and the calculated retention times by **Equation 5.1**, which gave the minimal variances for all the identified neutral N-glycans. Thirdly, with the equivalent “-OH” number as 4.0 for HexNAc, the equivalent “-OH” number for Neu5Ac/ α 2-3 was determined to be 7.0 (step size: 0.1, range 6-9) by using the identified N-glycans containing only Neu5Ac/ α 2-3. Lastly, the equivalent “-OH” number for Neu5Ac/ α 2-6 was determined to be 8.8 (step size: 0.1, range 6-9) by using the identified N-glycans containing both Neu5Ac/ α 2-3 and Neu5Ac/ α 2-6. The proposed “-OH” number for each monosaccharide is listed in **Table 5.1**. As demonstrated in **Figure 5.3**, a very good correlation was achieved between the calculated retention times and the experimental retention times (correlation coefficient 0.997, $R^2=0.9963$). Therefore, the predicted retention times for all the 318 SRM transitions can be obtained accordingly to the respective composition and the “-OH” number model for HILIC separation.

Table 5.1. Equivalent numbers of “-OH” group for different monosaccharides.

Monosaccharide	No. of “-OH”
Hex (Man, Glc, Gal)	5
HexNAc (GlcNAc, GalNAc)	4
Fuc	4
Neu5Ac (α 2-3 linkage)	7
Neu5Ac (α 2-6 linkage)	8.8

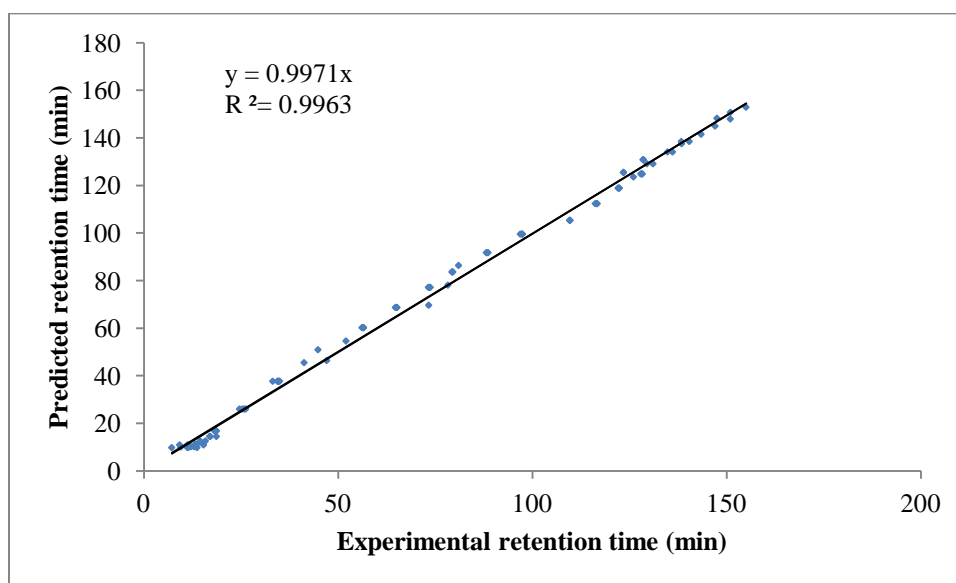


Figure 5.3. Experimental retention time vs. Predicted retention time by Equation 5.1 with well characterized N-glycans.

Evaluation of the LC-SRM-MS method. a. Increase of peak capacity by using multiple columns

The conventional HILIC separation of oligosaccharides was carried out by a single Penta-HILIC column (2.1 mm x 15 cm, 2.7 μ m) with a linear gradient of 78%B to 48% B in 75 min. The separation of the dextran ladder is shown in **Figure 5.4A**, which produced an average peak width of 0.45 min full width half maximum (FWHM) for GU3~GU27. The calculated peak capacity during the gradient time was 166.7 under such conditions. To increase the peak capacity for the LC system, two Penta-HILIC columns in series were applied with a linear gradient of 78%B to 48% B in 225 min after optimization, which gave an increased average peak width of 0.78 min at half maximum for the dextran ladder (**Figure 5.4B**). However, the use of two HILIC columns in series increased the theoretical peak capacity to 288.5 within the gradient time. Therefore, the double-column system was chosen in order to allocate all 318 transitions.

b. Gradient modification for optimal dwell time

For the 96 N-glycans from the known glycoproteins, the variances between predicted retention times and experimental retention times were among -4.4 min to +3.9 min for the double-column system with the linear gradient. Also, considering the 1.0 min peak width at the baseline and the reproducibility of the LC system, the detection window was set at 10 min for the SRM experiments. The concurrent SRM transitions at each time point during the LC run are illustrated in **Figure 5.5A**. It shows that the distribution of concurrent transitions was uneven during the whole run and that more transitions were monitored “simultaneously” in the middle of the run, with the largest number of 46.

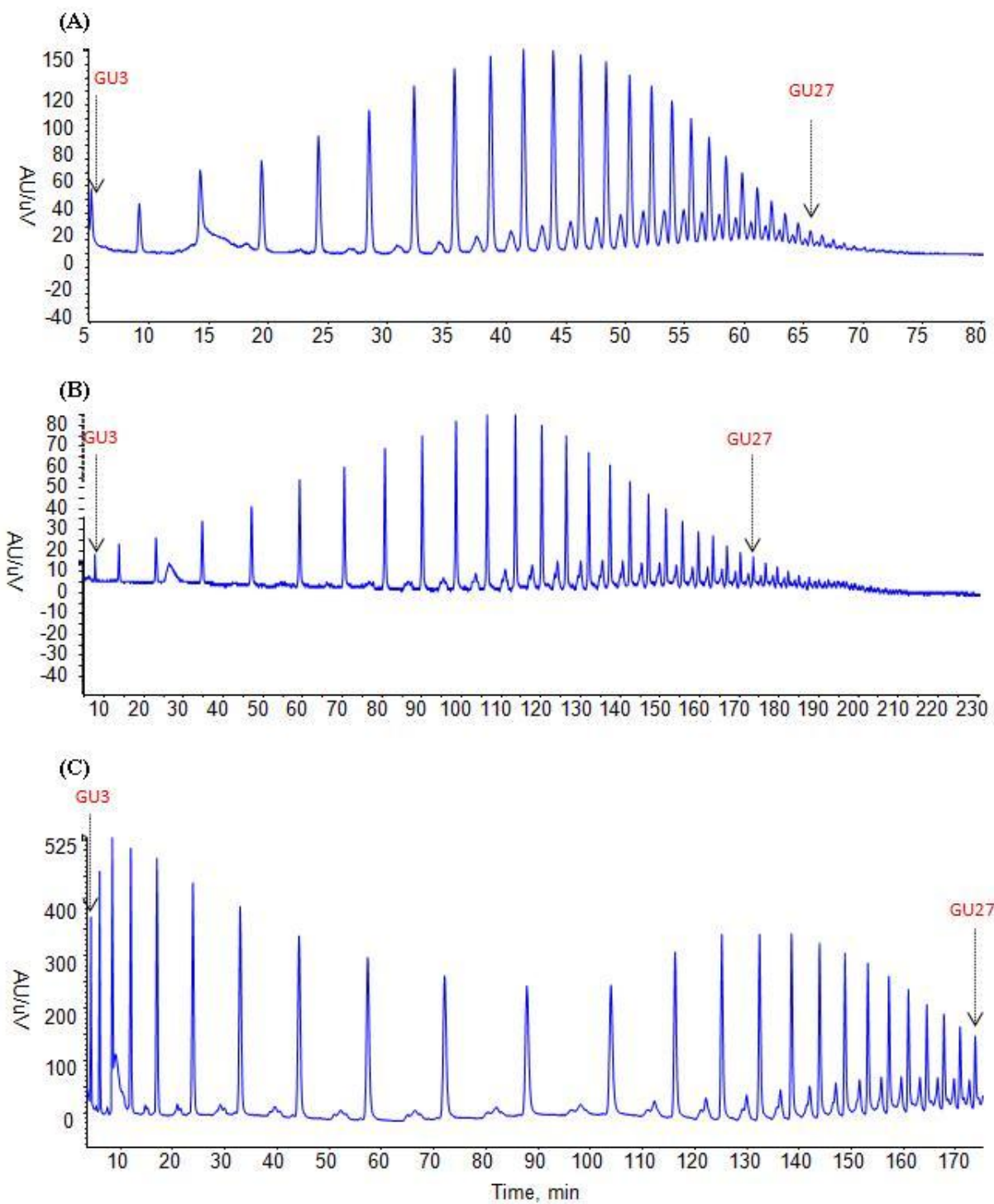
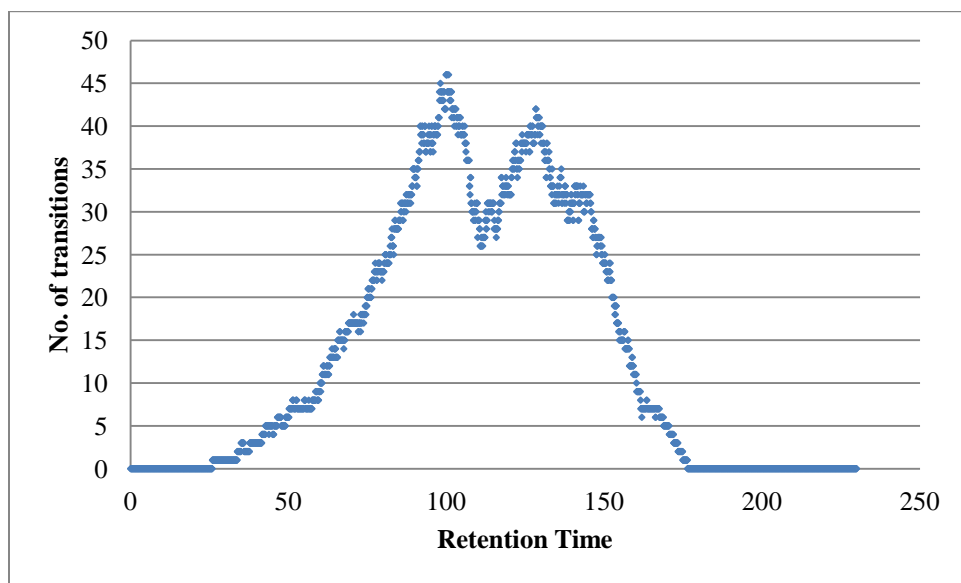


Figure 5.4. Dextran ladder separation under different LC conditions. (A) Single Penta-HILIC column with linear gradient; (B) Double Penta-HILIC columns with linear gradient; (C) Double Penta-HILIC columns with segmented gradient.

One of the essential factors for SRM scheduling is to decrease the number of concurrent SRM transitions monitored at any point in time, allowing both the cycle time and dwell time to remain optimal at high levels of SRM multiplexing. Therefore, the gradient was further optimized based on the transition distribution by DryLab. With such efforts, the gradient for the developed method contained three segments: 0-4 min, 70% B-69% B; 4-100 min, 69% B-64.5 % B; 100-175 min, 64.5% B-53.5% B. The separation of the dextran ladder is shown in **Figure 5.4C**, and the number of concurrent transitions is illustrated in **Figure 5.5B**. With the segmented gradient, the number of concurrent transitions was under 30 through the entire LC run without further prolonging the LC time.

Discovery of whole human serum N-glycans. The developed LC-SRM-MS method was applied to human serum samples to demonstrate its ability to identify a wide range of glycans in a complex sample (**Figure 5.6**). Due to the scheduling of the SRM experiments, the transitions would be detected only within the expected time range, which increase the reliability of the identification. From the 20 μ L human serum sample, 115 N-glycan structures were identified with 74 unique masses (**Table S5.1, Appendix D**), which were consistent with previous literature reports.^{16,17} Although a comprehensive characterization of all the structures wasn't fulfilled, the linkage information toward the Neu5Ac (α 2-6/ α 2-3) was revealed due to the retention time differences. Furthermore, the transition list was generated from GlycomeDB, which contains all the structures and annotations from all freely available databases with corrections. By referencing the discovered transitions to the database, it can significantly downsize the possibilities to the most likely existing structures and minimize the work of further structure confirmation/characterization. In addition, with SRM, specific transitions for the analytes can be monitored to investigate possible structures in further studies.

(A)



(B)

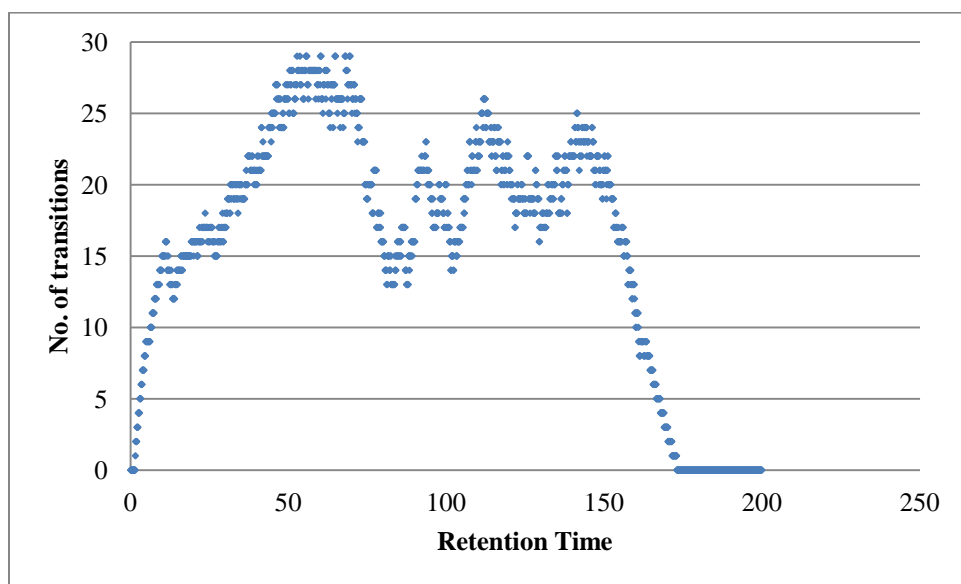


Figure 5.5. Number of concurrent SRM transitions during the LC gradient. (A) Double-column with linear gradient; (B) Double-column with segmented gradient.

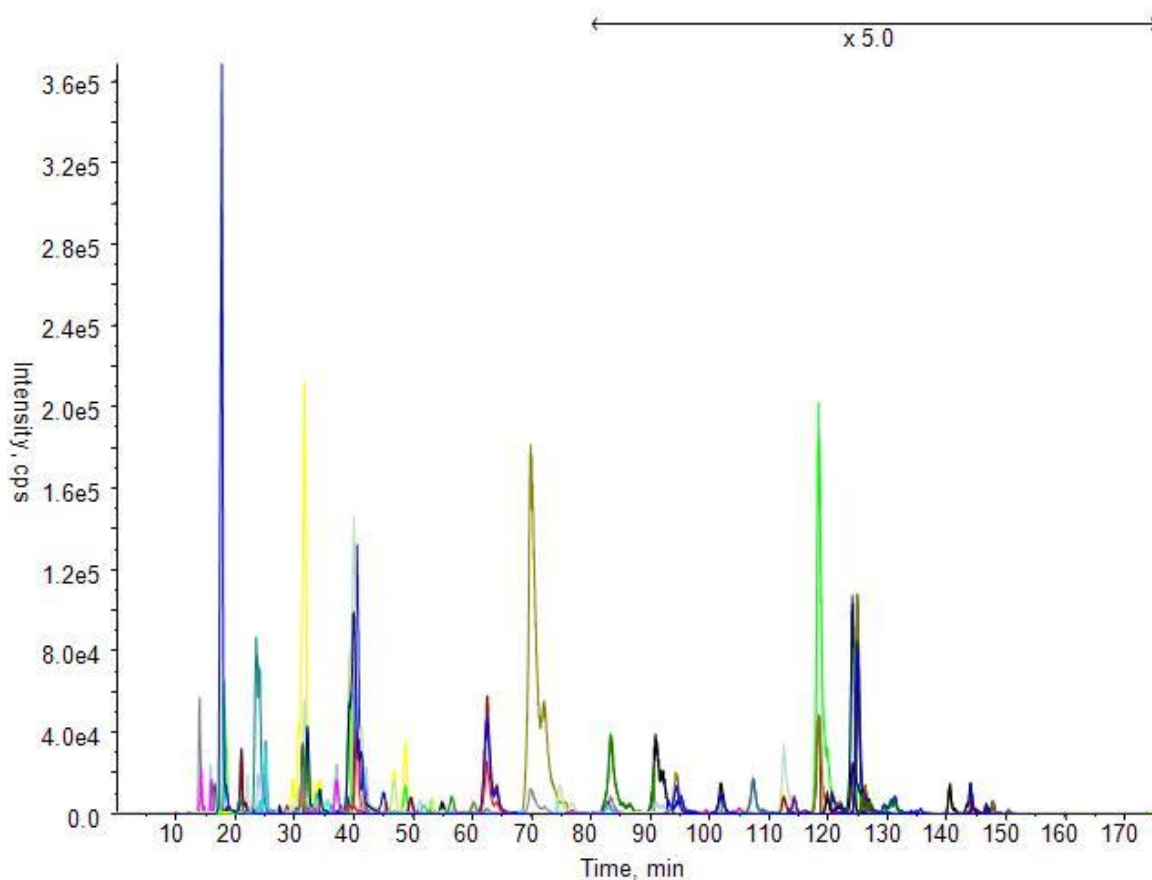


Figure 5.6. Targeted glycomics discovery for whole human serum N-glycans by HILIC LC-SRM-MS.

Relative quantitation of human serum N-glycans by SRM with single internal standard. The use of isotopic labeling is a “gold standard” for comparative quantitation, especially through *in vivo* approaches. However, the availability of isotopically labeled standards for the whole glycan pool is still under development. With the quantitative aspect of SRM experiment, we examined the possibility of using a single internal standard for comparative quantitation of a complex glycan pool, such as whole human serum N-glycans. By applying the maltopentaose as an internal standard from the first step of the sample preparation, it can

compensate for three major sources of error, including: differential sample loss during sample handling/processing, altered labeling efficiency for the ProA derivatives preparation, and variable instrument response from time to time.

For clarity, the individual glycan amounts from the 100 μL human serum sample were normalized as “1”. Therefore, the expected relative ratios for each glycan from 20 μL human serum, 50 μL human serum, 200 μL human serum, 500 μL human serum and 1000 μL human serum would be 0.2, 0.5, 2, 5, 10, respectively. The relative amount of each glycan can be calculated based on the following equation:

$$\text{Relative amount} = \frac{A_g}{A_{g100}} \times \frac{A_{m100}}{A_m}$$

where A_g is the peak area of a glycan in the measured sample, A_{g100} is the peak area of the corresponding glycan in the 100 μL human serum sample, A_{m100} is the peak area of the internal standard (maltopentaose) in the 100 μL human serum sample, and A_m is the peak area of the internal standard (maltopentaose) in the measured sample.

The results of relative quantitation for the 115 human serum N-glycans are shown in **Figure 5.7**. To examine the effect of using an internal standard on the reproducibility of LC-SRM-MS analysis, 3 replicates of the sample were analyzed for each glycan. The averaged coefficients of variation (CV) varied from 9.8% to 18.5% at 95% confidence (which means 109 out of 115 glycans were within the range), with the highest CV from the 1000 μL human serum sample. Thus, this study indicated that the SRM approach with a single internal standard provides an effective alternative to comparative glycomics.

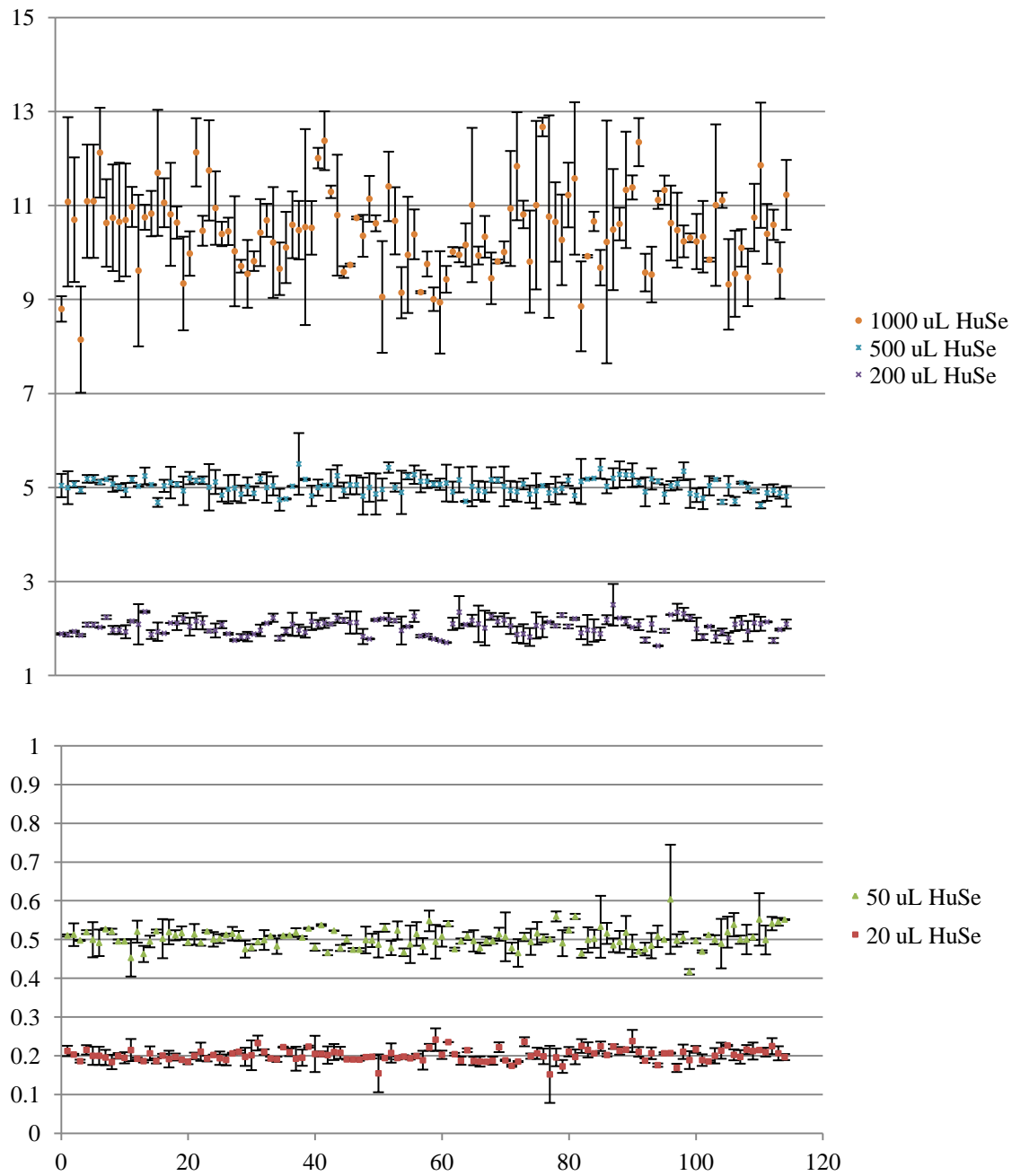


Figure 5.7. Relative quantitation of Human serum N-glycans by SRM with single internal standard.

Conclusions

Here, we developed a targeted glycomic approach to fulfill the requirement of large-scale analysis of diverse glycans by LC-SRM-MS. Also, a single internal standard was used to minimize the variability of sample preparation and MS analysis. Due to the sensitivity and specificity of SRM detection, the discovery of complex N-glycans from human serum was achieved based on the generation of a complete human N-glycan list. Also, with the predetermined retention time of each glycan composition for SRM scheduling, it provided further information regarding detailed structure characterization, such as Neu5Ac α 2-3/ α 2-6 linkages. Moreover, this LC-SRM-MS approach with a single internal standard provides a simple and cost-effective alternative for comparative glycomics.

References

- (1) Campbell, M. P.; Royle, L.; Radcliffe, C. M.; Dwek, R. A.; Rudd, P. M. *Bioinformatics* **2008**, *24*, 1214.
- (2) Roth, Z.; Yehezkel, G.; Khalaila, I. *International Journal of Carbohydrate Chemistry* **2012**, *2012*.
- (3) Royle, L.; Campbell, M. P.; Radcliffe, C. M.; White, D. M.; Harvey, D. J.; Abrahams, J. L.; Kim, Y. G.; Henry, G. W.; Shadick, N. A.; Weinblatt, M. E.; Lee, D. M.; Rudd, P. M.; Dwek, R. A. *Anal Biochem* **2008**, *376*, 1.
- (4) Klapoetke, S.; Zhang, J.; Becht, S.; Gu, X.; Ding, X. *J Pharm Biomed Anal* **2010**, *53*, 315.
- (5) Ahn, J.; Bones, J.; Yu, Y. Q.; Rudd, P. M.; Gilar, M. *J Chromatogr B Analyt Technol Biomed Life Sci* **2010**, *878*, 403.

- (6) Domann, P. J.; Pardos-Pardos, A. C.; Fernandes, D. L.; Spencer, D. I.; Radcliffe, C. M.; Royle, L.; Dwek, R. A.; Rudd, P. M. *Proteomics* **2007**, *7 Suppl 1*, 70.
- (7) Dreyfuss, J. M.; Jacobs, C.; Gindin, Y.; Benson, G.; Staples, G. O.; Zaia, J. *Anal Bioanal Chem* **2011**, *399*, 727.
- (8) Wolf-Yadlin, A.; Hautaniemi, S.; Lauffenburger, D. A.; White, F. M. *Proc Natl Acad Sci U S A* **2007**, *104*, 5860.
- (9) Lange, V.; Picotti, P.; Domon, B.; Aebersold, R. *Mol Syst Biol* **2008**, *4*, 222.
- (10) Zhang, H.; Liu, Q.; Zimmerman, L. J.; Ham, A. J.; Slebos, R. J.; Rahman, J.; Kikuchi, T.; Massion, P. P.; Carbone, D. P.; Billheimer, D.; Liebler, D. C. *Mol Cell Proteomics* **2011**, *10*, M110 006593.
- (11) Mani, D. R.; Abbatiello, S. E.; Carr, S. A. *BMC Bioinformatics* **2012**, *13 Suppl 16*, S9.
- (12) Cummings, R. D. *Mol Biosyst* **2009**, *5*, 1087.
- (13) Zhang, H.; Wang, Z.; Stupak, J.; Ghribi, O.; Geiger, J. D.; Liu, Q. Y.; Li, J. *Proteomics* **2012**, *12*, 2510.
- (14) Herrin, G. L.; McCurdy, H. H.; Wall, W. H. *J Anal Toxicol* **2005**, *29*, 599.
- (15) Ranzinger, R.; Herget, S.; von der Lieth, C. W.; Frank, M. *Nucleic Acids Res* **2011**, *39*, D373.
- (16) Aldredge, D.; An, H. J.; Tang, N.; Waddell, K.; Lebrilla, C. B. *J Proteome Res* **2012**, *11*, 1958.
- (17) Kronewitter, S. R.; de Leoz, M. L.; Peacock, K. S.; McBride, K. R.; An, H. J.; Miyamoto, S.; Leiserowitz, G. S.; Lebrilla, C. B. *J Proteome Res* **2010**, *9*, 4952.

CHAPTER 6

CONCLUSIONS

The ability to quantitatively determine changes is an essential component of comparative glycomics, and it can be accomplished by multiple strategies provided by this work.

The ^{18}O labeling approach introduces an isotopic label into the glycans prior to permethylation, which can eliminate errors caused by permethylation efficiency and after-clean-up. For MS analysis, this method can be adopted by labs equipped with MALDI/ESI-MS detectors that only need unit mass resolution. Also, this method is cost efficient and simple to implement, yet a powerful tool to the comparative glycomics toolbox.

Despite the advantages of permethylation for glycan analysis, the analysis of permethylated glycans has not yet been introduced into LC-MS based techniques due to the difficulties in separating isomeric glycan structures. On the other hand, the hydrophilic intrinsic characteristic of glycans has aroused great interest of HILIC separation techniques for glycomics analysis.

With a newly developed superficially porous Penta-HILIC material, chromatographic separation of glycans has been achieved for sialylated N-Glycan isomers differing in α 2-3 and α 2-6 linkages, and the relative quantitation of each sialic acid linkage isomer can be obtained from a straightforward LC-MS experiment. For MS analysis, an AB Sciex 4000 Q-Trap mass spectrometer is performed in SRM mode, which provides high selectivity, sensitivity, and large dynamic range for quantitation.

During the study of the SRM LC-MS approach for relative quantitation of SA linkage isomers, it was also revealed that relative quantitation by MS can be achieved for individual isomeric structures with the same glycan composition, but not applicable to individual structures among various compositions without an internal standard, due to the fact that the MS response varies from different glycan compositions. Therefore, an *in vivo* ¹⁵N labeling of mAb was harvested from cell culture by metabolic incorporation of stable isotope labels into glycans, so the labeled reference could serve as an internal standard for relative quantitation. Particularly, the ¹⁵N-labeled mAb can be an ideal internal standard for the glycomics investigation of mAb-based biopharmaceutical products. Moreover, they can be applied as an internal standard for comparative glycomics on the glycoprotein level.

Other than the object of interest oriented studies for comparative glycomics, such as the change of SA linkage ratios or the glycosylation level of mAb, investigators have been challenged to fulfill comprehensive glycomics studies of complex biological samples with minimum sample information provided. A hypothesis-driven experimental method is generated by utilizing the predictability of HILIC retention behavior for glycans and the knowledge of glycan biosynthesis pathways. As a proof-of-principle study, this targeted glycomics approach built a library of 318 well defined N-glycan structures with the predicted retention time by HILIC separation. This LC-SRM-MS method has been validated by profiling N-glycans from whole human serum, which gave 117 different N-glycans with 74 unique masses. With the application of a single internal standard at the beginning of the sample preparation, the maximum error observed was under 20% (for 109 out of 115 human serum N-glycans) with a dynamic range over 5 orders magnitude for relative quantitation. The ultimate goal for the targeted

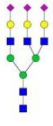
glycomics approach is to facilitate routine glycomics studies with increased selectivity, analytical precision and throughput.

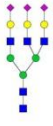
APPENDIX A

SUPPLEMENTAL INFORMATION TO CHAPTER 2:

A NOVEL METHOD FOR RELATIVE QUANTITATION OF N-GLYCANS BY ISOTOPIC
LABELING USING ^{18}O -WATER

Example for Mathematical Calculation of $^{18}\text{O}/^{16}\text{O}$ Ratio:



For , the measured relative intensities (%) of regular ^{16}O -N-glycan isotopic peaks were as follows:

$$R1=59.16, R2=97.68, R3=100, R4=64.56, R4=37.08, R5=16.11, R6=5.74$$

According to **Equation 2.1**,

$$p = \frac{59.16+97.68}{59.16+97.68+100+64.56+37.08+16.11+5.74} = 0.412$$

The measured relative intensities (%) of ^{18}O -N-glycan peaks were as follows:

$$U1=1.23, U2=6.2, U3+L1=63.58, U4+L2=100, U5+L3=96.43, U6+L4=64.11, U7+L5=33.27, \\ L6=10.6, L7=1.00$$

According to **Equation 2.2**,

$$UL = \frac{(1.23+6.2)/0.412}{1.23+6.2+63.58+100+96.43+64.11+33.27+10.6+1.00} = 0.056$$

The measured relative intensities (%) of ^{16}O and ^{18}O mixture peaks were as follows:

$$M1=31.59, M2=59.37, M3=94.09, M4=100, M5=70.89, M6=39.41, M7=17.8, M8=7.32$$

According to **Equation 2.3**,

$$\text{Ratio } (^{18}\text{O}/^{16}\text{O}) = \frac{(31.59+659.37+94.09+100+70.89+39.41+17.8+7.32)-(34.68+63.37)/0.412}{(34.68+63.37)/0.412 - (31.59+59.37+94.09+100+70.89+39.41+17.8+7.32)*0.056} = 1.012$$

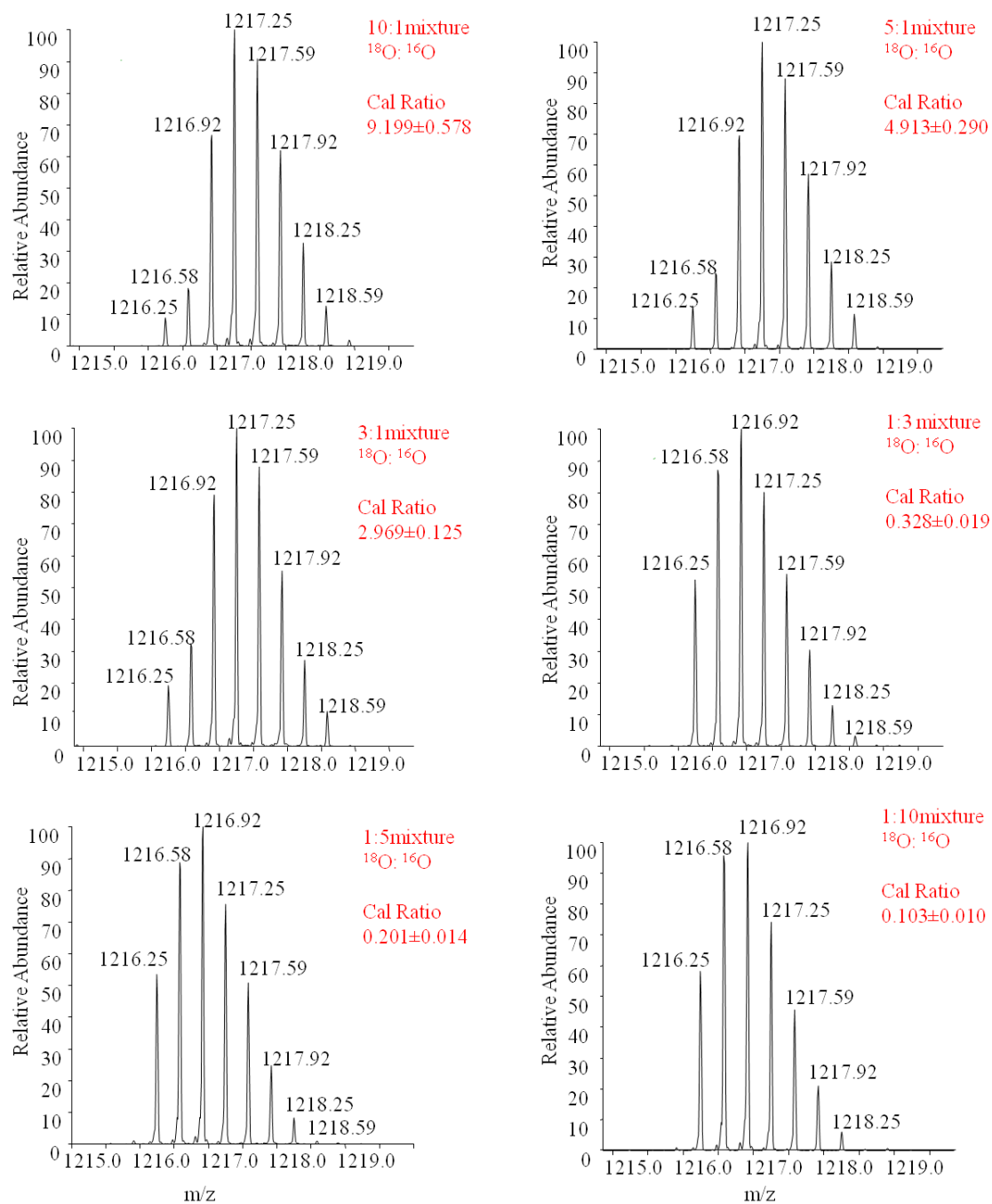


Figure S2.1. Quantitative analysis of fetuin N-glycan with ^{18}O -labeled internal standards at various ratios.

APPENDIX B

SUPPLEMENTAL INFORMATION TO CHAPTER 3:

AN LC-SRM APPROACH FOR THE SEPARATION AND QUANTITATION OF

SIALYLATED N-GLYCANS LINKAGE ISOMERS

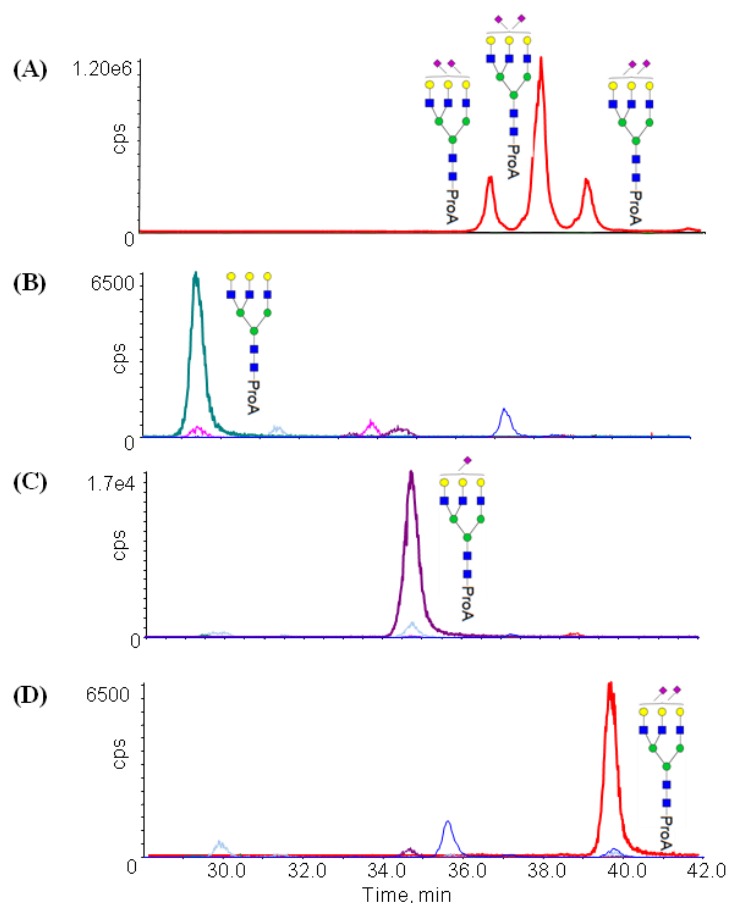


Figure S3.1. Sialidase S digestions for Tri-2SA fractions by SRM detection. (A) LC-SRM trace for Tri-2SA (m/z at 936.9) from analysis of the fetuin N-glycans. LC-SRM analysis illustrates (B) the disappearance of the red peak (Tri-2SA) and the appearance of the dark blue peak (Tri-0SA) after Sialidase S digestion for the first fraction; (C) the disappearance of the red peak (Tri-2SA) and the appearance of the purple peak (Tri-SA) after Sialidase digestion for the second fraction; and (D) no change of the red peak (Tri-2SA) after Sialidase S digestion for the third fraction. **Figures B-D** contain SRM traces for all three possible glycans resulting from this treatment, i.e., the Tri-0SA, Tri-SA and Tri-2SA, however the low levels make these difficult to see in all of the figures.

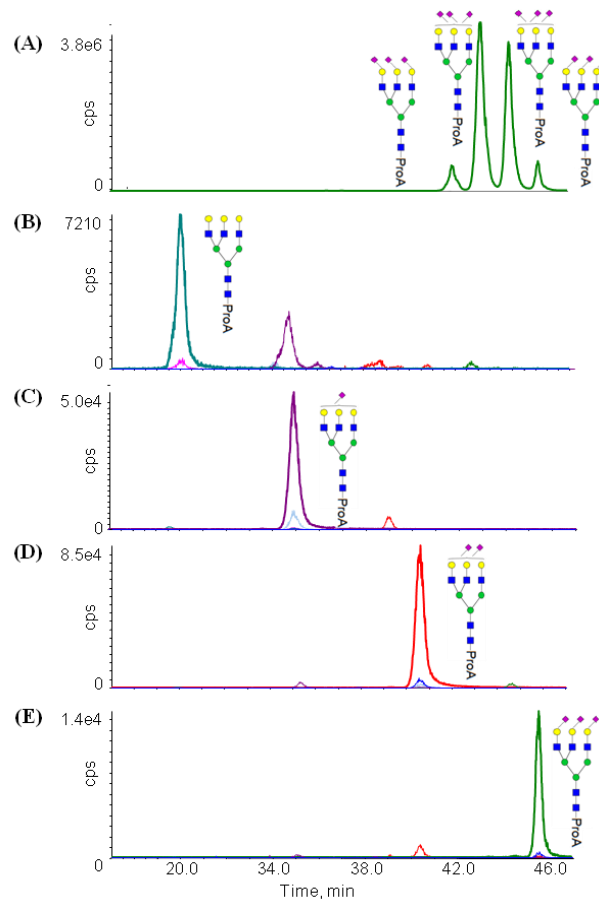


Figure S3.2. Sialidase S digestions for Tri-3SA fractions by SRM detection. (A) LC-SRM trace for Tri-3SA (m/z at 1033.9) from analysis of the fetuin N-glycans. LC-SRM analysis illustrates (B) the disappearance of the green peak (Tri-3SA) and the appearance of the dark blue peak (Tri-0SA) after Sialidase S digestion for the first fraction; (C) the disappearance of the green peak (Tri-3SA) and the appearance of the purple peak (Tri-SA) after Sialidase S digestion for the second fraction; (D) the disappearance of the green peak (Tri-3SA) and the appearance of the red peak (Tri-2SA) after Sialidase S digestion for the third fraction; and (E) no change of the green peak (Tri-3SA) after Sialidase S digestion for the fourth fraction. **Figures B-E** contain SRM traces for all four possible glycans resulting from this treatment, i.e., the Tri-0SA, Tri-SA, Tri-2SA and Tri-3SA, however the low levels make these difficult to see in all of the figures.

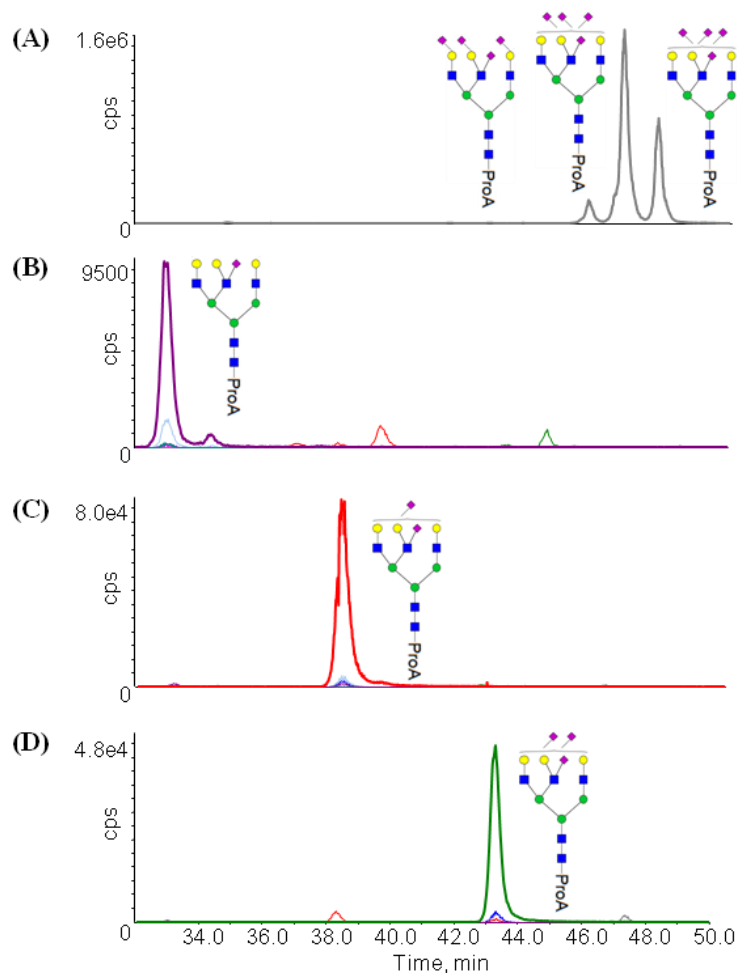


Figure S3.3. Sialidase S digestions for Tri-4SA fractions by SRM detection. (A) LC-SRM trace for Tri-4SA (m/z at 1130.9) from analysis of the fetuin N-glycans. LC-SRM analysis illustrates (B) the disappearance of the grey peak (Tri-4SA) and the appearance of the purple peak (Tri-SA) after Sialidase S digestion for the first fraction; (C) the disappearance of the grey peak (Tri-4SA) and the appearance of the red peak (Tri-2SA) after Sialidase S digestion for the second fraction; and (D) the disappearance of the grey peak (Tri-4SA) and the appearance of the green peak (Tri-3SA) after Sialidase S digestion for the third fraction. Figures B-D contain SRM traces for all five possible glycans resulting from this treatment, i.e., the Tri-0SA, Tri-SA, Tri-2SA, Tri-3SA and Tri-4SA, however the low levels make these difficult to see in all of the figures.

Table S3.1. SRM transitions for Sialidase S digestion of fetuin N-glycan studies.

Composition	Q1 (charge)	Q3 (charge)	CE (V)	Dwell (msec)
Bi-0SA	931.1 (+2)	441.4 (+1)	70	100
Bi-SA	1076.5 (+2)	441.4 (+1)	70	100
Bi-2SA	1222.1 (+2)	441.4 (+1)	70	100
Tri-0SA	1113.7 (+2)	441.4 (+1)	70	100
Tri-SA	1259.2 (+2)	441.4 (+1)	70	100
Tri-2SA	936.9 (+3)	441.4 (+1)	70	100
Tri-3SA	1033.9 (+3)	441.4 (+1)	70	100
Tri-4SA	1130.9 (+3)	441.4 (+1)	70	100

Table S3.2. P-Values obtained from Independent Two-Tailed Students T-test of the difference between the relative quantitation using UV and SRM detection when (I) the response for each glycoform is calculated relative to the summed response for all identified glycans and (II) the response for each glycoform is calculated relative to the summed response for all glycoforms with the same composition.

	P-Value	P-Value
Bi-2SA(3,3)	1.0E-05	0.5113
Bi-2SA(3,6)	8.7E-05	0.3489
Bi-2SA(6,6)	3.9E-05	0.0916
Tri-2SA(3,3)	5.5E-04	0.3409
Tri-2SA(3,6)	8.1E-04	0.4050
Tri-2SA(6,6)	0.0021	0.6826
Tri-3SA(3,3,3)	0.2697	0.9177
Tri-3SA(3,3,6)	6.0E-05	0.5113
Tri-3SA(3,6,6)	0.0146	0.0519
Tri-3SA(6,6,6)	0.0044	0.2180
Tri-4SA(3,3,3,6)	2.8E-05	0.0428
Tri-4SA(3,3,6,6)	2.2E-05	0.0594
Tri-4SA(3,6,6,6)	3.2E-05	0.0065

Bold values are significant at $P \leq 0.001$.

APPENDIX C

SUPPLEMENTAL INFORMATION TO CHAPTER 4:

EVALUATION OF AN ^{15}N -LABELED MONOCLONAL ANTIBODY (MAB) AS AN
INTERNAL STANDARD FOR QUANTITATIVE GLYCOMICS

Calculation of Under-labeling ratio (UL) from FT-MS spectra:

The relative isotopic peak intensities are listed in **Table S4.3A** and **Table S4.3B** from ^{14}N and ^{15}N samples, respectively.

The m/z at 1685.72 was recognized as the monoisotopic peak with 3 sites incorporated with ^{15}N .

So, the whole contribution from the underlabeling species was:

$$14.16/100*(100+76.82+37.64+9.95+1.72) = 32.02$$

Thus, the underlabeling ratio for all the species was:

$$32.02/(14.16+100+72.38+35.22+10.36+1.0) = 13.83\%$$

For this N-glycan, it has 4 labeling sites which can be incorporated with ^{15}N . If those sites were treated equally for labeling efficiency, then for each site, the under-labeling ratio would be:

$$\text{UL}=13.83\%/4= 3.46\%$$

Mathematic approaches for relative quantitation by SRM using ^{15}N -labeled mAb reference:

Isotopic contribution ratio by ^{13}C (I) was calculated from human serum IgG sample:

$$I = \frac{A_{\text{heavy}/442.3}}{A_{\text{light}/441.3} + A_{\text{heavy}/442.3}} \times 100\% \quad \text{(Equation 4.1)}$$

Underlabeling ratio (UL) was calculated from ^{15}N -labeled mAb reference:

$$UL = \frac{A_{\text{light}/441.3}}{A_{\text{light}/441.3} + A_{\text{heavy}/442.3}} \times 100\% \quad \text{(Equation 4.2)}$$

For the sample mixture, assume the area contributed by the sample is X (^{14}N), and the area contributed by the reference is Y (^{15}N). Hence,

$$A_{\text{light}/441.3} = X(1 - I) + Y(UL)$$

$$A_{\text{heavy}/442.3} = X(I) + Y(1 - UL)$$

By resolving the above equations,

$$X = \frac{A_{842.3/441.3} - A_{842.3/441.3}(UL) - A_{844.3/442.3}(UL)}{1 - I - UL}$$

$$Y = \frac{A_{844.3/442.3} - A_{842.3/441.3}(I) - A_{844.3/442.3}(I)}{1 - I - UL}$$

Therefore, for the relative quantitation

$$R\left(\frac{^{14}\text{N}}{^{15}\text{N}}\right) = \frac{X}{Y} = \frac{A_{842.3/441.3} - (A_{842.3/441.3})(UL) - (A_{844.3/442.3})(UL)}{A_{844.3/442.3} - (A_{842.3/441.3})(I) - (A_{844.3/442.3})(I)} \quad \text{(Equation 4.3)}$$

Taking the N-glycan F1A2 as an example with the detected peak areas of the light species (842.3/441.3) and the heavy species (844.3/442.3) from various sample mixtures listed in

Table S4.4:

a. Isotopic contribution ratio by ^{13}C (I) was calculated from human serum sample with

Equation 4.1:

$$I = \frac{A_{844.3/442.3}}{A_{842.3/441.3} + A_{844.3/442.3}} \times 100\% = \frac{1.22\text{E}+04}{(7.73\text{E}+05)+(1.22\text{E}+04)} \times 100\% = 1.55\%$$

b. Underlabeling ratio (UL) was calculated from ^{15}N -labeled mAb reference with **Equation 4.2:**

$$UL = \frac{A_{842.3/441.3}}{A_{842.3/441.3} + A_{844.3/442.3}} \times 100\% = \frac{2.29\text{E}+04}{(2.29\text{E}+04)+(4.60\text{E}+05)} \times 100\% = 4.74\%$$

c. The relative ratio of the light species and heavy species was calculated from each sample mixture with **Equation 4.3:**

$$R\left(\frac{^{14}\text{N}}{^{15}\text{N}}\right) = \frac{A_{842.3/441.3} - (A_{842.3/441.3})(UL) - (A_{844.3/442.3})(UL)}{A_{844.3/442.3} - (A_{842.3/441.3})(I) - (A_{844.3/442.3})(I)}$$

Thus,

For 10 μL human serum with reference,

$$R\left(\frac{^{14}\text{N}}{^{15}\text{N}}\right) = \frac{(7.63\text{E}+04) - (7.63\text{E}+04)(4.47\%) - (2.85\text{E}+05)(4.47\%)}{(2.85\text{E}+05) - (7.63\text{E}+04)(1.55\%) - (2.85\text{E}+05)(1.55\%)} = 0.262$$

For 25 μL human serum with reference,

$$R\left(\frac{^{14}\text{N}}{^{15}\text{N}}\right) = \frac{(2.19\text{E}+05) - (2.19\text{E}+05)(4.47\%) - (3.32\text{E}+05)(4.47\%)}{(3.32\text{E}+05) - (2.19\text{E}+05)(1.55\%) - (3.32\text{E}+05)(1.55\%)} = 0.653$$

For 50 μL human serum with reference,

$$R\left(\frac{^{14}\text{N}}{^{15}\text{N}}\right) = \frac{(3.42\text{E}+05) - (3.42\text{E}+05)(4.47\%) - (2.67\text{E}+05)(4.47\%)}{(2.67\text{E}+05) - (3.42\text{E}+05)(1.55\%) - (2.67\text{E}+05)(1.55\%)} = 1.27$$

For 100 μL human serum with reference,

$$R\left(\frac{^{14}\text{N}}{^{15}\text{N}}\right) = \frac{(5.29\text{E}+05) - (5.29\text{E}+05)(4.47\%) - (2.16\text{E}+05)(4.47\%)}{(2.16\text{E}+05) - (5.29\text{E}+05)(1.55\%) - (2.16\text{E}+05)(1.55\%)} = 2.45$$

For 250 μL human serum with reference,

$$R\left(\frac{^{14}\text{N}}{^{15}\text{N}}\right) = \frac{(1.03\text{E}+06) - (1.03\text{E}+06)(4.47\%) - (1.85\text{E}+05)(4.47\%)}{(1.85\text{E}+05) - (1.03\text{E}+06)(1.55\%) - (1.85\text{E}+05)(1.55\%)} = 5.62$$

With normalization by the 50 μL sample,

For 10 μL human serum sample, the ratio of sample over reference would be: $2.62 / 1.27 = 0.206$

For 25 μL human serum sample, the ratio of sample over reference would be: $6.53 / 1.27 = 0.515$

For 50 μL human serum sample, the ratio of sample over reference would be: $1.27 / 1.27 = 1.00$

For 100 μL human serum sample, the ratio of sample over reference would be: $2.45 / 1.27 = 1.93$

For 250 μL human serum sample, the ratio of sample over reference would be: $5.62 / 1.27 = 4.43$

Table S4.1. Transitions for SRM quantification. N-glycans identified from human serum IgG and ¹⁵N-labeled mAb reference.

Composition	Q1 (charge)	Q3 (charge)	Time (min)	CE (V)
M6	809.0 (+2)	441.3	30.80	70
F1A2	842.3 (+2)	441.3	27.50	70
¹⁵ N-F1A2	844.3 (+2)	442.3	27.50	70
A2G1	850.3 (+2)	441.3	29.30	70
¹⁵ N-A2G1	852.3 (+2)	442.3	29.30	70
M7	890.0 (+2)	441.3	34.40	70
F1A2G1	923.3 (+2)	441.3	31.20	70
¹⁵ N-F1A2G1	925.3 (+2)	442.3	31.20	70
A3G3S2	936.9 (+3)	441.3	47.70	70
M8	971.0 (+2)	441.3	37.80	70
F1A2G2	1004.4 (+2)	441.3	34.50	70
¹⁵ N-F1A2G2	1006.4 (+2)	442.3	34.50	70
M9	1052.1 (+2)	441.3	40.60	70
A2G2S1	1076.5 (+2)	441.3	39.50	70
F1A2G2S1	1149.5 (+2)	441.3	40.99	70
A2G2S2	1222.2 (+2)	441.3	45.50	70

Table S4.2. Relative quantitation using ¹⁵N-labeled mAb reference with Q3 resolution at “high”.

N-glycans	Normalized ratio				
	10 µL	25 µL	50 µL	100 µL	250 µL
F1A2/ ¹⁵ N-F1A2	0.213	0.499	1.00	1.98	4.42
A2G1/ ¹⁵ N-A2G1 (iso1)	0.203	0.505	1.00	1.832	3.91
A2G1/ ¹⁵ N-A2G1 (iso2)	0.194	0.515	1.00	1.91	4.20
F1A2G1/ ¹⁵ N-F1A2G1	0.206	0.498	1.00	1.92	3.98
F1A2G2/ ¹⁵ N-F1A2G2	0.255	0.551	1.00	1.60	3.65
M7/ ¹⁵ N-F1A2	0.193	0.488	1.00	1.92	5.44
M8/ ¹⁵ N-F1A2	0.240	0.504	1.00	1.91	4.96
M9/ ¹⁵ N-F1A2	0.228	0.516	1.00	2.02	4.20
A3G3S2/ ¹⁵ N-F1A2	0.183	0.525	1.00	2.13	5.10
A2G2S1/ ¹⁵ N-F1A2 (iso1)	0.198	0.393	1.00	1.88	4.74
A2G2S1/ ¹⁵ N-F1A2 (iso2)	0.210	0.486	1.00	1.90	4.43
F1A2G2S1/ ¹⁵ N-F1A2	0.199	0.448	1.00	1.90	4.71
A2G2S2/ ¹⁵ N-F1A2	0.215	0.528	1.00	2.02	4.53
Average	0.211	0.497	1.00	1.92	4.48
SD	0.0202	0.0396	0	0.121	0.507

Table S4.3. Isotopic distribution for the N-glycan F1A2 with FT-ICR detection. (A) Relative peak intensities for the isotopic peaks from human serum IgG; **(B)** Relative peak intensities for the isotopic peaks from ^{15}N -labeled mAb reference.

(A)

m/z	Isotopes	Relative Intensity (%)
1682.73	$^{13}\text{C}_0\text{ }^{15}\text{N}_0$	100
1683.74	$^{13}\text{C}_1\text{ }^{15}\text{N}_0$	76.82
1684.74	$^{13}\text{C}_2\text{ }^{15}\text{N}_0$	37.64
1685.74	$^{13}\text{C}_3\text{ }^{15}\text{N}_0$	9.95
1686.72	$^{13}\text{C}_4\text{ }^{15}\text{N}_0$	1.72

(B)

m/z	Isotopes	Relative Intensity (%)
1685.72	$^{13}\text{C}_0\text{ }^{15}\text{N}_3$	14.16
1686.72	$^{13}\text{C}_0\text{ }^{15}\text{N}_4$	100
1687.72	$^{13}\text{C}_1\text{ }^{15}\text{N}_4$	72.38
1688.73	$^{13}\text{C}_2\text{ }^{15}\text{N}_4$	35.22
1689.73	$^{13}\text{C}_3\text{ }^{15}\text{N}_4$	10.36
1690.75	$^{13}\text{C}_4\text{ }^{15}\text{N}_4$	1.00

Table S4.4. Peak areas for the N-glycan F1A2 (light and heavy species) by SRM detection.

	842.3/441.3 Peak Area (blue SRM traces)	844.3/442.3 Peak Area (red SRM traces)
Human Serum (sample only)	7.73E+05	1.22E+04
¹⁵N-labeled mAb (reference only)	2.29E+04	4.60E+05
10 μL human serum + reference	7.63E+04	2.85E+05
25 μL human serum + reference	2.19E+05	3.32E+05
50 μL human serum + reference	3.42E+05	2.67E+05
100 μL human serum + reference	5.29E+05	2.16E+05
250 μL human serum + reference	1.03E+06	1.85E+05

APPENDIX D

SUPPLEMENTAL INFORMATION TO CHAPTER 5:

TARGETED GLYCOMICS BY SCHEDULED SELECTED REACTION MONITORING
(SRM) COUPLED WITH HILIC SEPARATION FOR GLOBAL GLYCAN PROFILING

Table S5.1. Detection and identification of N-glycans and isomers from whole human serum.

ID	m/z	Charge state	Composition					GU (Experimental)
			HexNAc	Hex	Fuc	Neu5Ac (α 2-3)	Neu5Ac (α 2-6)	
22	1130.65	1	2	3	0	0	0	4.31
41	1292.70	1	2	4	0	0	0	5.35
134	1333.73	1	3	3	0	0	0	5.16
134_iso	1333.73	1	3	3	0	0	0	5.60
15	1454.75	1	2	5	0	0	0	6.83
174	1479.79	1	3	3	1	0	0	5.89
16	808.90	2	2	6	0	0	0	7.53
176	821.42	2	3	4	1	0	0	6.95
176_iso	821.42	2	3	4	1	0	0	6.95
136	829.42	2	3	5	0	0	0	7.28
132	849.93	2	4	4	0	0	0	7.19
38	870.44	2	5	3	0	0	0	6.88
17	889.93	2	2	7	0	0	0	8.27
147_1	893.94	2	3	4	0	1	0	7.83
147_2	893.94	2	3	4	0	0	1	8.22
32	902.45	2	3	5	1	0	0	7.67
40	910.44	2	3	6	0	0	0	8.02
44	922.96	2	4	4	1	0	0	7.51
1	930.96	2	4	5	0	0	0	7.50
1_iso	930.96	2	4	5	0	0	0	7.85
36	943.47	2	5	3	1	0	0	7.20
61	951.47	2	5	4	0	0	0	7.49
148_1	966.97	2	3	4	1	1	0	8.61
148_2	966.97	2	3	4	1	0	1	9.20
19	970.96	2	2	8	0	0	0	9.03
119_1	974.96	2	3	5	0	1	0	8.49
119_2	974.96	2	3	5	0	0	1	8.93
31	983.47	2	3	6	1	0	0	8.48
79_2	995.48	2	4	4	0	0	1	8.82
51	1003.99	2	4	5	1	0	0	8.19
63	1011.98	2	4	6	0	0	0	8.51
45	1024.50	2	5	4	1	0	0	7.81
24	1032.50	2	5	5	0	0	0	8.17
21	1051.98	2	2	9	0	0	0	10.17

Table S5.1. Continued.

ID	m/z	Charge state	Composition					GU (Experimental)
			HexNAc	Hex	Fuc	Neu5Ac (α 2-3)	Neu5Ac (α 2-6)	
120_1	1055.99	2	3	6	0	1	0	9.54
82_1	1068.51	2	4	4	1	1	0	9.21
5_1	1076.50	2	4	5	0	1	0	9.08
5_2	1076.50	2	4	5	0	0	1	9.57
222	1077.01	2	4	5	2	0	0	9.04
287	1085.01	2	4	6	1	0	0	9.58
583_2	1089.02	2	5	3	1	0	1	9.60
518_1	1097.02	2	5	4	0	1	0	8.97
518_2	1097.02	2	5	4	0	0	1	9.31
177	1105.52	2	5	5	1	0	0	9.31
2	1113.52	2	5	6	0	0	0	9.02
71	1134.04	2	6	5	0	0	0	8.89
185_2	1141.54	2	4	4	2	0	1	10.49
8_1	1149.53	2	4	5	1	1	0	10.01
8_2	1149.53	2	4	5	1	0	1	10.33
191	1150.04	2	4	5	3	0	0	9.50
382_1	1157.53	2	4	6	0	1	0	10.31
382_2	1157.53	2	4	6	0	0	1	10.63
505	1158.04	2	4	6	2	0	0	9.99
50_1	1170.05	2	5	4	1	1	0	9.64
50_2	1170.05	2	5	4	1	0	1	10.07
241_1	1178.04	2	5	5	0	1	0	10.10
186	1178.55	2	5	5	2	0	0	9.80
12	1186.55	2	5	6	1	0	0	10.10
35_1	1222.05	2	4	5	0	2	0	11.24
35_2	1222.05	2	4	5	0	1	1	11.83
125_1	1222.56	2	4	5	2	1	0	10.66
125_2	1222.56	2	4	5	2	0	1	11.25
86_1	1230.56	2	4	6	1	1	0	11.24
86_2	1230.56	2	4	6	1	0	1	11.84
240	1231.07	2	4	6	3	0	0	10.84
517_1	1242.56	2	5	4	0	2	0	10.56
517_2	1242.56	2	5	4	0	1	1	11.06
517_3	1242.56	2	5	4	0	0	2	11.61
482_1	1243.07	2	5	4	2	1	0	10.56
482_2	1243.07	2	5	4	2	0	1	10.83
46_1	1251.07	2	5	5	1	1	0	10.52

Table S5.1. Continued.

ID	m/z	Charge state	Composition					GU (Experimental)
			HexNAc	Hex	Fuc	Neu5Ac (α 2-3)	Neu5Ac (α 2-6)	
46_2	1251.07	2	5	5	1	0	1	11.03
245_1	1259.07	2	5	6	0	1	0	11.21
245_2	1259.07	2	5	6	0	0	1	11.68
398	1267.58	2	5	7	1	0	0	10.87
398_iso	1267.58	2	5	7	1	0	0	11.00
9_1	1295.08	2	4	5	1	2	0	11.71
9_2	1295.08	2	4	5	1	1	1	12.19
9_3	1295.08	2	4	5	1	0	2	13.11
3	1296.09	2	6	7	0	0	0	11.10
483_2	1315.59	2	5	4	1	1	1	11.85
138_1	1323.59	2	5	5	0	2	0	11.85
138_2	1323.59	2	5	5	0	1	1	12.32
138_3	1323.59	2	5	5	0	0	2	12.62
392_1	1332.10	2	5	6	1	1	0	11.68
392_2	1332.10	2	5	6	1	0	1	12.31
144_2	1396.62	2	5	5	1	1	1	12.85
43_1	936.75	3	5	6	0	2	0	12.88
43_2	936.75	3	5	6	0	1	1	13.51
43_3	936.75	3	5	6	0	0	2	13.78
575_1	937.09	3	5	6	2	1	0	12.29
575_2	937.09	3	5	6	2	0	1	12.90
864_1	942.42	3	5	7	1	1	0	12.90
864_2	942.42	3	5	7	1	0	1	13.51
14_2	985.43	3	5	6	1	1	1	13.78
14_3	985.43	3	5	6	1	0	2	14.44
7_2	1033.78	3	5	6	0	2	1	15.18
7_3	1033.78	3	5	6	0	1	2	15.74
7_4	1033.78	3	5	6	0	0	3	16.35
85_2	1039.45	3	5	7	1	1	1	15.19
85_3	1039.45	3	5	7	1	0	2	15.74
249_1	1058.46	3	6	7	0	2	0	14.22
249_2	1058.46	3	6	7	0	1	1	14.88
249_3	1058.46	3	6	7	0	0	2	15.46
72_3	1082.46	3	5	6	1	1	2	15.85
72_4	1082.46	3	5	6	1	0	3	16.40
252_2	1155.49	3	6	7	0	2	1	16.66

Table S5.1 Continued.

ID	m/z	Charge state	Composition					GU (Experimental)
			HexNAc	Hex	Fuc	Neu5Ac (α 2-3)	Neu5Ac (α 2-6)	
252_3	1155.49	3	6	7	0	1	2	17.12
516_1	1156.17	3	6	7	4	1	0	15.45
516_2	1156.17	3	6	7	4	0	1	15.76
59_1	1252.52	3	6	7	0	4	0	17.68
59_2	1252.52	3	6	7	0	3	1	18.43
59_3	1252.52	3	6	7	0	2	2	19.07
59_4	1252.52	3	6	7	0	1	3	19.93